



# รายงานวิจัยฉบับสมบูรณ์

# โครงการ การศึกษาหน้าที่ของ GW182 ในกุ้งกุลาดำที่ติดเชื้อไวรัส โรคดวงขาว

โดย น.ส. อรชุมา อิฐสถิตไพศาล

มีนาคม 2561

สัญญาเลขที่ TRG5780032

## รายงานวิจัยฉบับสมบูรณ์

โครงการ การศึกษาหน้าที่ของ GW182 ในกุ้งกุลาดำที่ติดเชื้อไวรัส โรคดวงขาว

## น.ส. อรชุมา อิฐสถิตไพศาล ภาควิชาชีวเคมี คณะวิทยาศาสตร์ มหาวิทยาลัยมหิดล

สนับสนุนโดยสำนักงานกองทุนสนับสนุนการวิจัยและคณะ วิทยาศาสตร์ มหาวิทยาลัยมหิดล

(ความเห็นในรายงานนี้เป็นของผู้วิจัย สกว.และต้นสังกัดไม่จำเป็นต้องเห็นด้วยเสมอไป)

## รูปแบบ Abstract (บทคัดย่อ)

Project Code: TRG5780032

Project Title: การศึกษาหน้าที่ของ GW182 ในกุ้งกุลาดำที่ติดเชื้อไวรัสโรคดวงขาว

Investigator: น.ส. อรชุมา อิฐสถิตไพศาล ภาควิชาชีวเคมี คณะวิทยาศาสตร์ มหาวิทยาลัยมหิดล

E-mail Address: ornchuma.its@mahidol.ac.th

Project Period: 2 ਹੈ

Keywords: GW182, miRNA, Penaeus vannamei, dsRNA

(คำหลัก)

#### Abstract:

Shrimp, especially Penaeus vannamei, plays an important role in Thai aquaculture industry. Many diseases are caused by viral infection in shrimp, such as White Spot Syndrome Virus (WSSV) and Yellow Head Virus (YHV) which leads to a high mortality rate of shrimp in 3-5 days and subsequent economic losses. GW182 is considered as one of the core proteins of a miRNA-induced silencing complex (miRISC) that downregulates target mRNAs that are partially complement to the small RNA, called miRNA, in the complex. This pathway regulates gene expression and fights against viral infection, which GW182 is as an Argonaute-binding partner in the miRNA pathway. For more comprehensive understanding in the miRNA pathway against viral infection in shrimp, an investigation into expression of P. vannamei GW182 during virus infection has been carried out using doublestranded RNA to knockdown GW182 (dsRNA-GW182). It was hypothesized that similar to other genes involved in RNA interference, the GW182 expression is upregulated during viral infection. The results revealed that PvGW182 mRNA level was significantly up-regulated after 24 hours post YHV injection, while the PvGW182 mRNA level was consistent during WSSV infection. To facilitate a further study into the function of GW182 during viral infection, an RNAi technique was used to knockdown the expression of GW182. The results showed that GW182 is upregulated in response to an injection of dsRNA. Hence, it is not surprising that the injection of 2.5 µg/g shrimp of dsRNA-GW182#1 in this study could only reduce the expression of GW182 by 60% on day 3. Further study of the GW182 function using dsRNA-GW182 is underway to determine the PvGW182 mRNA level in shrimp infected with virus.

กุ้งขาวแวนนาไมเป็นกุ้งชนิดหนึ่งที่มีความสำคัญต่ออุตสาหกรรมการเพาะเลี้ยงสัตว์น้ำของไทย ปัญหา จากการเลี้ยงกุ้งส่วนหนึ่งมีสาเหตุมาจากการติดเชื้อไวรัส ยกตัวอย่างเช่น ไวรัสตัวแดงดวงขาว (WSSV) และ ไวรัสหัวเหลือง (YHV) ซึ่งไวรัสเหล่านี้มีผลต่ออัตราการตายของกุ้งสูงถึง 100% ภายใน 3 - 5 วัน ซึ่งส่งผล กระทบต่อเศรษฐกิจการส่งออกกุ้งเป็นจำนวนมาก โปรตีน GW182 เป็นหนึ่งในองค์ประกอบสำคัญของกลุ่ม โปรตีน (miRISC) โดยทำงานร่วมกับโปรตีน Argonaute ที่ทำหน้าที่ควบคุมการแสดงออกของยีนต่างๆ รวมถึง การยับยั้งการติดเชื้อไวรัสในกุ้ง โดยการยับยั้งการแสดงออกของยืนเป้าหมาย เพื่อเพิ่มความเข้าใจกลไกการ ยับยั้งการแสดงออกของยีนด้วยการอาศัยไมโครอาร์เอ็นเอในกุ้งระหว่างที่มีการติดไวรัส หน้าที่ของยืน GW182 ในกุ้งขาวที่มีการติดไวรัสด้วยการยับยั้งการแสดงออกของยืน GW182 โดยอาศัยอาร์ เอ็นเอสายคู่ที่จำเพาะต่อยืน GW182 (dsRNA-GW182) ภายใต้สมมติฐานว่า การยับยั้งการแสดงออกของยืน GW182 อาจจะส่งผลให้กุ้งขาวติดเชื้อไวรัสหัวเหลืองได้มากขึ้นและเร็วขึ้น ในงานวิจัยนี้ ผลจากการศึกษาการ แสดงออกของยืน GW182 ในระหว่างที่มีการติดเชื้อไวรัสพบว่า หลังจากที่กุ้งได้รับไวรัสหัวเหลือง 48 ชั่วโมง กุ้งมีระดับการแสดงออกของยืน GW182 เพิ่มขึ้น ในขณะที่การติดเชื้อไวรัสตัวแดงดวงขาวไม่มีผลต่อการ แสดงออกของยืน GW182 ในกุ้ง นอกจากนี้การยับยั้งการแสดงออกของยืน GW182 ด้วยการใช้ dsRNA-GW182 พบว่าการใช้ 2.5 ไมโครกรัมของ dsRNA-GW182 ตำแหน่งที่ 1 ต่อน้ำหนักกุ้ง 1 กรัม สามารถยับยั้ง การแสดงออกของยืน GW182 ได้ดีที่สุด และการยับยั้งการแสดงออกของยืน GW182 สูงถึง 60% ในวันที่ 2 หลังจากฉีด dsRNA-GW182 ตำแหน่งที่ 1 ทั้งนี้การศึกษาหน้าที่ของยืน GW182 ยังคงดำเนินการต่อไป โดย จะทำการยับยั้งการแสดงออกของยืน GW182 แล้วฉีดไวรัส เพื่อศึกษาการติดโรคหัวเหลือง และอัตราการตาย ของกุ้งโดยเปรียบเทียบกับกุ้งที่ฉีดด้วยน้ำเกลือ และ dsRNA-GFP ซึ่งเป็นอาร์เอ็นเอสายคู่ที่ไม่เกี่ยวข้องกับยืน ของกุ้ง

## **Executive summary**

In this project, the open-reading frame of a GW182 gene from *P. monodon* was cloned. The genetic information was used to design double-stranded RNAs to knockdown the expression of GW182 in *P. vannamei* prior to the exposure of shrimp to WSSV and YHV to determine whether the absence of the GW182 transcript would affect the susceptibility of shrimp towards those two viruses. This project was significantly delayed by the challenge in knocking down GW182, despite the investigator's many attempts to optimize the knockdown condition. As a result, the principle investigator proposed to conclude the project with a corresponding author paper that investigated one of a proteins found in *Enterocytozoon hepatopenaei*, an emerging pathogen. The paper has been accepted by *Parasites & Vectors* on Feb 28, 2018. This project produced one Ph.D. student and one M.Sc. students from Department of Biochemistry, Faculty of Science, Mahidol University.

## **Table of Content**

EXE	CUTIVE SUMMARY	5
<u>FIN</u>	AL REPORT	7
1	OBJECTIVES	7
1.1	TO CLONE PMGW182 FROM THE ALREADY IDENTIFIED RRM REGION OF PMGW182	7
1.2		7
1.3		7
		7
2	MATERIALS AND METHODS	
2.1	CLONING OF A FULL-LENGTH OPEN READING FRAME (ORF) OF PMGW182	7
2.2	•	7
2.3		7
2.4		7
2.5		13
2.6		13
2.7		13
2.8		13
2.9	•	14
2.10		16
2.13		16
2.13		17
2.13	3 STATISTICAL ANALYSIS	18
3	RESULTS	19
3.1	CLONING OF A FULL-LENGTH OPEN READING FRAME (ORF) OF PMGW182	19
3.2	SEQUENCE AND PHYLOGENIC ANALYSIS	20
3.3	TISSUE DISTRIBUTION STUDY OF GW182	21
3.4	EXPRESSION PROFILE OF PVGW182 MRNA DURING VIRUS INFECTION	23
3.5	PRODUCTION OF DSRNA BY IN VIVO BACTERIAL EXPRESSION	25
3.6	KNOCKDOWN EFFICIENCY OF PVGW182 BY SPECIFIC DSRNA TARGETING GW182 GENE	26
3.7	EXPRESSION PROFILE OF PVGW182 MRNA DURING DSRNA-GFP INJECTION	37
3.8	EFFECT OF PvGW182 SUPPRESSION IN YHV INFECTION	39
4	DISCUSSION	41
4.1	PvGW182 mRNA is upregulated at 24 hours by YHV infection but not by WSSV	
	ECTION.	41
4.2		-
	/182).	42
•	-v-)·	-
5	CONCLUSIONS	47
6	FUTURE DIRECTION: STUDYING THE KNOCKDOWN EFFECT OF PVGW182 IN YHV-	
	ECTED SHRIMP	48
	EOLED OLIMINA	-70
7	REFERENCES	49
8	OUTPUT จากโครงการวิจัยที่ได้รับทนจาก สกว.	56

## **Final Report**

## 1 Objectives

- 1.1 To clone PmGW182 from the already identified RRM region of PmGW182
- 1.2 To characterize the functions of PmGW182 in WSSV replication in P. monodon
- 1.3 To investigate the roles of PmGW182 in miRNA-mediated gene silencing

## 2 Materials and methods

## 2.1 Cloning of a full-length open reading frame (ORF) of PmGW182

cDNA synthesized from total RNA from *P. vannamei* ovary was used as a template for amplification by Q5 DNA polymerase. The resulting amplicon was cloned sequenced. The amino acid sequence was shown in Figure 2.1

## 2.2 Sequence and phylogenic analysis

Multiple sequence alignment of the full-length GW182, also known as TNRC6A, TNRC6B, TNRC6C and Gawky was performed by ClustalW. The neighbor-joining tree was constructed by MEGA 5.05 programs. Bootstrap values from 1000 replicates are indicated at the nodes.

## 2.3 Tissue distribution study of GW182

#### 2.3.1 Total RNA extraction and reverse transcription

Total RNA was isolated from gill using RiboZol<sup>TM</sup> RNA extraction solution (Amresco, USA), following a protocol from the manufacturer. DNA templates were removed using RQ1 DNase (Promega, USA). The concentration of RNA was determined by Nanodrop. The  $A_{260}/A_{280}$  ratio of 1.8-2.0 was used as an indicator of the purity of RNA samples. 2  $\mu$ g of total RNA was used as a template for cDNA synthesis by Impromp-II<sup>TM</sup> reverse transcriptase (Promega, USA), according to the manufacturer's protocol, and oligo-dT<sub>20</sub> primer (Table 2.1).

#### 2.3.2 Multiplex PCR reaction

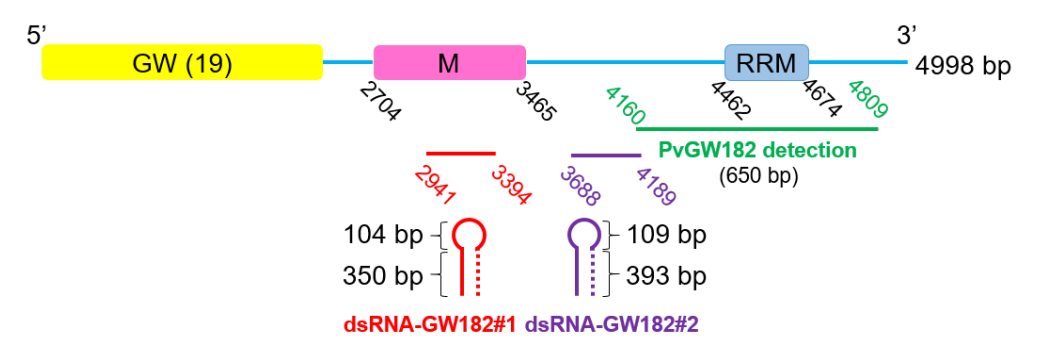
PCR reactions were performed using Platinum Hot Start PCR master mix (Invitrogen, USA) according to the manufacturer protocol. The PCR reaction The fragment of *GW182* gene was amplified by specific primer pairs, 1 μM OI020GW; 5'---ggt gga ctc ctg ggg aaa t -3' and 1 μM OI021GW; 5'-tca gag gtg aga agg cca t-3'. Specific primer pairs for the actin gene of *P. vannamei* (*PvActin*) were used as an internal control (0.05 μM Actin\_F; 5'-CCT CGC TGG AGA AGT CCT AC3' and 0.05 μM Actin\_R; 5'-TGG TCC AGA CTC GTC GTA CTC-3') The multiplex PCR protocol for both *EhSWP1* and *PvActin* was as follows: denaturation at 95 °C for 1 min followed by 30 cycles of 20 s denaturation at 95 °C, 15 s annealing at 55 °C and 60 s extension at 72 °C, with a final extension for 5 min at 72 °C. The amplicons were analyzed by 1.5% agarose gel electrophoresis with ethidium bromide staining.

#### 2.4 Construction of dsRNAs

A recombinant plasmid encoding an inverted-repeat disrupted by a loop was used as a template for *in vivo* dsRNA expression. The plasmid for expressing dsRNA-GFP, which was used as a non-specific dsRNA, was constructed from pET-3a-stGFP which was kindly provided by Asst. Prof. Chalermporn Ongvarasopone.

## 2.4.1 <u>Design sense-loop and antisense of dsRNA specific to PvGW182 gene</u>

Two regions from the full-length amino acid sequence of PmGW182 were selected as a target for constructing dsRNA to knockdown the GW182 gene (Figure 2.1). The first construction, called dsRNA-GW182#1, was designed to cover the M-domain. The second construction, called dsRNA-GW182#2, was designed to cover a non-conserved sequence to avoid non-specific knockdown.



dsRNA-GW182	Amino acid (AA) position at	Nucleotide sequence at
#1	981 - 1131	2941 - 3394
#2	1230 - 1396	3688 - 4189
PvGW182 detection	1388 - 1603	4160 - 4809

Figure 2.1 A schematic diagram of dsRNA-GW182#1 and #2 and regions on PvGW182 that they target.

**Product size** (dq) 454 350 502 393 cDNA synthesis Sense-loop of Sense-loop of Antisense of Antisense of **Purposes** GW182#1 GW182#1 GW182#2 GW182#2 dsRNAdsRNAdsRNAdsRNA-Non-conserved Restriction site Target genes M-domain of PmGW182 PmGW182 region of BamHI BamHI HindIII HindIII Xbal Xhol Xbal Xho CCTATCTAGAGTAGTGCAGGGGATGCTTGGCGT GATTCTCGAGAGTAGTGCAGGGGGATGCTTGGCGT CAGTGGATCCGCTGTTAACATAGAGAG GCCAGGATCCGTCTGTGACGAGTTCTTGTTAATG TTAAAAGCTTGTTCGACGTGAGGGAGAAAG TATACTCGAGCTGCTCGGACCCTCTAACAG TATA<u>TCTAGA</u>CTGCTCGGACCCTCTAACAG TTAAAAGCTTCATTCCAAGCTGACCCACTT Sequences  $(5' \rightarrow 3')$ Table 2.1 Sequences and names of primers in used Oligo-dT<sub>20</sub> O1046GW OI048GW O1049GW O1046GW OI047GW OI048GW OI049GW OI047GW **Primers** 

Table 2.1 Sequences and names of primers in used (cont.)

Primers	Sequences (5'→ 3')	Target genes	Purposes	Product size (bp)	Reference
Actin_F	GACTCGTACGTGGCGACGAGG	e e	An internal control	C L	
Actin_R	AGCAGCGGTGGTCATCTCCTGCTC	<b>p</b> -actin	for multiplex RT-PCR	ncc	(Posifi et al., 2016)
PS013GW	CCAATGGCAAAAGTGGGTCA	2,470		Ç	
PS014GW	AGACTGGGAAGTTGGTGGAG	7VG/V 182	FVGW 182 Multiplex K1-FCK	000	i nis study
WSSV (VP28)_F	WSSV (VP28)_F CCGCTCGAGACTCTTTCGGTCGTGGCGCC				
WSSV (VP28)_F	WSSV (VP28)_R GGCACCATCTGCATACCAGTG	VP28	WSSV detection	420	(Attasart et al., 2009)
YHV(hel)_F	CAAGGACCACCTGGTACGGTAAGAC	NA PERSONAL PROPERTY OF THE PERSONAL PROPERTY		C	
YHV(hel)_R	GCGGAAACGACTGACGCTACATTCAC	Y nv nelicase	Y NV detection	000	(Posifi et al., 2016)

## 2.4.2 <u>Amplification of sense-loop and antisense template strands for dsRNA expression</u>

The sense-loop and antisense strands template were amplified separately from *P. vannamei* gill cDNA template using primers shown in Table 2.1. Recipes for PCR reactions and thermocycling conditions are shown in Table 2.2 and Table 2.3.

Table 2.2 Recipes of PCR reactions for amplifying sense-loop and antisense strand template for expressing of dsRNA-GW182

dsRNA-	Component	1 Reac	tion set up (50 µl)	
GW182 construction	Component	Volume (μl) for sense-loop	Volume (µI) for antisense	Final conc.
	water	42.75	42.75	
	10X Standard <i>Taq</i> buffer	5	5	1X
	10 mM dNTPs	1	1	0.2 mM
	10 μM OI046GW	1	-	0.2 μΜ
#1	10 μM OI047GW	1	-	0.2 μΜ
	10 μM OI048GW	-	1	0.2 μΜ
	10 μM OI049GW	-	1	0.2 μΜ
	Taq DNA polymerase	0.25	0.25	0.2 Unit
	cDNA template	1	1	
	water	42.75	42.75	
	10X Standard <i>Taq</i> buffer	5	5	1X
	10 mM dNTPs	1	1	1X 0.2 mM 0.2 μM 0.2 μM 0.2 μM 0.2 μM 0.2 μM
	10 μM Ol068GW	1	-	
#2	10 μM Ol069GW	1	-	0.2 μΜ
	10 μM OI070GW	-	1	0.2 μΜ
	10 μM Ol071GW	-	1	0.2 μΜ
	Taq DNA polymerase	0.25	0.25	0.2 Unit
	cDNA template	1	1	

Table 2.3 Thermocycling condition of PCR reactions for amplifying sense-loop and antisense strand template for expressing of dsRNA-GW182

Step	Temp (°C)	Time	Cycles
Initial denaturation	95	1 min	1
Denaturation	95	20 s	30
Annealing	53	20 s	
Extension	68	1 min	

Final extension	68	1 min	1
-----------------	----	-------	---

The 454 and 350 bp amplicons for the sense-loop and antisense strand template of dsRNA-GW182#1 and the 503 and 393 bp amplicons for the sense-loop and antisense of dsRNA-GW182#2 were analyzed by 1.5% agarose gel electrophoresis with ethidium bromide staining. Then, the expected DNA amplicons were purified and digested with specific enzymes. The sense-loop of GW182#1 and GW182#2 were cut by *Xbal/Bam*HI and *Xbal/HindIII*, respectively. The antisense of GW182#1 and GW182#2 were cut by *Xhol/Bam*HI and *HindIII/Xhol*, respectively.

#### 2.4.3 <u>Ligation reactions</u>

Amplicons and a pET28a vector that were cut with the same pair of restriction enzymes were ligated to construct a recombinant plasmid of sense-loop and antisense of dsRNA-GW182 called pET28a-sl-GW182#1, pET28a-sl-GW182#2, pET28a-a-GW182#1, and pET28a-a-GW182#2. An insert-to-vetor ratio used in the ligation was 3:1 which is normally used for sticky end ligation.

Ligation reactions were performed using T4 DNA ligase (Thermoscientific, USA). The vector and cut PCR amplicon were ligated according to the manufacturer's protocol at 22 °C for 1 hour.

The pET28a-sl-GW182#1, pET28a-sl-GW182#2, pET28a-a-GW182#1 and pET28a-a-GW182#2 plasmids that already confirmed by DNA sequence analysis were digested with specific enzymes. The pET28a-sl-GW182#1 and an antisense amplicon of dsRNA-GW182#1 were digested with *Bam*HI and *Xho*I to construct a recombinant plasmid pET28a-GW182#1, while the pET28a-sl-GW182#2 and an antisense amplicon of dsRNA-GW182#2 were digested with *Hin*dIII and *Xho*I to construct a recombinant plasmid pET28a-GW182#2. The pET28a-GW182#1 and pET28a-GW182#2 plasmid were transformed into HT115 *E. coli* strain for dsRNA production (Figure 2.2).

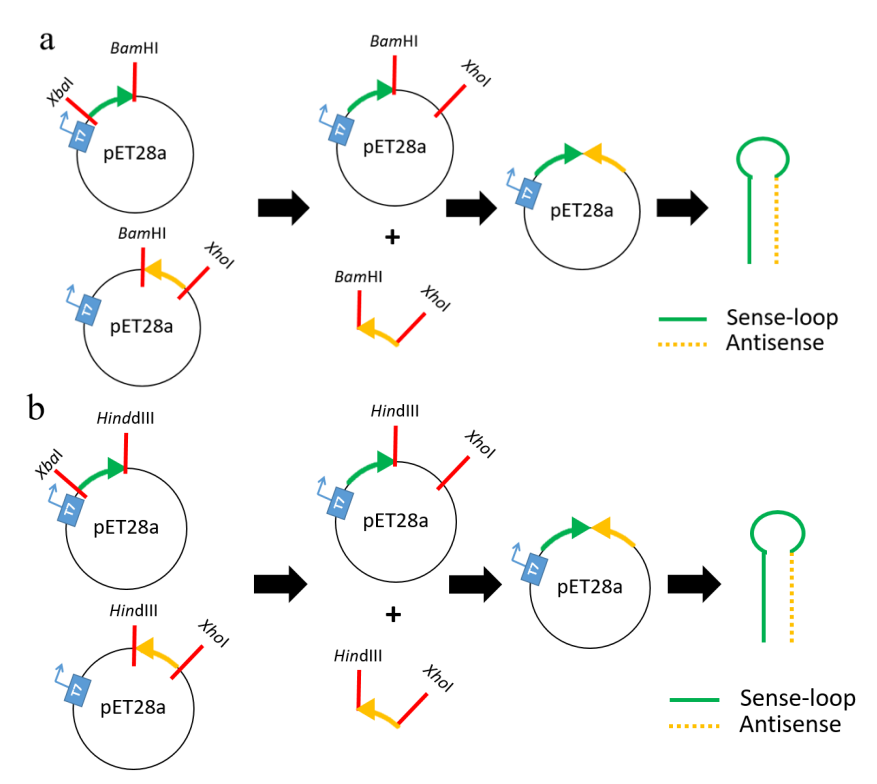


Figure 2.2 A schematic of recombinant plasmids pET28a for (a) dsRNA-GW182#1 and (b) dsRNA-GW182#2

## 2.5 Transformation of DNA plasmid into competent DH50 E. coli strain

 $6~\mu l$  of the ligated pET28 vector was added to  $50~\mu l$  of *E. coli* competent cell and incubated on ice for 30~min before 30~sec heat shock at  $42^{\circ}C$  and 2~min incubation on ice.  $250~\mu l$  of LB media without antibiotics was added before further incubation for 1~hour at  $37^{\circ}C$  and 250~rpm. The bacterial culture was spread onto a LB agar plate with  $50~\mu g/m l$  kanamycin. Then, the plate was incubated overnight at  $37^{\circ}C$ . The colonies were selected and cultured in 5~m l of LB media containing with  $50~\mu g/m l$  kanamycin at  $37^{\circ}C$  for overnight. Finally, plasmids were extracted from the overnight culture for identification of positive clones by restriction endonuclease digestion.

#### 2.6 In vivo bacterial expression of dsRNA

The pET28a-dsRNA-PvGW182 plasmids were transformed into the ribonuclease (RNase) III-deficient *E. coli* HT115 strain (Timmons et al., 2001). A single colony was picked and grown overnight at 37°C in 5 ml LB media containing 100 µg/ml kanamycin and 12.5 µg/ml tetracycline. On the next day, each bacterial starting culture was diluted 100-fold in fresh, antibiotic-supplemented media to obtain starting culture at cell density (OD<sub>600</sub>) of ~0.1. The culture was incubated at 37°C with constant shaking at 250 rpm until the OD<sub>600</sub> reached approximately 0.4. Then, the T7 promoter of RNA polymerase was induced by adding 0.4 mM isopropyl- $\beta$ -D-thiogalactopyranoside (IPTG) before further incubation for 3 hours and determined the final OD<sub>600</sub> for calculating the dsRNA yield. Cells were harvested by centrifugation at 3500 × g for 5 min at 4°C. The dsRNA was extracted according to Posiri et al., 2013.

#### 2.7 Extraction of dsRNA

The ethanol extraction method (Posiri et al., 2013) was used to purify dsRNA from  $E.\ coli$  cells. Briefly, cell pellet containing dsRNA-expressing  $E.\ coli$  was resuspended with 5 ml 75% ethanol in 1X PBS per 1 OD cell and incubated at room temperature for 5 min or at -20°C overnight prior to centrifugation at  $6000 \times g$  for 5 min at 4°C. The fixed pellet was resuspended in 1 ml of 150 mM NaCl RNase-free and centrifuged at  $8000 \times g$  for 10 min at 4°C. The dsRNA-containing supernatant was collected and kept in -20°C for storage.

## 2.8 Validation of dsRNA

To verify quality and quantity of dsRNAs, the purified dsRNAs were digested with RNase A or RNase III. There are 3 RNase reactions including an untreated dsRNA (U), a dsRNA treated with RNase A (A) and a dsRNA treated with RNase III (III) that were performed according to Table 2.4 and incubated at  $37^{\circ}$ C for 5 min. 4  $\mu$ I of the digestion reactions were analyzed by 1.5% agarose gel electrophoresis. The concentration of dsRNAs was determined by comparing band intensity with a known amount of DNA marker band. Finally, the yield of dsRNA was calculated according to Equation 2.1.

Equation 2.1 The yield of dsRNA ( $\mu$ g/OD) =  $\frac{concentration\ of\ dsRNA\ \times total\ volume\ of\ dsRNA}{final\ OD_{600}\ cell\ \times total\ volume\ of\ bacterial\ culture}$ 

Table 2.4 Recipes of enzymatic reactions for verifying dsRNA construction

Component (μl)	U	Α	III
RNasee-free water	7	6.5	6

5X RNase A buffer	2	2	
100 ng/μl of dsRNA	1	1	1
0.01 μg/μl RNase A		0.5	
10X Short cut RNase III buffer			1
10X MnCl <sub>2</sub>			1
1.5U/µl of ShortCut RNase III			1
Total volume	10	10	10

Table 2.5 Recipes of 5X RNase A buffer

Component	Volume (ml)
1 M Tris-Cl, pH 8.0	10
0.5 M EDTA	10
3 M Sodium acetate	100
ddH <sub>2</sub> O	80
Total	200

## 2.9 Determination of GW182, YHV and WSSV mRNA expression.

 $_2$   $_{\mu g}$  of individual RNA sample were used in the first strand cDNA synthesis reaction as described in 2.3.1. Primers for PvGW182, YHV helicase, and VP28 were used (Table 2.1).  $\beta$ -actin primers were used as an internal control to normalize for RNA loading.

## 2.9.1 RT-PCR

YHV and WSSV specific genes were individually amplified using primers shown in Table 2.1. Recipes of PCR reactions and thermocycler profiles for amplifying different amplicants are shown in Table 2.6 and Error! Reference source not found..

Table 2.6 Recipes of a PCR reaction for amplifying YHV helicase and WSSV (VP28) genes

Target	Reaction set	t up (25 μl)		Reference
amplicons	Component	Volume (µI)	Final conc.	
YHV helicase	water	19.875		(Posiri et al., 2016)
(850 bp)	10X ThermoPol <i>Taq</i> buffer	2.5	1X	
	10 mM dNTPs	1	0.4 mM	
	10 μM YHV(hel)_F	0.25	0.1 μΜ	
	10 μM YHV(hel)_R	0.25	0.1 μΜ	
	Taq DNA polymerase	0.125	0.2 Unit	
	cDNA template	1		
WSSV (VP28)	water	19.375		(Adapted from Attasart
(420 bp)	10X ThermoPol <i>Taq</i> buffer	2.5	1X	et al., 2009)
	10 mM dNTPs	1	0.4 mM	
	10 μM WSSV(VP28)_F	0.5	0.2 μΜ	
	10 μM WSSV(VP28)_R	0.5	0.2 μΜ	

Taq DNA polymerase	0.125 0.2 Unit	
--------------------	----------------	--

Table 2.7 Thermocycling condition for the PCR reaction of YHV helicase and WSSV VP28 genes

Step	Temp (°C)	Time	Cycles
Initial denaturation	95	5 min	1
Denaturation	95	30 s	
Annealing	55	30 s	30
Extension	68	45 s	
Final extension	68	5 min	1

The PCR products were analyzed using 1.5% agarose gel electrophoresis with ethidium bromide staining.

## 2.9.2 <u>Semi-quantitative PCR analysis</u>

Multiplex-PCR reactions were performed as shown in Table 2.8 and Table 2.9. The GW182 gene (650 bp) was amplified at nucleotide position 4160-4809 which does overlap with the region that is targeted by dsRNA-GW182#2, nucleotide position 3688-4189 (Figure 2.3). The overlapping of these two regions does not affect the PvGW182 mRNA detection. Because the oligo-dT $_{20}$  primer was used to convert RNA to cDNA which provides cDNA products only from mRNAs.  $\beta$ -actin (550 bp) was used as an internal control for loading control in PCR reaction and calculating relative PvGW182 gene expression (Equation 3.2).

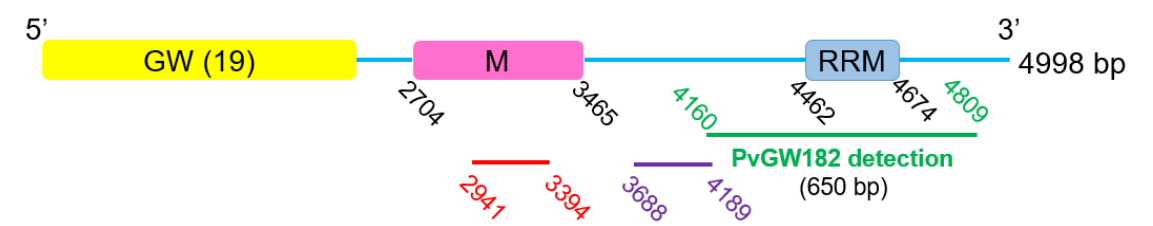


Figure 2.3 The schematic diagram of dsRNA-GW182#1 and #2 target regions and the PvGW182 detection region.

The red and purple lines under the GW182 domain diagram show the regions that are targeted by two dsRNA-GW182, while the green line represents the region that is used to detect PvGW182 expression.

Equation 3.2

Relative PvGW182 gene expression (arbitrary unit) =  $\frac{Band\ intensity\ of\ PvGW182}{Band\ intensity\ of\ \beta-actin}$ 

Table 2.8 Recipes of a multiplex-PCR reaction for amplifying beta-actin and PvGW182 genes

	1 Reaction set up (25 μl)		
Gene	Component	Volume (μl)	Final conc.
β-actin (550 bp) and PvGW182 (650 bp)	water	17.125	
	10X ThermoPol <i>Taq</i> buffer	2.5	1X

10 mM dNTPs	0.5	0.2 mM
1 μM Actin_F	1.25	0.05 μΜ
1 μM Actin_R	1.25	0.05 μΜ
10 μM PS013GW	0.625	0.25 μM
10 μM PS014GW	0.625	0.25 μM
Taq DNA polymerase	0.125	0.2 Unit
cDNA template	1	

Table 2.9 Thermocycling condition for the multiplex-PCR reaction of β-actin and PvGW182

Thermocycling condition						
Step	Temp (°C)	Time	Cycles			
Initial denaturation	95	5 min	1			
Denaturation	95	30 s				
Annealing	60	30 s	30			
Extension	68	45 s				
Final extension	68	5 min	1			

The PCR products were analyzed by 1.5% agarose gel electrophoresis with ethidium bromide staining. Band intensity was quantitated using the Scion Image software (version 4.0.2) before calculating relative expression (Equation 3.2).

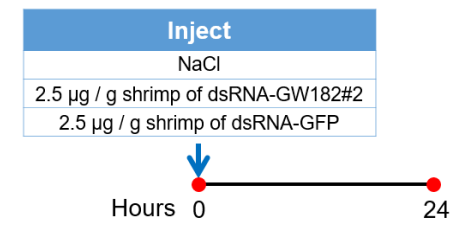
## 2.10 Virus challenge

To observe how GW182 mRNA expression level was altered upon virus infection, shrimp (2-3 g) were injected intramuscularly with 100  $\mu$ l of a 10<sup>-5</sup> dilution of WSSV or 10<sup>-7</sup> dilution of YHV stock in 150 mM NaCl that resulted in 100% shrimp mortality 4-5 days. 100  $\mu$ l of 150 mM NaCl injection was used as an injection control group. After injection, gills of control and virus injection groups were collected for RNA purification as described above. The resulting total RNAs were stored at -80°C for later analysis of  $\beta$ -actin, GW182, VP28 and YHV helicase expression.

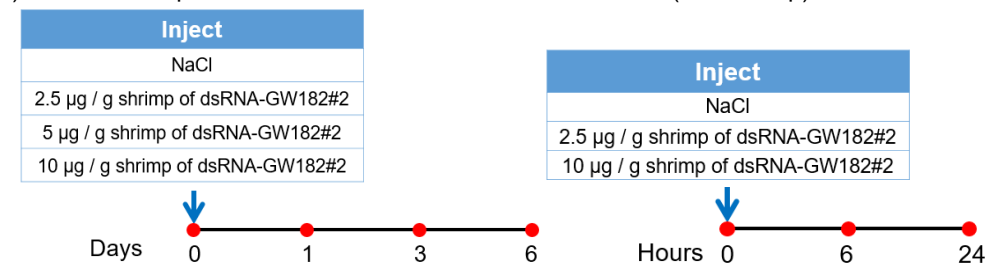
#### 2.11 Injection of dsRNAs

Shrimp (2-3 g) were injected with 100  $\mu$ l of the dsRNA-GFP or dsRNA-GW182 in 150 mM NaCl at specific concentrations according to Figure 2.4. A control group was injected with 100  $\mu$ l of 150 mM NaCl. The final concentration of dsRNAs depended on each experiment (Figure 2.4). Gills of the control shrimp and the dsRNA-injected shrimp were collected for RNA purification as described above. The resulting total RNAs were stored at -80°C for later analysis of GW182 gene.

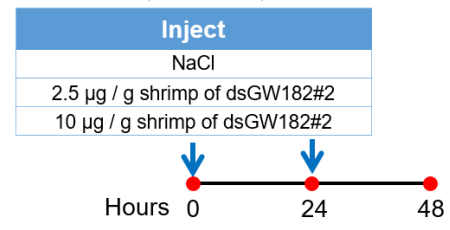
a) Test dsRNA-GW182 specific knockdown PvGW182 gene (40 shrimp)



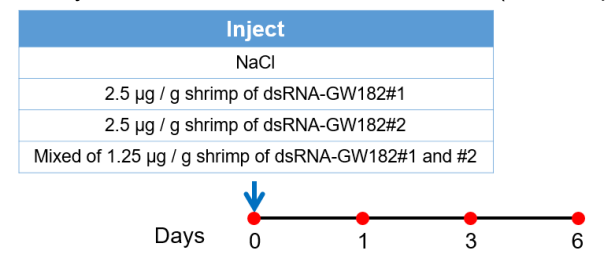
b) Time-dose dependent of dsRNA-GW182#2 concentrations (100 shrimp)



c) Double injection of dsRNA-GW182#2 (40 shrimp)



d) Test knockdown efficiency of two dsRNA-GW182 constructions (75 shrimp)



e) Time-course of PvGW182 mRNA suppression by dsRNA-GW182#1 (35 shrimp)

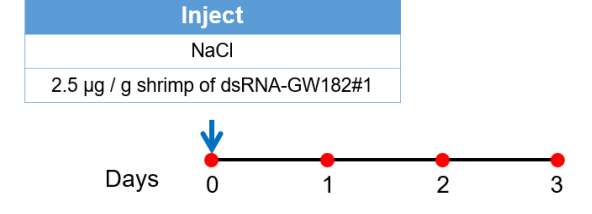


Figure 2.4 A schematic of injection plans for PvGW182 gene suppression. 2-3 g of shrimp were used in these experiments. Sample collection points are shown as red dots.

## 2.12 Injection of dsRNA-GW182#1 and YHV challenge

Shrimp (2-3 g) were injected with 100  $\mu$ l of the 2.5  $\mu$ g/g shrimp of dsRNA-GFP or dsRNA-GW182. A control group was injected with 100  $\mu$ l of 150 mM NaCl. Three day later, all shrimp were injected with 10<sup>-7</sup> dilution of YHV. Gills were collected at specific time points (Figure 2.5) for RNA purification as described above. The resulting total RNAs were stored at -80°C for later analysis of GW182 gene,  $\beta$ -actin and YHV helicase.

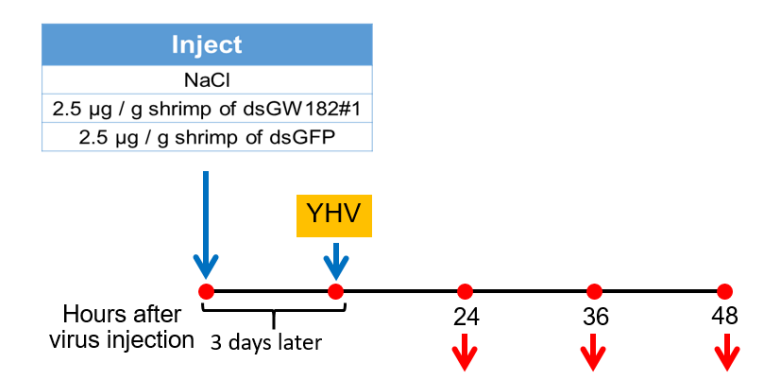


Figure 2.5 A schematic of injection plans for PvGW182 gene suppression and challenge YHV. A blue arrow represents injection. A red arrow represents collection samples.

## 2.13 Statistical analysis

Both PCR and mortality results were statistically analyzed by GraphPad Prism 7 software. Student t-test was used for analysis. The data were performed as mean ± standard error (Standard error of mean, SEM).

## 3 Results

## 3.1 Cloning of a full-length open reading frame (ORF) of PmGW182



makn nsk picdpnpll scqdvlsv pssgdlgfy alsake cvdd clvsplsvs ssgssdte af slivk ccvgggl cirm dshceah qantvtnlpn pefpt nkvpdt std nsk picdpnpll scqdvlsv pssgdlgfy alsake cvdd clvsplsvs ssgssdte af slivk ccvgggl cirm dshceah qantvtnlpn pefpt nkvpdt std nsk picdpnpll scqdvlsv pssgdlgfy alsake cvdd clvsplsvs ssgssdte af slivk ccvgggl cirm dshceah qantvtnlpn pefpt nkvpdt std nsk picdpnpll scqdvlsv pssgdlgfy alsake cvdd clvsplsvs ssgssdte af slivk ccvgggl cirm dshceah qantvtnlpn pefpt nkvpdt std nsk picdpnpll scqdvlsv pssgdlgfy alsake cvdd clvsplsvs ssgssdte af slivk ccvgggl cirm dshceah qantvtnlpn pefpt nkvpdt std nsk picdpnpl scqdvlsv pssgdlgfy alsake cvdd clvsplsv ssgssdte af slivk ccvgggl cirm dshceah qantvtnlpn pefpt nkvpdt std nsk picdpnpl scqdvlsv pssgdlgfy alsake cvd clvsplsv ssgssdte af slivk ccvgggl cirm dshceah qantvtnlpn pefpt nkvpdt std nsk picdpnpl scqdvlsv pssgdlgfy alsake cvd clvsplsv ssgs psgdlgfy alvetfgmvceaqserdvdhkssssqsilsvddtaevaanetsnvpvssagrespvtdggadgaradpylppqpvkslsvifsstplhghfstasphissgdeepqgtsg psrpssttapgspglggslrgmpitpsgqqgvvktvaassqccvgeaeasctthvlhntsqpaqqpvaavaqaaahtqaslnipgsmannnansqlqgsnpsfnqe tkqaiasllqisatcnqyasfptsskfqaagkpgkfgfasfphgfikvnr<mark>WG</mark>iprglglvgggesaan<mark>gWG</mark>tsapqta<mark>gWG</mark>ssganqagsqgq<mark>WG</mark>gapnraggap nt spg qggslk paqqn sgp sqqps spag qqnt qt ggt ggq qgp agvnn qqqt qqgn sgq ggn snntwa qaagk gl pag sg sgd aqkrhme qql qsirealls squared by the squared squar $e\underline{g\textbf{WG}} genvnqettwd|pgspepckdanaph|k|nvnngcd|wenn|rnggaappktqqap \\ \textbf{WG} htpatnyggt\\ \textbf{Wg} edddatdssnvwtgvpsnnpq\\ \textbf{WG} ant$ pnppnm<mark>WG</mark>ggappkknsewaaggsgtgggntqs<mark>gWG</mark>dhgpqrsgvenppse<mark>WG</mark>pggphkpgphvgphagphshsgphsgphsgphsgshgglhsg  $hhvgphsgphntphgaphngphsgshtgphgphgphgphgphgaphgnlthsgppggpggptqwngpkdmkpsgpvgaps\textcolor{red}{\textbf{GW}} eepspptqrrddgt$ av<mark>WG</mark>npqqqanvsrwkempnpnmmgrpnmpgpqqgrmpgppvppgikpdqrm<mark>WG</mark>qhgrngswsdpphdtgsgm<mark>WG</mark>eepksg<mark>gWG</mark>eppitsps WGtkpktptggpvgpgWGetdmelqgWGhqnkkedieaalrnnnmglddtlmelsnrgiagmggssagdawrnppleehapfdltnpnfqqrfpptlhhlpftnq qgssgnsp<mark>hyralmqhiqmayqaqylnpqilnqplapst|m||nnm|s</mark>hinmlqkftqqqaiwqaqahinknssqt||shvsitktkqqiqn|qnqiaaqqalyvkqqq qhqhhhqqlnshmtggppgtqndffnkpslpdqlcssfdflavnnnpaiinvgqqqgsrlhqwklpslendepdfirapgapgkpsmpqsqsspnltpllgpsnstward frameword and the state of the statsInrtses<mark>gw</mark>pesssggsvdvannpgvekvvpnmdsrwvassqanasgsygldikpfepgkpwmmknieddpnitpgsvtqsplalgikesvdllssisktsttnta sdmagplts fsltsntws fnpgpghhaansplsgdnklssgtngksgsawnessqggsnnlasel WGapgnklrgpppgmsvgssnnkigvgvsggs WGalgrick for the state of the s $stswsgeqqrnppssalhsaavvaapgawtnsqlpsqlp{\underline{stwlii}} rnltpqidgstlktlcmqhgplvnfylslnhgfalvnygsreeaakaqgnlnncllsnttilaefand$ sevkqvmgqpthqgqaapptpgptnassWGxsgrgstptsqssggskvdsWGngnssnlwssgpggssslwsxanigegdphratpsslkpylpdglltses m

Figure 3.1 The amino acid sequence of *P. monodon* GW182. The GW/WG repeats, M-domain and RRM domain are highlighted in yellow, pink and blue respectively

The amino acid sequence of *P. monodon* GW182 obtained from this study (Figure 3.1) contains 19 GW/WG repeats that are characteristic of proteins in this family in the N-terminus followed by a middle "M" domain and a C-terminus RRM domain. The M-domain was used as a target site of dsRNA#1.

## 3.2 Sequence and phylogenic analysis

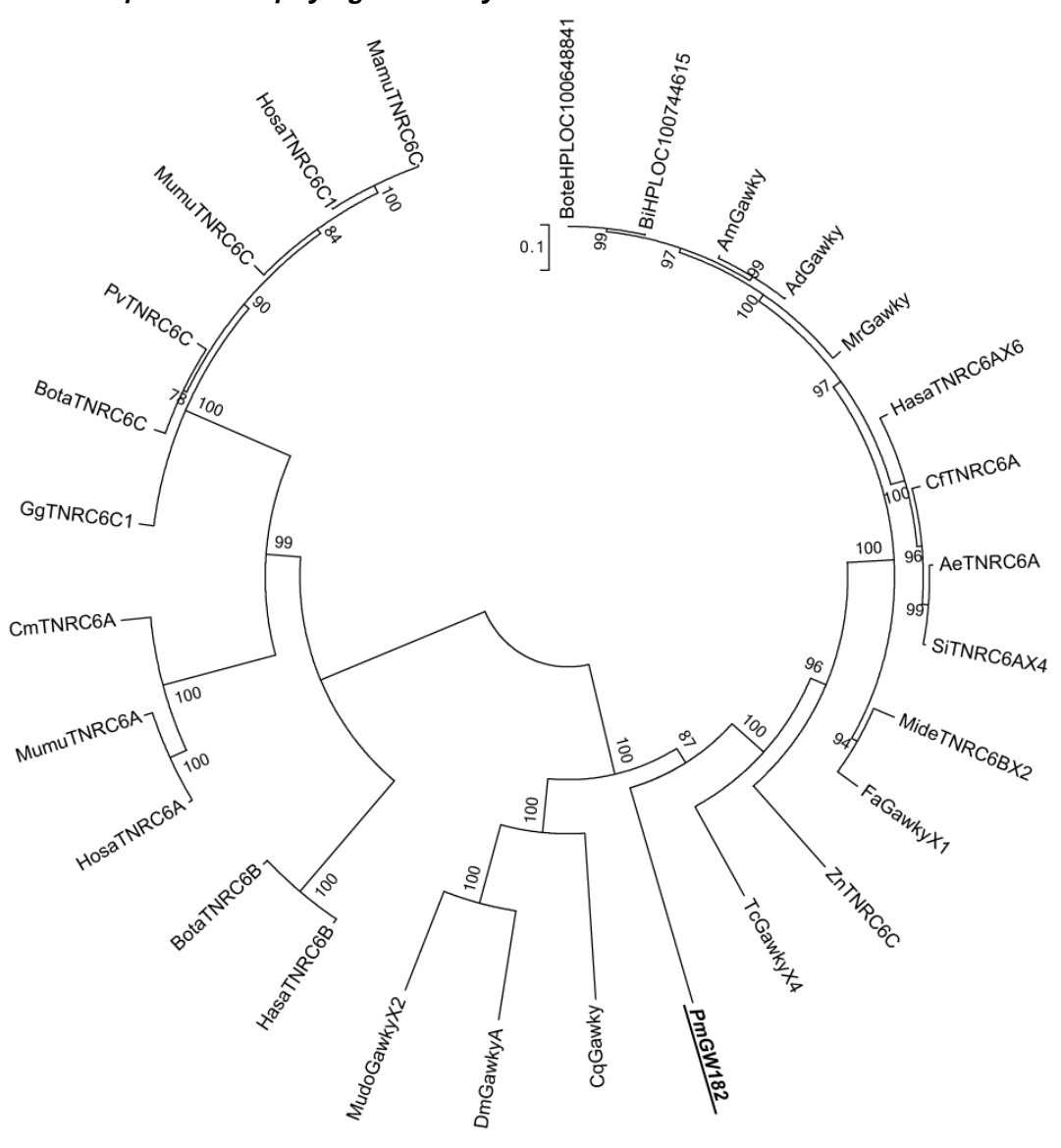


**Figure 3.2 Phylogenetic tree of GW182.** Multiple sequence alignment of the full-length GW182, also known as TNRC6A, TNRC6B, TNRC6C and Gawky was performed by ClustalW. The neighbor-joining tree was constructed by MEGA 5.05 programs. Bootstrap values from 1000 replicates are indicated at the nodes. Abbreviations are listed in Table 3.1

Species	Proteins		Abbreviations	Gene ID
Acromyrmex	TNRC6A		AeTNRC6A	332026373
Apis dorsata	Protein Gawky-like		AdGawky	572313755
Apis mellifera	Protein Gawky-like, p	artial	AmGawky	571575378
Bombus impatiens	Hypothetical	protein	BiHPLOC100744615	350414279
Bombus terrestris	Hypothetical	protein	BoteHPLOC100648841	340727004
Bos taurus	TNRC6B		BotaTNRC6B	300798505
	TRNC6C		BotaTRNC6C	297487379
Camponotus	TRNC6A		CfTRNC6A	307185285
Chelonia mydas	TRNC6A		CmTRNC6A	465985792
Culex	Gawky		CqGawky	167871061
Drosophila	Gawky, isoform A		DmGawkyA	22759367
Fopius arisanus	Gawky, isoform X1		FaGawkyX1	755941666
Gallus gallus	TNRC6C, isoform 1		GgTNRC6C1	363740794
Harpegnathos saltator	TNRC6A, isoform X6		HasaTNRC6AX6	749786937
Homo sapiens	TNRC6A		HosaTNRC6A	116805348
	TNRC6B		HosaTNRC6B	229904901
	TNRC6C, isoform 1		HosaTNRC6C1	217416332
Macaca mulatta	TNRC6C		MamuTNRC6C	386781810
Megachile rotundata	Protein Gawky-like		MrGawky	383860126
Microplitis demolitor	TNRC6B, isoform X2		MideTNRC6BX2	665811907
Mus musculus	TNRC6A		MumuTNRC6A	117190552
	TNRC6C		MumuTNRC6C	124378035
Musca domestica	Gawky, isoform X2		MudoGawkyX2	755885525
Penaeus monodon	Gawky		PmGW182	This study
Pteropus vampyrus	TNRC6C		PvTNRC6C	759125534
Solenopsis invicta	TNRC6A, isoform X4		SiTNRC6AX4	751215275
Tribolium castaneum	Gawky, isoform X4		TcGawkyX4	642933103
Zootermopsis	TNRC6C		ZnTNRC6C	646705102

Table 3.1 Proteins in the GW182 family used for multiple sequence alignment and phylogenetic analysis

## 3.3 Tissue distribution study of GW182

A region of 162-nucleotide long in the 3' RACE fragment was selected as a template for a semiquantitative PCR to determine tissue distribution pattern of GW182 in *P. monodon*. It was found that GW182 express in every tissue used in the study at comparable level across all tissues.

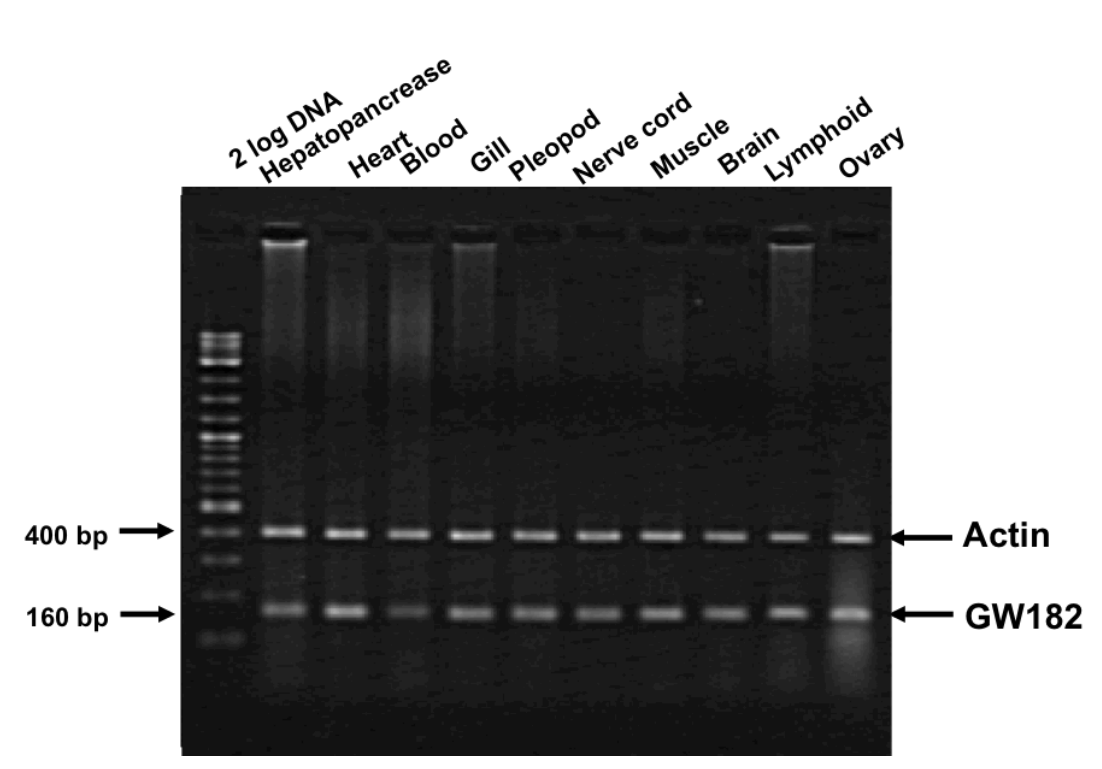


Figure 3.3 Tissue distribution of GW182.

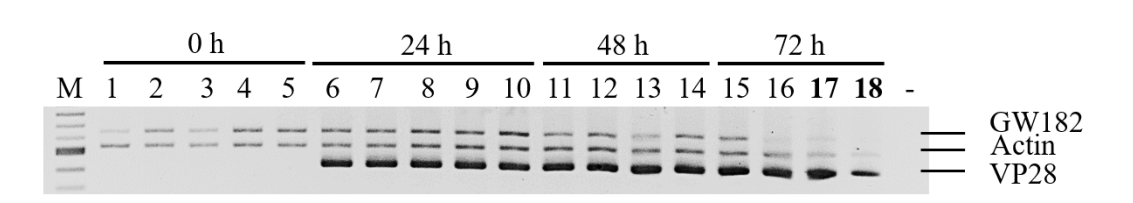
## 3.4 Expression profile of PvGW182 mRNA during virus infection

## 3.4.1 PvGW182 mRNA expression profile during WSSV infection

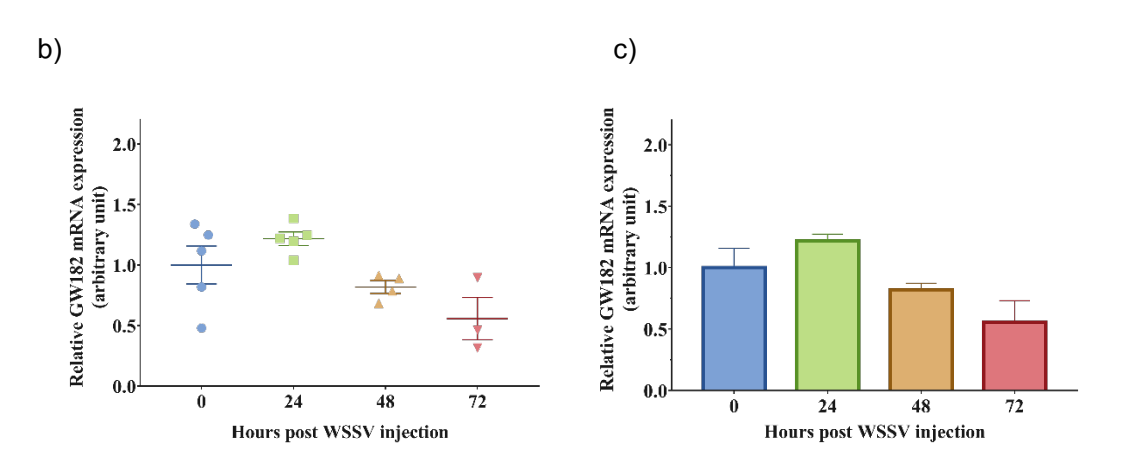
To study the effect of WSSV infection on the expression of PvGW182, shrimp were injected with WSSV. Total RNAs were extracted from gills and treated with DNase prior converting to cDNA. Then, multiplex PCR detection of an internal control  $\beta$ -actin gene and PvGW182 was performed (Figure 3.4). Successful amplification of the  $\beta$ -actin gene with the amplicon size of 550 bp indicated that the RNA samples were intact. The equal intensity of the bands of the  $\beta$ -actin amplicon in each sample was indicative of an equal amount of the added RNA template. Amplification of WSSV VP28 gene, used to follow the infection, showed that WSSV was detectable at 24 hpi.

The first experiment for studying the alteration of PvGW182 mRNA level during WSSV infection was to compare the relative expression level of PvGW182 with the pre-injection group (0 hpi) (Figure 3.4a-c). Since shrimp gills were collected individually and the PvGW182 mRNA expression could be varied, the experiment should have an injection control (NaCl group) in every time points. Therefore, the second experiment was performed and the relative expressions level of PvGW182 mRNA were compared between WSSV challenge and NaCl injection groups at 12, 24 and 48 hpi (Figure 3.4d-f).

Even though the relative PvGW182 mRNA levels were analyzed differently, the results from these experiments displayed a similar trend. At 72 hours post injection (hpi), there were a few samples from which the intensity of the  $\beta$ -actin band was low. This indicates that the RNA samples from dead shrimp had already degraded during collection. Using the expression level of  $\beta$ -actin to normalize the expression level of PvGW182, the result shows that, despite the slight upregulation of PvGW182 at 24 hpi, the statistical analysis by the student t-test method that compared the WSSV-injected group to the NaCl-injected group at individual time-points indicated that the difference is not statistically significant (Figure 3.4). Therefore, the PvGW182 mRNA level was not altered during WSSV infection.



a)



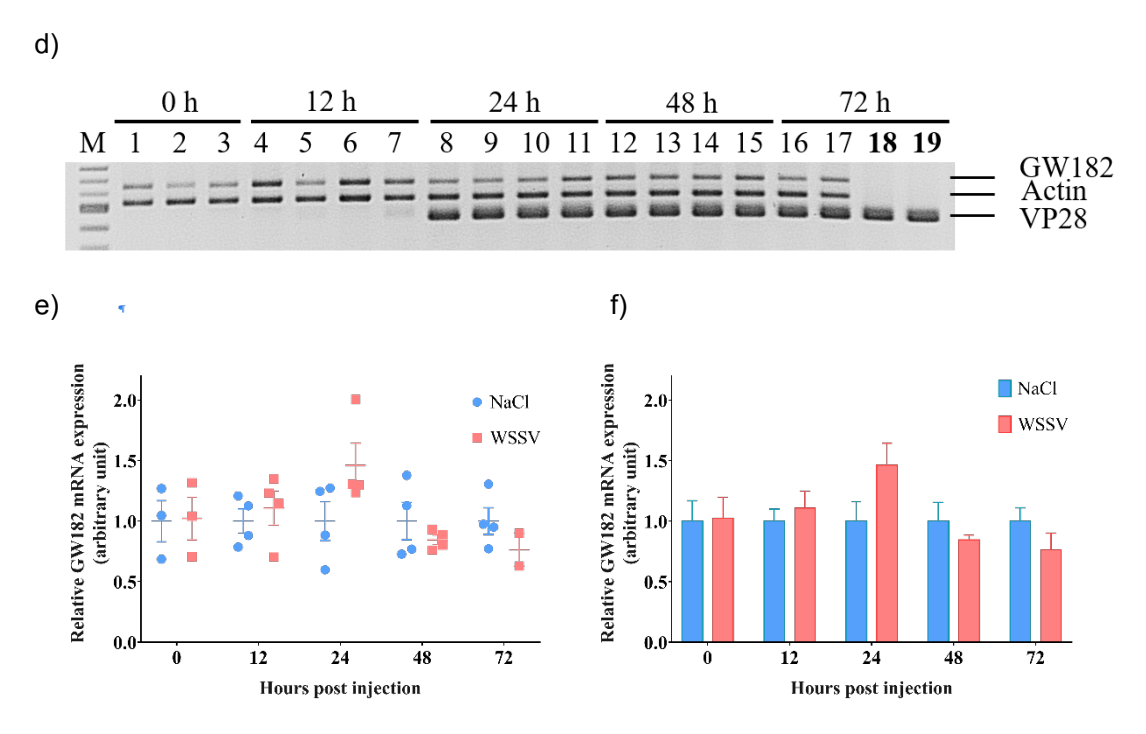


Figure 3.4 Time-course expression profile of PvGW182 in gills after WSSV challenge at various hours post injection from two independent experiments. (a-c) shows results from the first experiment, while (d-f) shows results from the second trial. (a, d) 1.5% agarose gels stained with ethidium bromide shows RT-PCR products for PvGW182 (650 bp),  $\beta$ -actin (550 bp) and VP28 (420 bp) at various times post WSSV challenge from each experiment. Bold number represents samples collected from dead shrimp. Quantification of band intensity from the agarose gel. (b, e) The scatter plot represents the relative PvGW182 expression in individual shrimp at the various time points. (c, f) The bar graph represents the average relative PvGW182 expression in an arbitrary unit (mean  $\pm$  SEM) in WSSV challenge compared (b, c) with shrimp at 0 hours and (e, f) with NaCI-injected shrimp.

## 3.4.2 <u>PvGW182 mRNA expression profile during YHV infection</u>

To study whether the PvGW182 expression level changes during YHV infection, shrimp were injected with YHV. Then, shrimp gills were collected at various time points. Total RNAs were extracted and converted to cDNA templates. Multiplex-PCR of  $\beta$ -actin and PvGW182 was performed to determine the mRNA level of the internal control and PvGW182 expression, while singleplex PCR of YHV helicase was used for YHV detection (Figure 3.5). The  $\beta$ -actin bands appeared at an expected intensity and size of approximately 550 bp in every lane indicating that the qualities and quantities of collected samples were good.

The results showed that the helicase gene of YHV was first found in shrimp at 24 hpi and the band intensity increased during the course of infection. The relative expression of PvGW182 was calculated in an arbitrary unit compared with the NaCl group. The bar graph represents an average PvGW182 expression in each group (Figure 3.5). Statistical analysis by the student t-test method revealed that the PvGW182 mRNA expression level was significantly increased at 24 hpi upon YHV infection (p < 0.05).

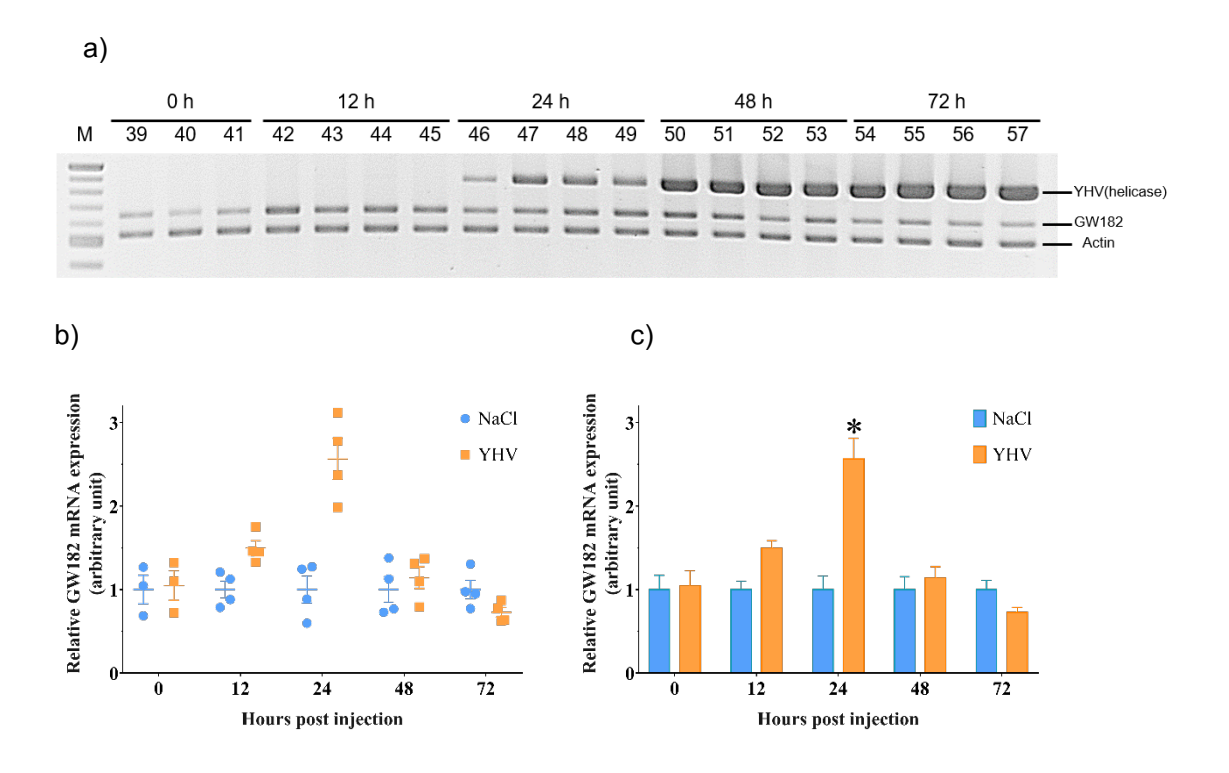


Figure 3.5 Time-course expression profiles of PvGW182 in gills after YHV challenge at 12, 24, 48 hpi. (a) The PCR reactions were analyzed by 1.5% agarose gels stained with ethidium bromide shows RT-PCR products for PvGW182 (650 bp),  $\beta$ -actin (550 bp) and YHV helicase (850 bp) at various times post YHV challenge. Quantification of band intensity from the agarose gel. (b) The scatter plot represents the relative PvGW182 expression in individual shrimp at the various time points. (c) The bar graph represents the average relative PvGW182 expression in an arbitrary unit normalized with  $\beta$ -actin (mean  $\pm$  SEM) in YHV challenge compared with the NaCl group at each time point. The asterisk (\*) represents the significant difference from student t-test statistical analysis with the p-value < 0.01 when compared between NaCl and YHV at specific time point.

## 3.5 Production of dsRNA by in vivo bacterial expression

To investigate the functions of PvGW182 using the RNAi technique, the pET28a-PvGW182#1 and #2 vectors were transformed into the HT115 *E. coli* strain for expressing dsRNA. The expression of hairpin dsRNA-GW182 under the T7 promoter in the HT115 *E. coli* strain was induced by IPTG. After purification of dsRNA by the ethanol extraction method (Posiri et al., 2013), the double-stranded nature of the resulting RNA was verified by a RNase digestion assay. DsRNA should only be cleaved by a dsRNA-specific RNase III, but not RNase A which specifically cleaves ssRNAs after the 3'end of unpaired C and U residues. The RNase digestion reactions were analyzed by 1.5% agarose gel electrophoresis (Figure 3.6).

As expected, the resulting dsRNAs were completely cleaved by RNase III (Lane III) giving rise to a low molecular weight nucleic acid band below 200 bp. The slight increase in the migration rate of the band in the RNase A-treated lane confirmed that the dsRNA contains a single-stranded loop that was cleaved by RNase A. Therefore, these results indicated that the synthesized dsRNA was obtained with a good quality.

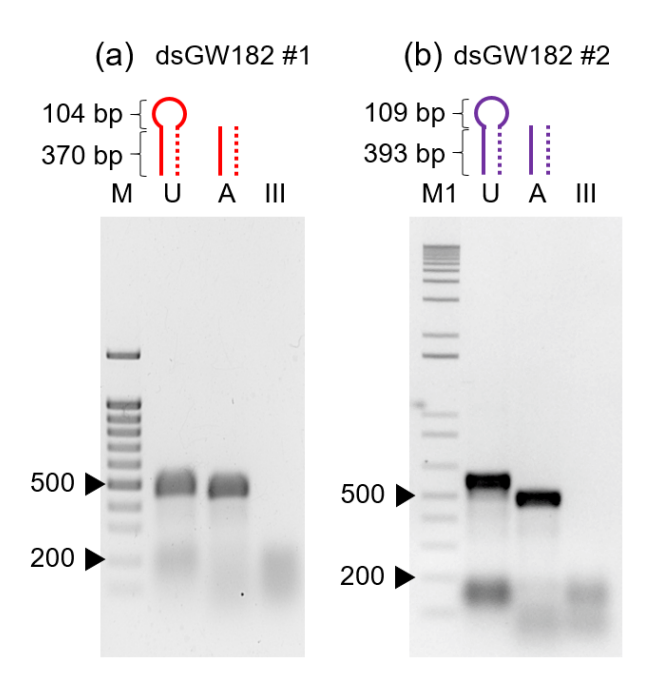


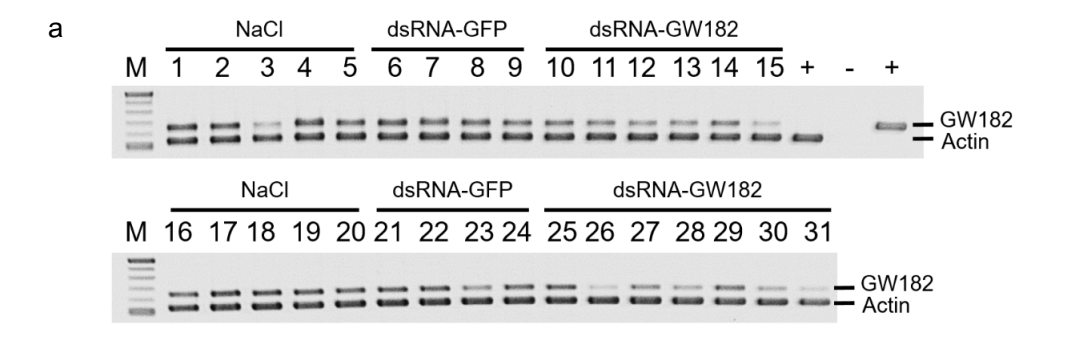
Figure 3.6 1.5% Agarose gel electrophoresis of (a) dsRNA-GW182#1 and (b) dsRNA-GW182#2 from the *in vivo* bacterial expression system. The number on the left side represents DNA-size in a base pair. Abbreviations: U, untreated; A, treated RNase A; III, treated RNase III; M, a 100-bp DNA marker (Siberian Enzyme, Russia); M1, a 1-kb plus DNA marker (New England Biolabs, USA).

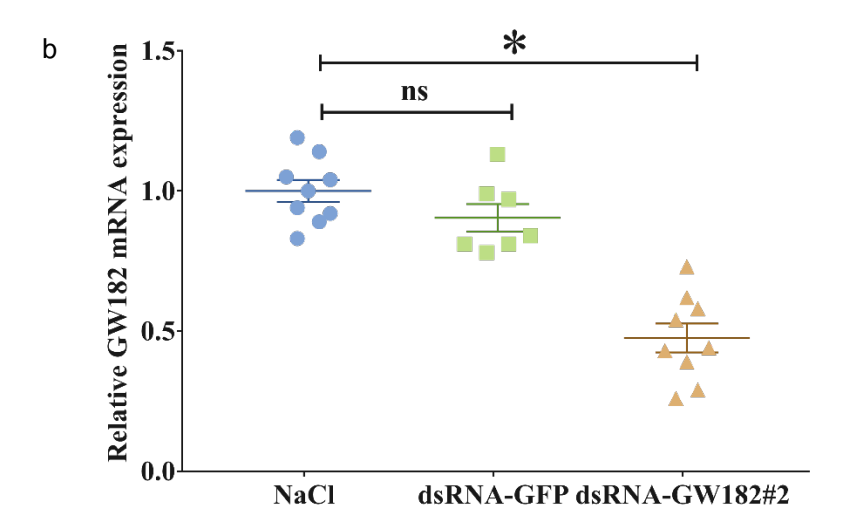
500 bp of 100 bp DNA ladder.

## 3.6 Knockdown efficiency of PvGW182 by specific dsRNA targeting GW182 gene

## 3.6.1 Suppression of PvGW182 by specific dsRNA targeting GW182 gene

Since the yield of the dsRNA-GW182#2 was higher than the dsRNA-GW182#1, the dsRNA-GW182#2 was first used as a dsRNA specific to GW182 to suppress PvGW182. Shrimp were injected with 150 mM NaCl, 2.5  $\mu$ g/g shrimp of dsRNA-GFP or dsRNA-GW182#2 and collected gills at 24 hpi (Figure 3.7). The result showed that between NaCl and dsRNA-GFP injected group, there was no difference of PvGW182 expression, whereas the injection of dsRNA-GW182#2 suppressed the PvGW182 mRNA level by about 50% compared to NaCl group. This indicated that PvGW182 mRNA level can be suppressed specificically by dsRNA targeting GW182 gene, not by any dsRNA.





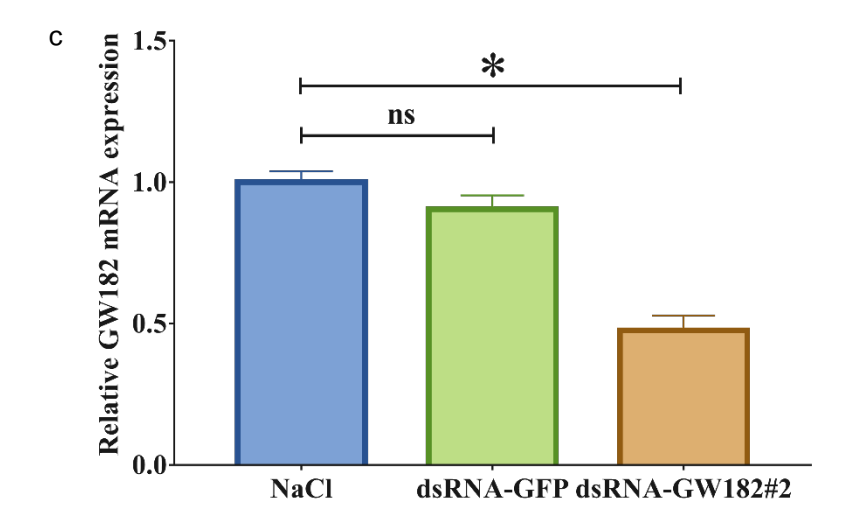


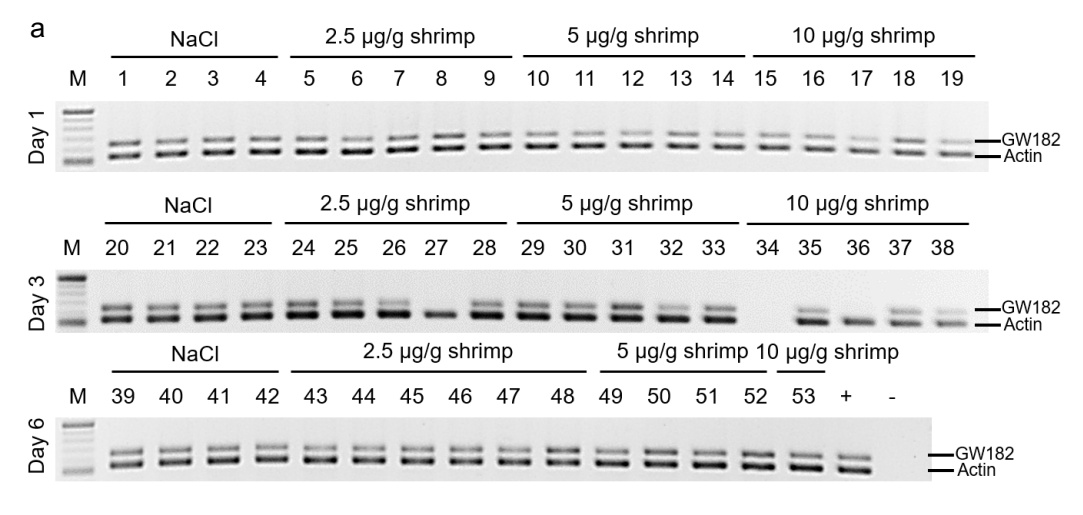
Figure 3.7 Comparison of PvGW182 mRNA expression level in gills after 24 hours post injection with NaCl (blue), dsRNA-GFP (green) or dsRNA-GW182#2 (orange). (a) The PCR reactions were analyzed by 1.5% agarose gels stained with ethidium bromide shows RT-PCR products for PvGW182 (650 bp) and  $\beta$ -actin (550 bp) at 24 hpi. Quantification of band intensity from the agarose gel. (b) The scatter plot represents the relative PvGW182 expression in individual shrimp at 24 hpi. (c) The bar graph represents the average relative PvGW182 expression normalized with  $\beta$ -actin (mean  $\pm$  SEM) in dsRNA groups compared with the NaCl group. The asterisk (\*) represents the significant difference from student t-test statistical analysis with the p-value < 0.001.

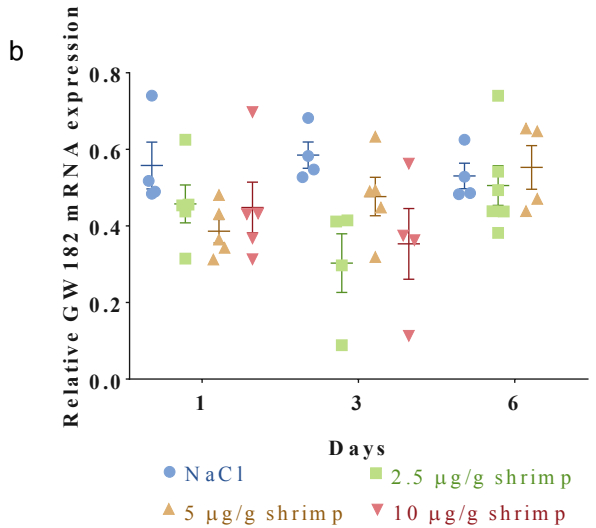
#### 3.6.2 Time- and dose- dependent on dsRNA-GW182#2

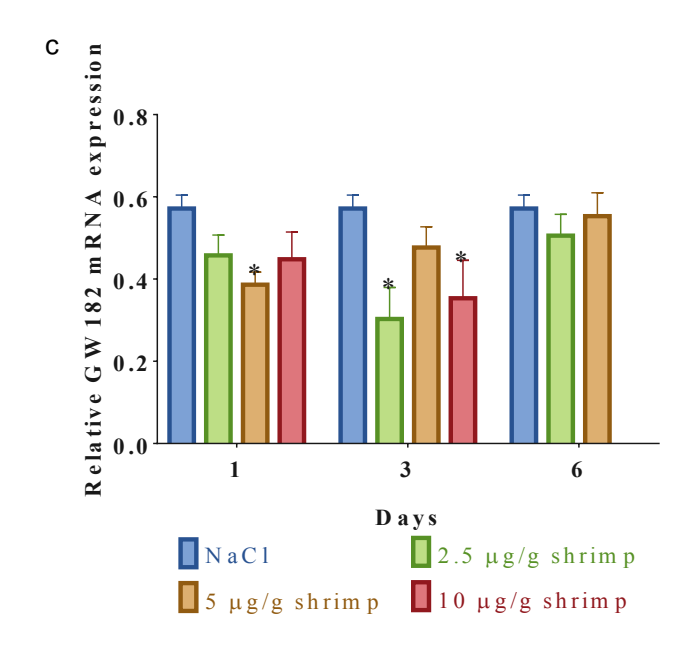
To investigate whether the efficiency of knockdown PvGW182 can be improved by increasing the dose of dsRNA-GW182. Shrimp were injected with NaCl and various concentrations of dsRNA-GW182#2 including 2.5, 5 and 10  $\mu$ g/g shrimp. Gills were collected at 1, 3 and 6 dpi and also performed a cumulative mortality assay. Overall, the result revealed that an increasing of dsRNA-GW182#2 dosage could not improve the knockdown efficiency. The injection of 2.5  $\mu$ g/g shrimp of dsRNA-GW182#2 showed the highest efficiency about 48% after 3 days post injection compared with NaCl injection. Meanwhile, the higher doses of dsRNA-GW182#2 showed no enhancement of knockdown efficiency. Instead, they increase the shrimp mortality.

The cumulative mortality of shrimp injected with the higher doses reached 50% cumulative mortality within 4-5 days compared to more than 5 days for those injected with lower doses. This indicated that not only did the higher dose of dsRNA fail to enhance the knockdown efficiency, it was also toxic to shrimp.

To further investigate whether the higher dose of dsRNA-GW182#2 injection can improve knockdown efficiency, shrimp were injected with two concentrations of dsRNA-GW182#2 including a low dose of 2.5  $\mu$ g/g shrimp and a high dose of 10  $\mu$ g/g shrimp. Then, gills were collected at 6 and 24 hpi. The results showed that at 6 hpi the administration of a high dose of dsRNA-GW182#2 significantly suppressed PvGW182 expression approximately 25% and at 24 hpi, the PvGW182 mRNA expression was suppressed 36% and 22% by the dose of 2.5  $\mu$ g/g shrimp and 10  $\mu$ g/g shrimp, respectively. This suggested that the high dose injection showed suppressed PvGW182 expression faster than the lower dose, however; the high dose of dsRNA-GW182#2 could not improve the knockdown efficiency.







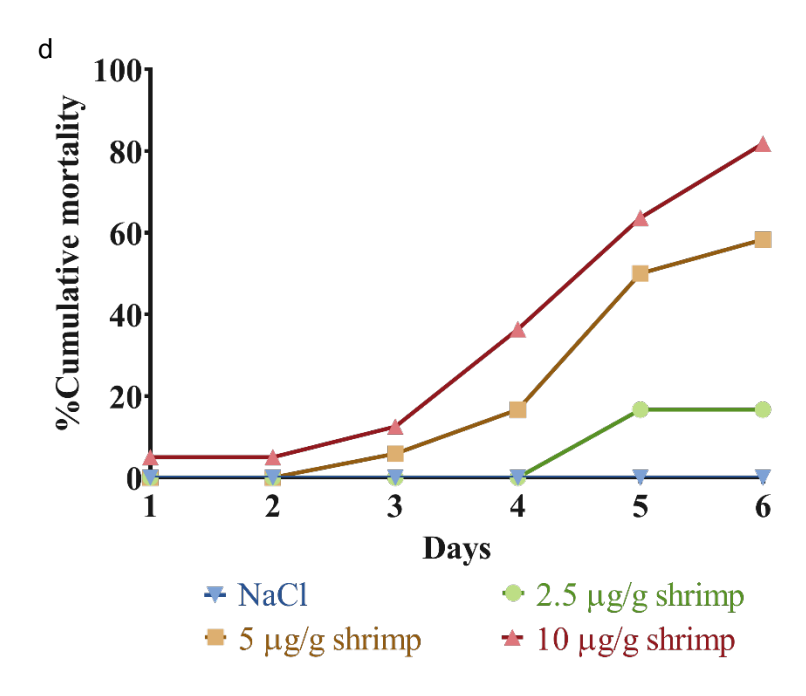


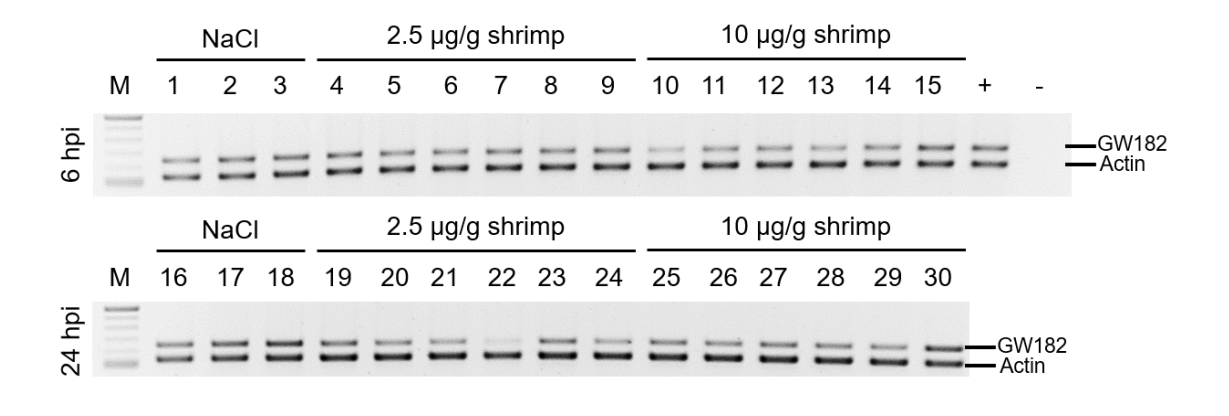
Figure 3.8 Time- and dose- dependent of PvGW182 expression profile in gills after injection of various concentration of dsRNA-GW182#2 at 1, 3 and 6 days post injection. (a) 1.5% agarose gels stained with ethidium bromide shows RT-PCR products for PvGW182 (650 bp) and  $\beta$ -actin (550 bp) at various times post injection. Quantification of band intensity from the agarose gel. (b) The scatter plot represents the relative PvGW182 expression in individual shrimp at the various time points. (c) The bar graph represents the average relative PvGW182 expression normalized with  $\beta$ -actin (mean  $\pm$  SEM) in various concentrations of dsRNA-GW182#2 groups compared with the NaCl group. The asterisk (\*) represents the significant difference from student t-test statistical analysis with the p-value < 0.05. (d) The %cumulative shrimp mortality of NaCl and the various concentrations of dsRNA-GW182#2 injections.

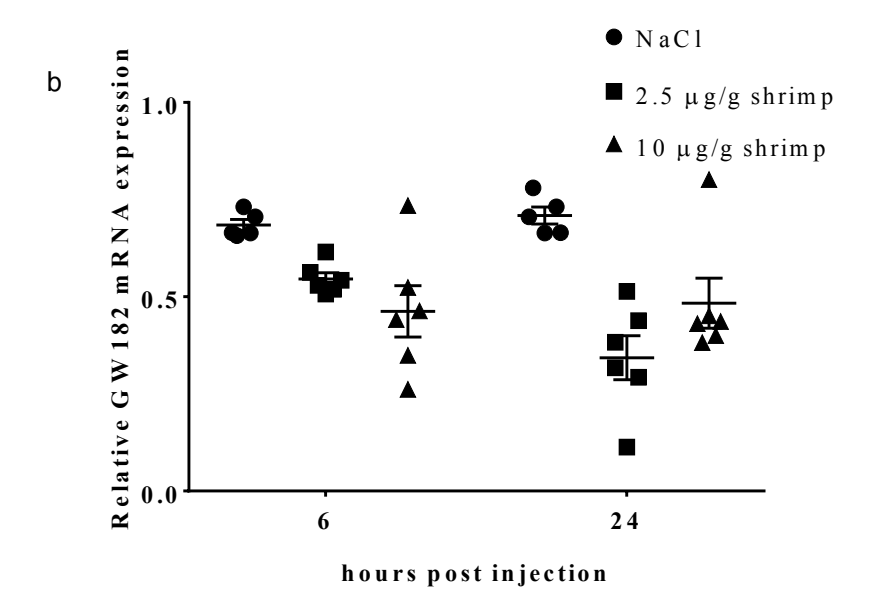
## 3.6.3 Improving the PvGW182 knockdown efficiency by double injection

A double injection of dsRNA-GW182#2 was performed to improve the knockdown efficiency. The PvGW182 mRNA level was compared. Three injection schemes were used: dual injection of NaCl, dual injection of 2.5  $\mu$ g/g shrimp or dual injection of 10  $\mu$ g/g shrimp. The results showed that at 24 h after the first injection, the PvGW182 in shrimp receiving 2.5  $\mu$ g/g shrimp of dsRNA-GW182#2 was significantly suppressed about 40%. Unfortunately, the dual injection with either 2.5  $\mu$ g/g shrimp or 10  $\mu$ g/g shrimp of dsRNA-GW182#2 significantly suppressed PvGW182 expression about 20%. This suggested that the double injection does not increase knockdown efficiency.

Together, from the administration of dsRNA-GW182#2 to find the optimal condition, the proper condition to suppress PvGW182 mRNA expression when using dsRNA-GW182#2 is a single injection of 2.5  $\mu$ g/g shrimp of dsRNA-GW182#1. Although, the 36% of the dsRNA-GW182#2 knockdown efficiency still low, the higher injection of dsRNA-GW182#2 more than 2.5  $\mu$ g/g shrimp and the double injection of dsRNA-GW182#2 did not improve the knockdown efficiency.

а





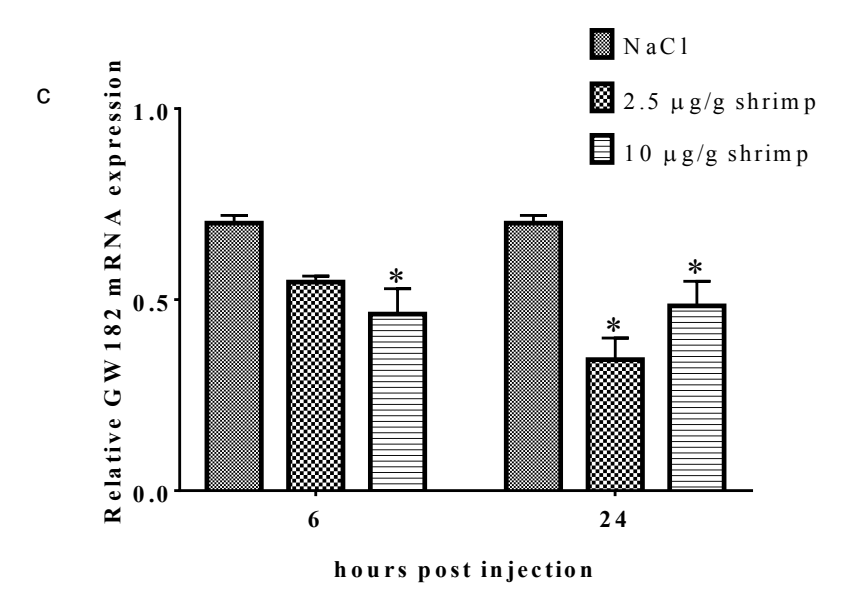
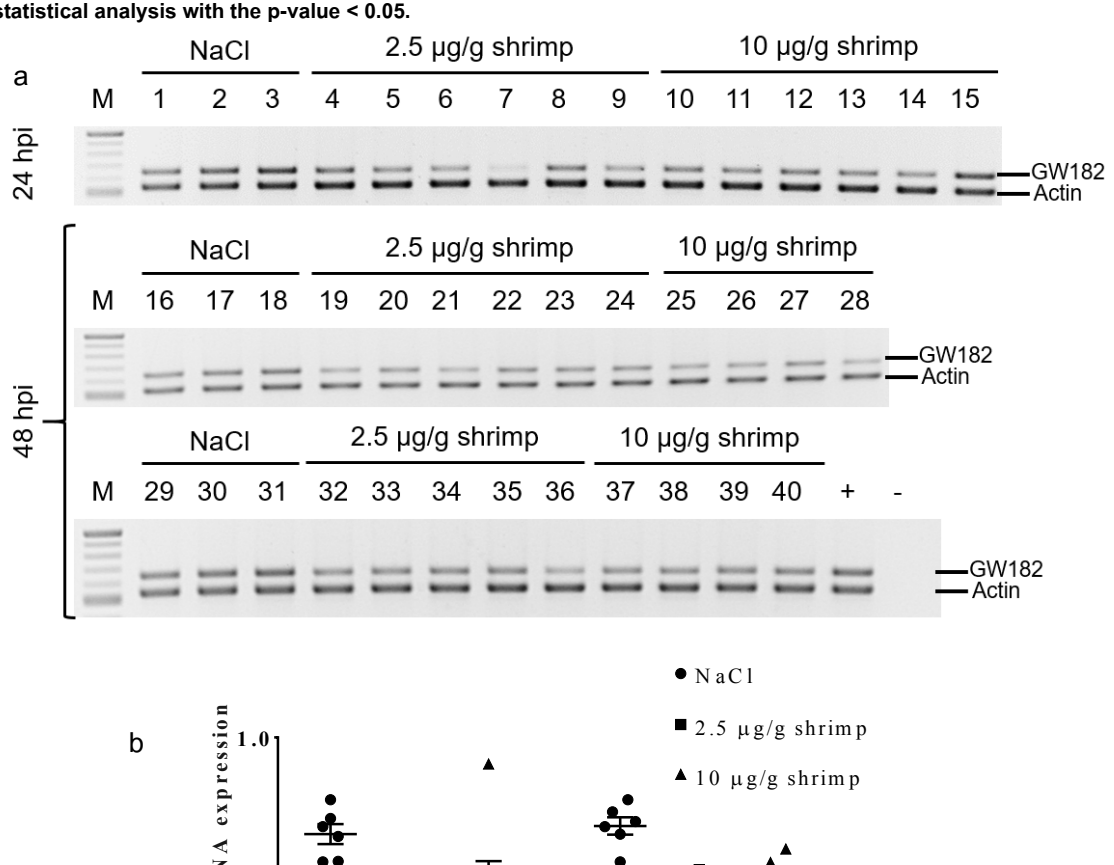
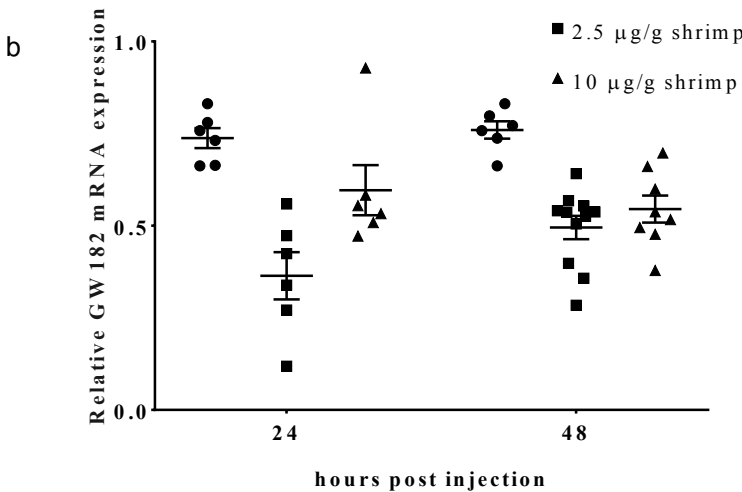


Figure 3.9 Time- and dose- dependent of PvGW182 expression profile in gills after injection of various concentration of dsRNA-GW182#2 at 6 and 24 hours post injection. (a) 1.5% agarose gels stained with ethidium bromide shows RT-PCR products for PvGW182 (650 bp) and  $\beta$ -actin (550 bp) at various times post injection. Quantification of band intensity from the agarose gel. (b) The scatter plot represents the relative PvGW182 expression in individual shrimp at the various time points. (c) The bar graph represents the average relative PvGW182 expression normalized with  $\beta$ -actin (mean  $\pm$  SEM) in various concentrations of dsRNA-GW182#2

groups compared with the NaCl group. The asterisk (\*) represents the significant difference from student t-test statistical analysis with the p-value < 0.05.





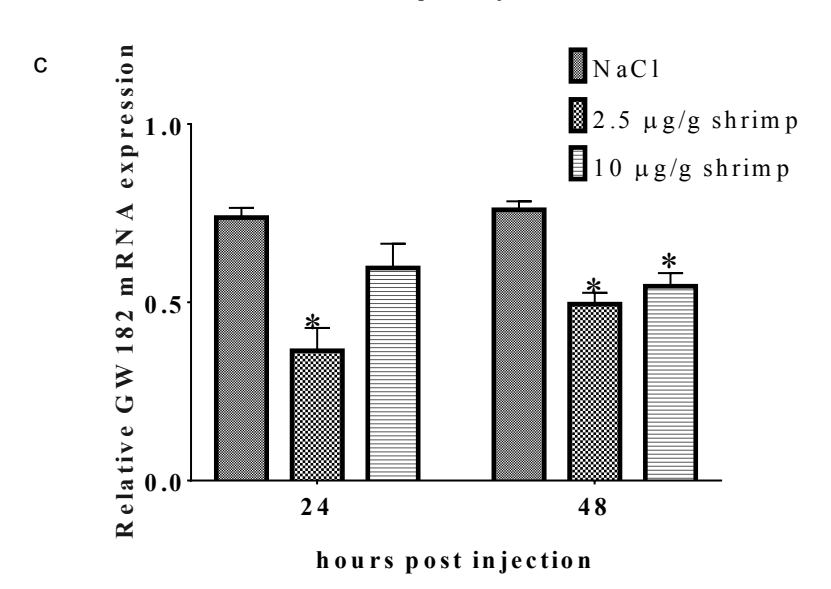
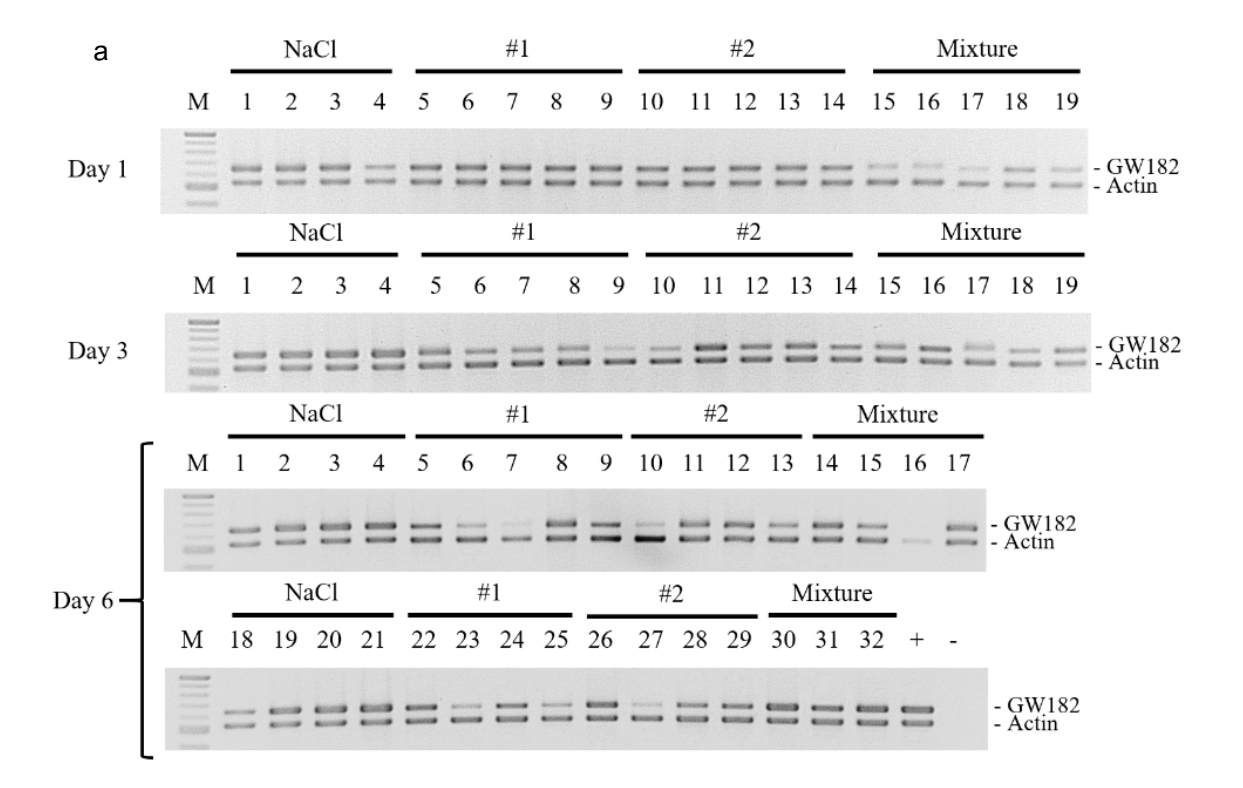


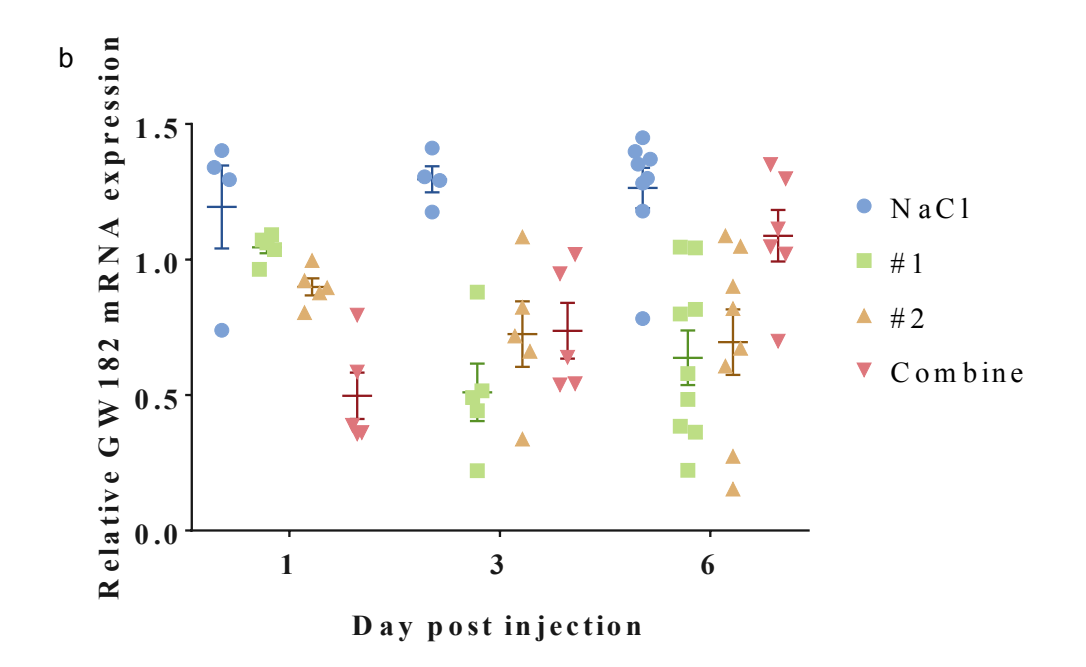
Figure 3.10 Time-dose dependent of PvGW182 expression profile in gills after injection of various concentration of dsRNA-GW182#2 at 24 hours post first injection and 48 hours post first injection (twice injection for 24 hours). (a) 1.5% agarose gels stained with ethidium bromide shows RT-PCR products for PvGW182 (650 bp) and  $\beta$ -actin (550 bp) at various times post injection. Quantification of band intensity from the agarose gel. (b) The scatter plot represents the relative PvGW182 expression in individual shrimp at the various time points. (c) The bar graph represents the average relative PvGW182 expression normalized with  $\beta$ -actin (mean  $\pm$  SEM) in various concentrations of dsRNA-GW182#2 groups compared with the NaCl group. The asterisk (\*) represents the significant difference from student t-test statistical analysis with the p-value < 0.01.

# 3.6.4 <u>Comparison of the PvGW182 knockdown efficiency by two dsRNA-GW182</u> constructions

To compare the knockdown efficiency of two construction, shrimp were injected with 2.5  $\mu$ g/g shrimp of dsRNAs or NaCl as outlined. Gills were individually collected after day 1, 3 and 6 post injection to observe the mRNA level of GW182 (Figure 3.11). The results showed that the 1:1 mixture of dsRNA-GW182#1:dsRNA-GW182#2 partially decreased the level of GW182 expression by approximately 58% after 24 hours of injection. After 3 days, injection of dsRNA-GW182#1 showed suppression of GW182 by approximately 61%, whereas administration of dsRNA-GW182#2 or the dsRNA mixture brought about approximately 44% suppression. At day 6, the expression of GW182 returned to the pre-knockdown level. In the groups injected with dsRNA-GW182#1 or #2, however, the expression of GW182 was still downregulated by approximately 50% (Figure 3.11).

These indicated that either dsRNA-GW182 #1, dsRNA-GW182#2 or the mixture of dsRNA-GW182 could partially knockdown GW182 expression. The dsRNA-GW182#1 provided the highest knockdown efficiency (61%) from the relative GW182 mRNA expression at day 3 after injection (Figure 3.11). While the combinatorial injection approach appeared to be more efficient on day 1, individual dsRNA was more efficient at GW182 suppression at 3 and 6 days. The lower efficiency of dsRNAs mixture might be caused by the half-diluted concentration of each dsRNA. Therefore, the dsRNA-GW182#1 was used for PvGW182 suppression.





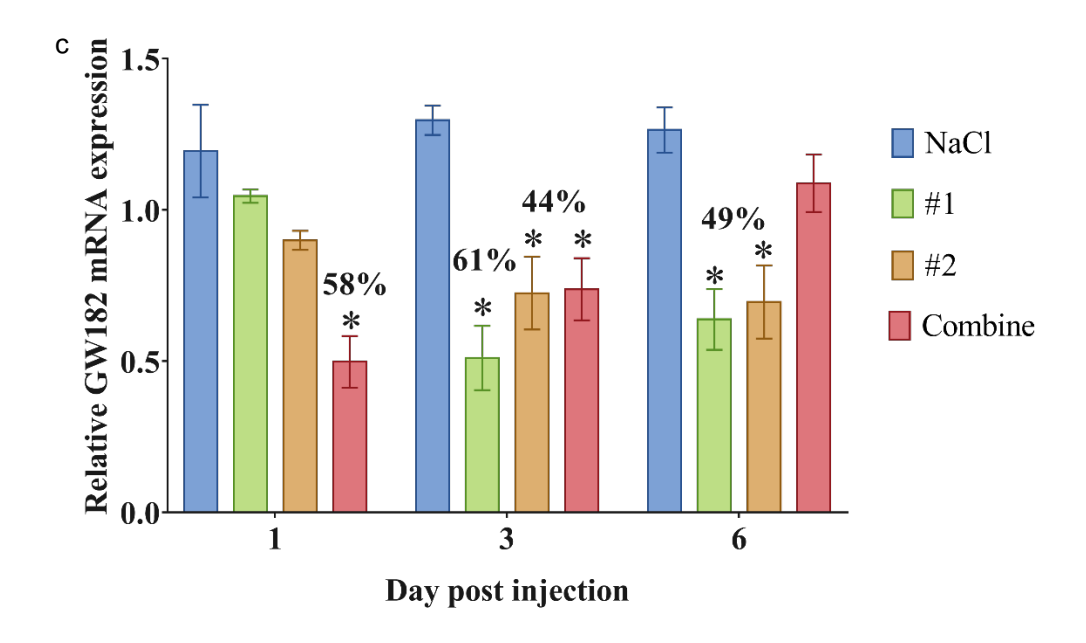
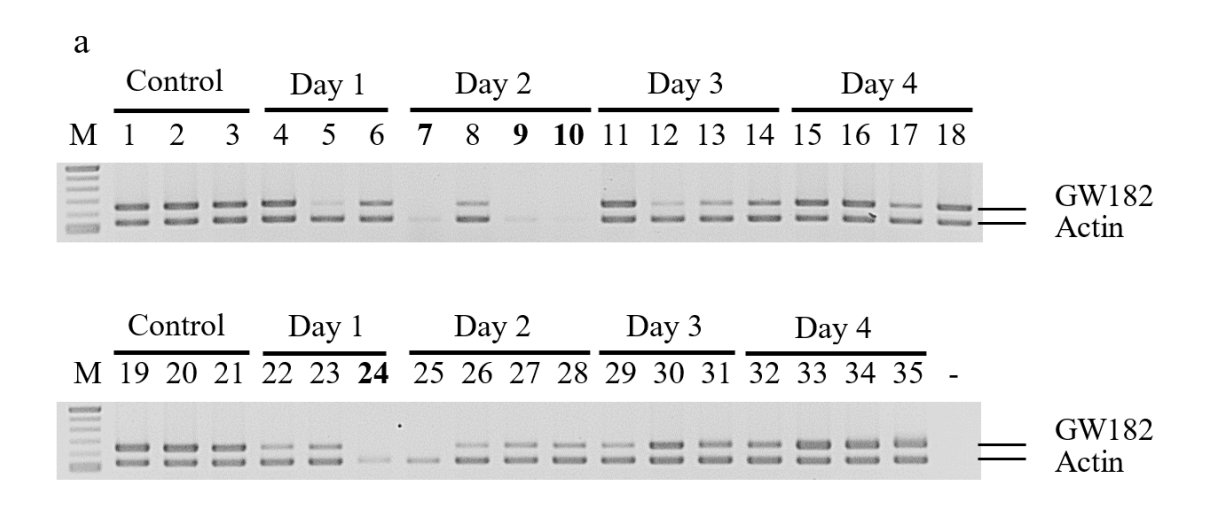


Figure 3.11 Time-course expression profile of PvGW182 in gills response to various constructions of dsRNA-GW182 injection on day 1, 3 and 6. (a) 1.5% Agarose gels of RT-PCR products for PvGW182 and  $\beta$ -actin. The injection of individual dsRNA-GW182#1 and #2 represents as group 1 and 2. Whereas, the injection of 1:1 mixture of dsRNA-GW182#1 and #2 represents as the mixture. (b) The scatter plot represents the relative PvGW182 expression in individual shrimp at the various time points. (c) The bar graph represents the average relative PvGW182 expression normalized with  $\beta$ -actin (mean ± SEM) in the dsRNA-GW182 injection. The asterisk (\*) represents the significant difference from student t-test statistical analysis with the p-value < 0.05. The number above bar represents the percentage of knockdown efficacy.

## 3.6.5 Suppression of PvGW182 using dsRNA-GW182#1 in P. vannamei

Previous experiment revealed that the dsRNA-GW182#1 provided the highest knockdown efficiency. Thus, the dsRNA-GW182#1 was used as a dsRNA specific to GW182.

A time-course effect of PvGW182 suppression by the dsRNA-GW182#1 was performed to observe a long-term knockdown efficiency. Shrimp were injected with 2.5 µg/g shrimp of the dsRNA-GW182#1. The monitoring of PvGW182 suppression was studied by collecting the individual shrimp gills on day 0, 1, 2, 3 and 4 (Figure 3.12). The results showed that the shrimp received dsRNA-GW182#1 showed up to 63% knockdown PvGW182 on day 2 when compared with the pre-injected shrimp (Figure 3.12). Furthermore, the PvGW182 mRNA level was recovered same level as the pre-injection on day 4. However, the study of PvGW182 suppression by dsRNA-GW182 injection is still undergoing. The next experiment will be to compare the relative of PvGW182 mRNA level with an injection of non-related dsRNA which is dsRNA-GFP and NaCl group at these time points. Then, the shrimp receiving dsRNA-GW182 will be further injected with virus to study the PvGW182 function during viral infection.



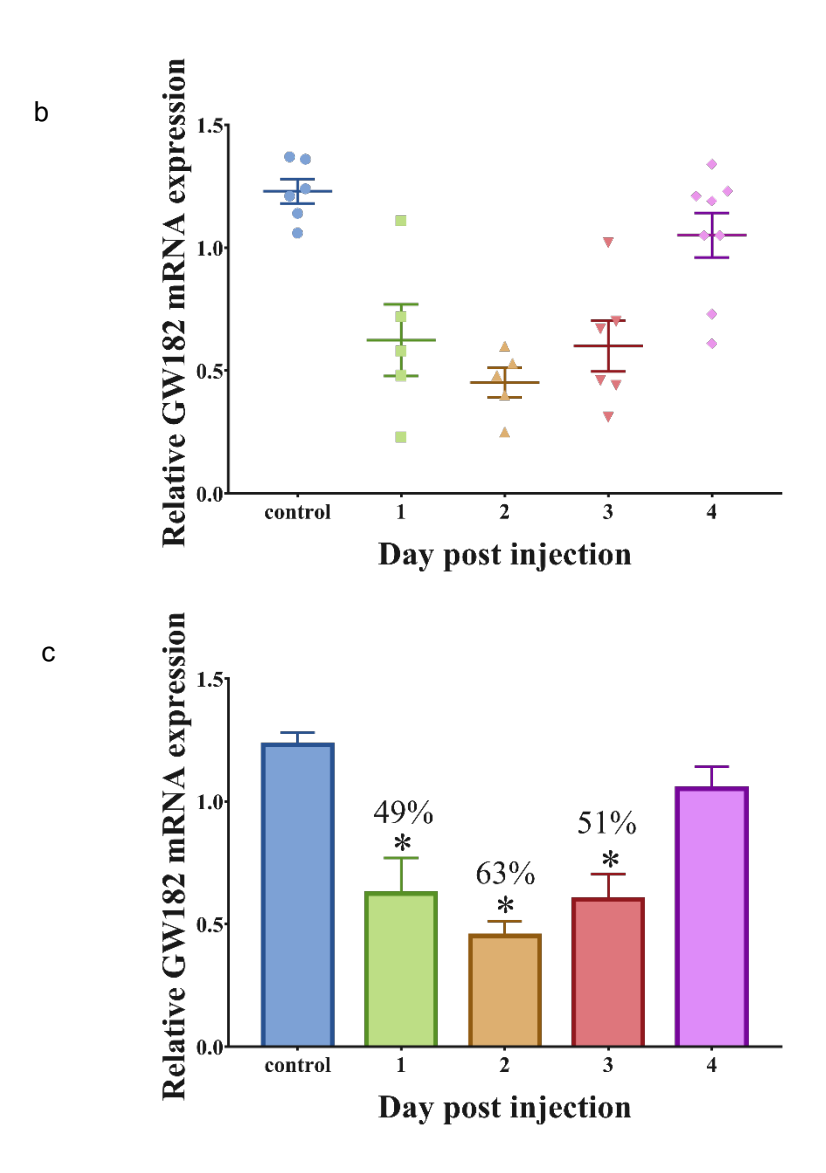


Figure 3.12 Time-course expression profile of PvGW182 in gills response to 2.5  $\mu$ g/g shrimp of dsRNA-GW182 injection on day 1, 2, 3 and 4. (a) 1.5% Agarose gel of PvGW182 mRNA expression in gills response to 2.5  $\mu$ g/g shrimp of dsRNA-GW182 injection on day 1, 2, 3 and 4. RT-PCR products for PvGW182 and  $\beta$ -actin. A bold number represents an excluded sample. (b) The scatter plot represents the relative PvGW182 expression in individual shrimp at the various time points. (c) The bar graph represents the average relative PvGW182 expression normalized with  $\beta$ -actin (mean  $\pm$  SEM) in the dsRNA-GW182 injection. The asterisk (\*) represents the significant difference from student t-test statistical analysis with the p-value < 0.01. The number above bar represents the percentage of knockdown efficacy.

### 3.7 Expression profile of PvGW182 mRNA during dsRNA-GFP injection

Because of the low efficiency of GW182 knockdown by dsRNA-GW182s, we hypothesized that the expression of PvGW182 might be up-regulated upon dsRNA injection. To study whether the PvGW182 mRNA expression level changed during dsRNA injection, shrimp were injected with dsRNA-GFP, a non-related dsRNA, followed by monitoring the PvGW182 mRNA level.

The results showed that the PvGW182 mRNA expression level was significantly up-regulated at 3 h after dsRNA-GFP injection compared to the pre-injection control (0 hpi) and remained steady from 6 to 12 hpi before it

gradually decreased after 24 hpi (Figure 3.13). This suggested that the presence of dsRNA could trigger the PvGW182 mRNA expression level after 3 hpi.

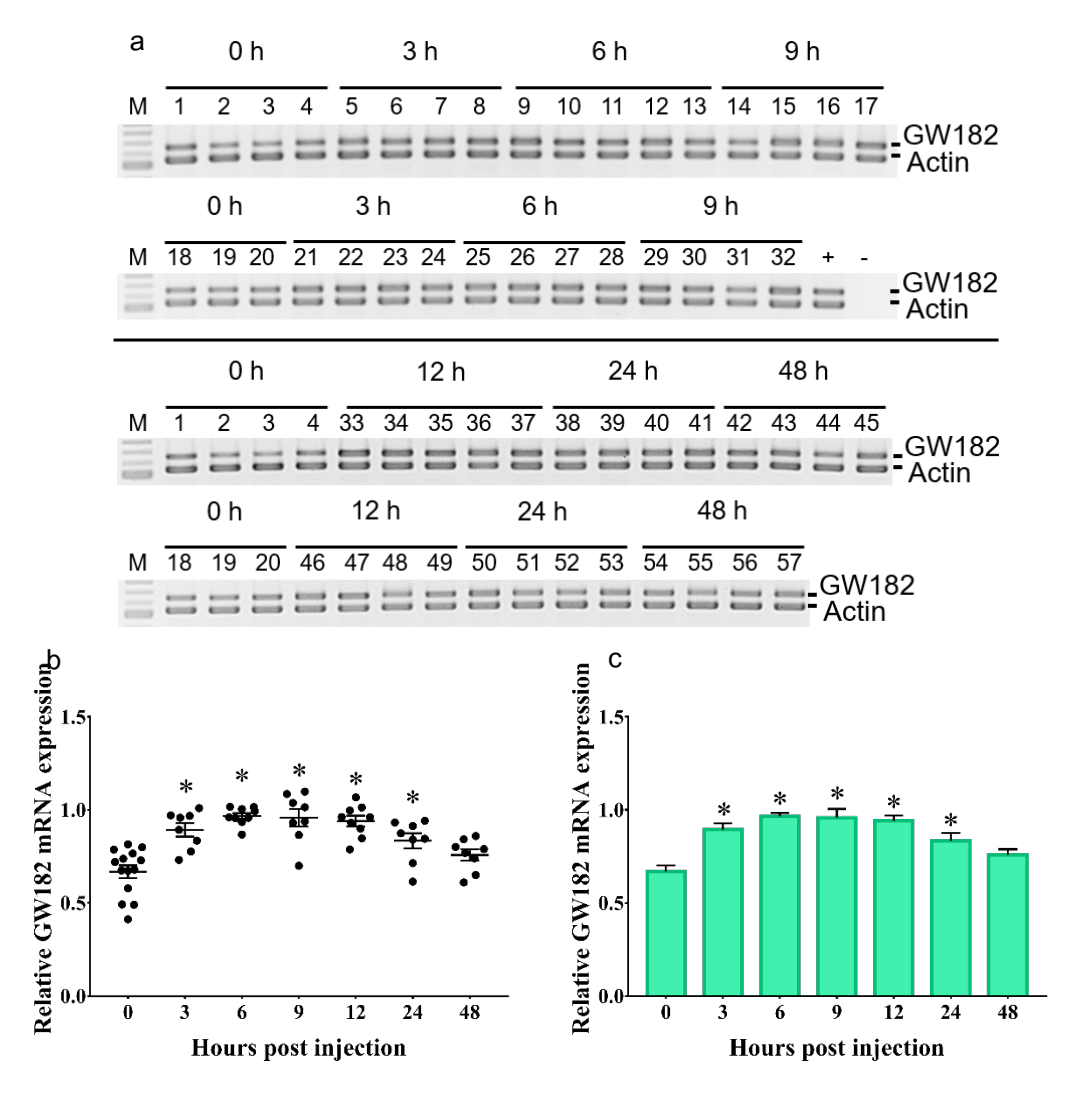


Figure 3.13 Time-course expression profile of PvGW182 in gills response to 2.5  $\mu$ g/g shrimp of dsRNA-GFP injection at 0, 3, 6, 9, 12, 24 and 48 hours. (a) 1.5% Agarose gel of PvGW182 mRNA expression in gills response to 2.5  $\mu$ g/g shrimp of dsRNA-GFP injection at specific time points. RT-PCR products for PvGW182 and  $\beta$ -actin. (b) The scatter plot represents the relative PvGW182 expression in individual shrimp at the various time points. (c) The bar graph represents the average relative PvGW182 expression normalized with  $\beta$ -actin (mean  $\pm$  SEM) in the dsRNA-GW182 injection. The asterisk (\*) represents the significant difference compared to 0 hpi by student t-test statistical analysis with the p-value < 0.01.

#### 3.8 Effect of PvGW182 suppression in YHV infection

Because the expression level of PvGw182 was up-regulated upon YHV infection, we hypothesized that PvGW182 might be necessary for YHV infection. To test that hypothesis, shrimp were divided into 3 groups: a NaCl-injected group, a dsRNA-GFP-injected group, and a dsRNA-GW182#1-injected group. Three days after the first injection, all shrimp were injected with YHV. Gills were collected after day 1, 2 and 3 after YHV injection.

The preliminary results (Figure 3.14) showed that the control group (day 0) was free from YHV infection. YHV could be detected on Day 1 in the group that was injected with NaCl followed by YHV, but not in the other two groups. On day 2 post YHV injection, all shrimp in the NaCl-injected group and 75% of shrimp in the dsRNA-GFP-injected group were positive for YHV. In contrast, noticeably fewer shrimp in the group that was injected with dsRNA-GW182 followed up by YHV showed the sign

of YHV infection. However, on day 3, more shrimp in the dsRNA-GW182-injected group showed the sign of YHV replication. Overall, the PvGW182 suppression might affect the YHV replication.

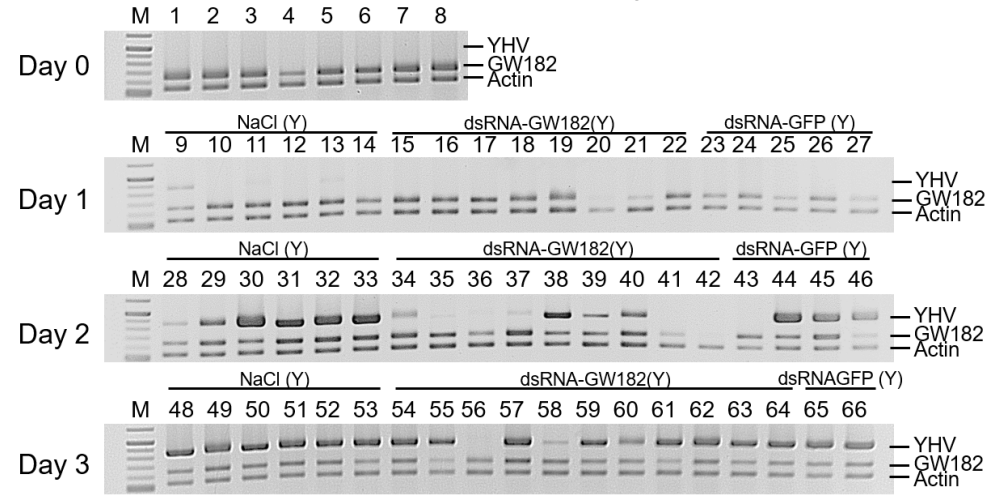


Figure 3.14 1.5% Agarose gel of RT-PCR products of YHV,  $\beta$ -actin and PvGW182 mRNA expressions. Shrimp were divided into 4 group: a pre-injection, NaCl(Y), dsRNA-GW182(Y) and dsRNA-GFP(Y).

#### **Discussion**

White spot syndrome virus (WSSV) and Yellow head virus (YHV) cause the most lethal virus disease in Penaeid shrimp. The infected shrimp shows 100% cumulative shrimp mortality in 3-5 days. An innate immune system especially RNA interference (RNAi) is still elucidated. The functions of RNAi components are necessary to fulfill RNAi pathway for applying and developing a novel method to prevent and help shrimp from virus infection.

RNAi components in shrimp have been studied by observing expression profiles of RNAi components response to viruses. Most RNAi components mRNA levels are altered during virus infection (Chen et al., 2012; Huang and Zhang, 2012; Phetrungnapha et al., 2015; Yang et al., 2014). Moreover, the knockdown of some RNAi components could affect viral infections either enhancing or inhibition viral infections (Huang and Zhang, 2012; Phetrungnapha et al., 2013; Su et al., 2008).

Previous works mentioned that during virus infection in human cells, the level of GW182 expression is unchanged either during transcription or translation. However, the studies of GW182 function were examined by knocking out or over-expressing of a GW182 gene. The results showed that GW182 plays a role in enhancing WNV and HCV replication (Bukong et al., 2013; Chahar et al., 2013). On the other hand, the GW182 knockdown in HIV-1 infected cells suggested that GW182 functions in an immune system response to HIV infection (Chable-Bessia et al., 2009). Therefore, the functions of GW182 during virus infection may be either recruiting or interfering viral infection depends on viruses. In shrimp, based on previous studies of other RNAi components (Table 2. 2), this research hypothesizes that GW182 may play a role in an innate immune system to suppress viral replication. Hence, knocking down of GW182 by the RNAi technique will cause high mortality rate of YHV infected shrimp.

# 3.9 PvGW182 mRNA is upregulated at 24 hours by YHV infection but not by WSSV infection.

In shrimp, the role of GW182 during virus infection has not been previously characterized. Therefore, *P. vannamei* GW182 mRNA expression was determined during either WSSV or YHV infection. The results showed that the PvGW182 expression was not significant different in WSSV infected shrimp compared to NaCl-injected shrimp (Figure 4.1), while the PvGW182 mRNA level increased at 24 hours post-injection in YHV infected shrimp (Figure 4.2).

Our results suggested that PvGW182 can be triggered in a different way based on the type of virus because the expression of PvGW182 mRNA was upregulated by an RNA virus but not a DNA virus. Upregulation of GW182 upon RNA virus infection has been reported in human (Table 2.3). Nevertheless, there has been no any evidence to exclude the possibility that the transcript level of GW182 may respond to other DNA virus.

In previous works, the expression profiles during viral infection of other genes in the RNAi pathway in shrimp have been studied (Table 0.1). These studies showed that the RNAi components up-regulate in virus-infected shrimp, except PvAgo2, PmAgo3 which remained unchanged and MjAgo1C which down regulates. Previous studies only look at the expression of the aforementioned genes in response to either DNA or RNA virus. According to the result that the PvGW182 gene was only modified by YHV infection, an investigation of the PvGW182 gene will be focused on YHV-infected shrimp.

Table 0.1 Studies of mRNA expression profile upon virus infection.

RNAi	DNA or RNA	Virus	Expression profile	Reference	
TXIV II	virus	virus challenge (mRNA lev		el)	
PvDicer-1	RNA	TSV	<b>1</b>	Yao et al., 2010	
PmDicer-1	DNA	GAV	•	Su et al., 2008	
PvDicer-2	DNA	WSSV	•	Chen et al., 2011	
PmTRBP-1	DNA	WSSV	•	Yang et al., 2013	
PmAgo1	RNA	YHV	•	Unajak et al., 2006	
MjAgo1A	DNA	WSSV	•	Huang and Zhang,	
, 5-		,,,,,,,,,,,,,,,,,,,,,,,,,,,,,,,,,,,,,,,	_	2012	
MjAgo1B	DNA	WSSV	<b>1</b>	Huang and Zhang,	
MJAGOTB				2012	
M: A == 4 C	DNA	WSSV	•	Huang and Zhang,	
MjAgo1C				2012	
PvAgo2	DNA	WSSV	-	Nilsen et al., 2017	
PmAgo2	DNA	WSSV	•	Yang et al., 2014	
D 4 0	RNA	YHV	-	Phetrungnapha et	
PmAgo3				al., 2013	
MjMov-10	DNA	WSSV	1	Phetrungnapha et	
				al., 2015	
D. OWAGO	DNA	WSSV	-	This study	
PvGW182	RNA	YHV	•	This study	

# 3.10 PvGW182 was suppressed by injection of specific-dsRNA targeting GW182 (dsRNA-GW182).

#### 3.10.1 The knockdown efficiency of dsRNA-GW182s

The dsRNA-GW182#2 was first used to find an optimal condition to knockdown PvGW182 due to the high yield of dsRNA-GW182#2. However, an increasing dose of dsRNA-GW182#2 and a double injection could not increase the knockdown efficiency. Moreover, an excess dsRNA-GW182#2 also resulted in a high shrimp mortality rate within 5 days. The toxicity in shrimp from dsRNA-GW182#2 may be from a high uptake of contaminants from  $E.\ coli$  proteins during the ethanol extraction step. Therefore, a single injection of 2.5  $\mu$ g/g shrimp was used in other experiments.

In addition, the knockdown efficiency of dsRNA-GW182#1 and dsRNA-GW182#2 was compared. These results revealed that all dsRNAs targeting PvGW182 could partially knockdown PvGW182 expression by about 40-60% when compared with NaCl injection group. The mixture of the two dsRNA-GW182 showed no enhancement of knockdown efficiency because of the half-diluted of dsRNA-GW182 concentration. Therefore, the dsRNA-GW182#1 was selected for PvGW182 suppression as it provides higher effective than other conditions.

The preliminary result for PvGW182 knockdown showed that the administration of  $2.5~\mu g/g$  shrimp of dsRNA-GW182#1 showed the most effective modifies (63%) on day 2 after injection. However, the knockdown efficiency of dsRNA-GW182#1 was quite low when compared with other dsRNAs targeting RNAi components (Table 0.2).

Table 0.2 Studies of knockdown efficiency of RNAi components by dsRNA injection

Target gene	Function	Knockdown efficiency	Reference		
PmAgo3	Interacting other proteins to form RISC that specific in siRNA pathway	100%	Phetrungnapha et al., 2013		
MjTRBP	Stabilizing Dicer	100%	Wang et al., 2012		
MjelF6	Preventing ribosome assembly	100%	Wang et al., 2012		
PmDicer-	Generating small RNAs in the RNAi pathways	~ 85%	Su et al., 2008		
MjMov-10	Interacting with Ago1 and Ago2 to form RISC and guiding miRNA to target mRNA cleavage	~ 60%	Phetrungnapha et al., 2015		
PmDicer-	Generating small RNAs in the RNAi		Personal communication with		
2	pathways	Could not	Ongvarrasopone's laboratory		
PmSid-1	A dsRNA selective channel	knockdown	Personal communication with Dr. Pongsopee Attasart		
	Note: Pv = <i>P. vannamei</i> , Pm = <i>P. monodon</i> , Mj = <i>M. japonicus</i>				

The low knockdown efficiency of dsRNA-GW182s could be from 1) an increasing of PvGW182 mRNA level in shrimp receiving any dsRNAs, 2) the selection of dsRNA-GW182 regions (Mohammed et al., 2017; Perkin et al., 2017), and 3) the half-life of either dsRNA-GW182s or PvGW182 gene (Behm-Ansmant et al., 2006; Posiri et al., 2016; Yodmuang et al., 2006).

Comparison of PvGW182 mRNA level response to dsRNA-GFP, a non-related dsRNA, and dsRNA-GW182s (Figure 0.1), the result revealed that PvGW182 mRNA was triggered by dsRNA-GFP. According to 24 hours post dsRNA-GFP injection, the PvGW182 was up-regulated. This could be the reason that PvGW182 was only slightly suppressed at 24 hpi. The response of GW182 upon the injection of non-specific dsRNA is light with a previous report by Labreuche et al., 2010 that showed that a non-specific of dsRNA induced LvAgo1, a major component in RNAi pathway. This not only showed that PvGW182 was partially suppressed, but also that PvGW182 is involved in siRNA pathway

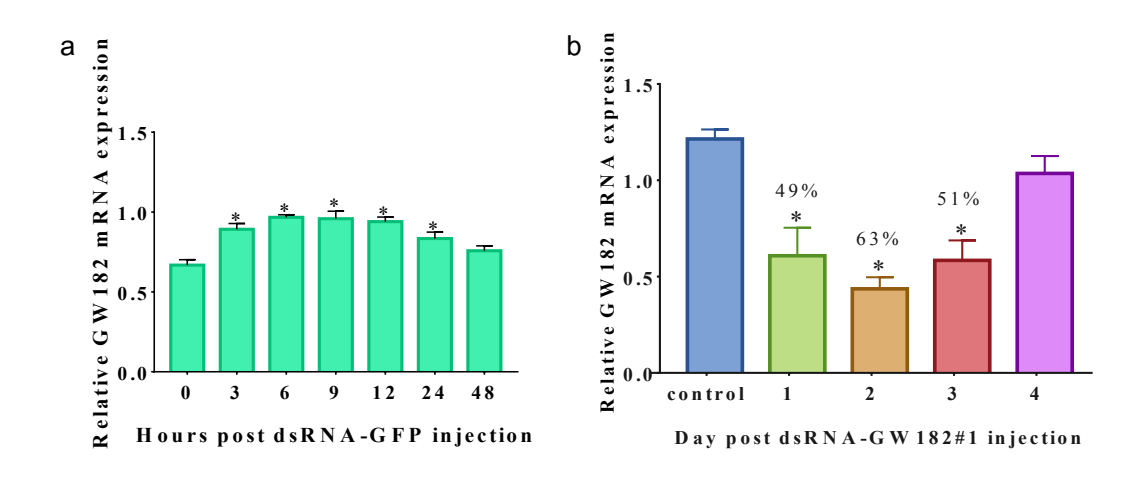


Figure 0.1 Comparison of the PvGW182 mRNA level in (a) the dsRNA-GFP injection experiment and (b) the dsRNA-GW182#1 injection experiment. The asterisk (\*) represents the significant difference by the student t-test with p-value > 0.01.

It has been reported that the region of mRNA target affects the knockdown efficiency. For instance, the knockdown of chitin synthase A, a major component in chitin synthesis pathway in the potato tuber moth, by three different target regions showed that the dsRNA that targets a 5' target provided the highest knockdown efficiency (Mohammed et al., 2017). Conversely, the results reported by the Oppert's laboratory demonstrated that the 3' target region provided the highest knockdown effect on the cathepsin L gene, a lysosomal cysteine proteinase, compared to dsRNAs targeting 5' and middle regions in *Tribolium castaneum* (Perkin et al., 2017). Therefore, the differences in the knockdown effect are probably due to the target region on the mRNA itself.

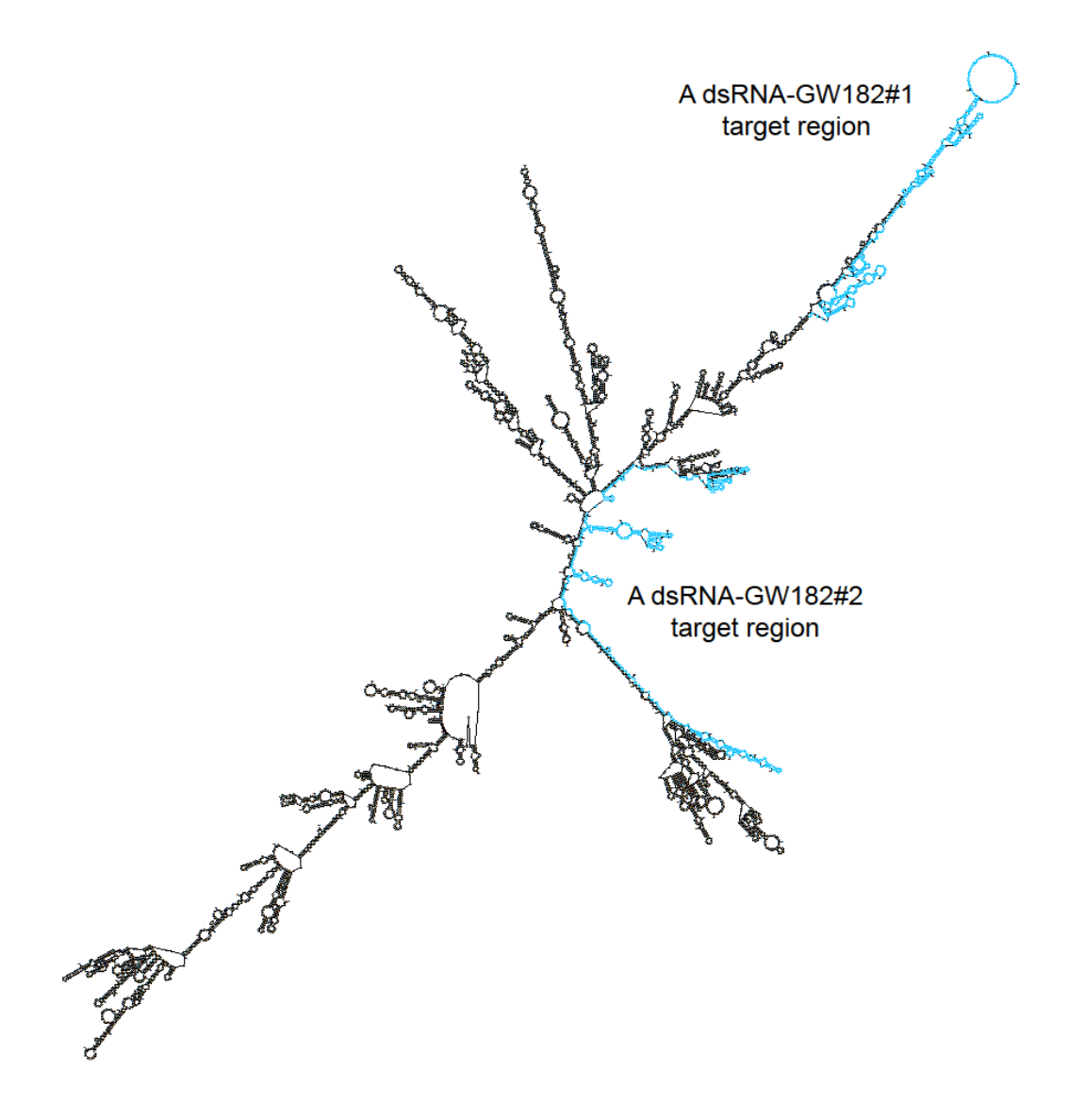
During the last step in the RNAi pathway when the siRNA binds to the target mRNA site. The siRNA knockdown efficiency depends on three major factors including a secondary structure of mRNA target, a thermodynamic of siRNA-mRNA binding and a localization of local protein factors for an mRNA target. (Holen et al., 2002; Luo and Chang, 2004; Pascut et al., 2015; Schubert et al., 2005; Shao et al., 2007; Sun et al., 2013).

The secondary structure of target mRNA plays a crucial role in RNAi knockdown efficiency (Luo and Chang, 2004; Schubert et al., 2005). The exact identities of the siRNA that were involved in the knockdown process are unknown because the injected dsRNA is further diced by Dicer into siRNAs.

According to the secondary structures of PvGW182 mRNA regions targeted by dsRNA-GW182#1 and dsRNA-GW182#2 were predicted by the Mfold program. The result showed that the secondary structures of the mRNA target consist of stems, loops, and hairpins (Figure 0.2). The target sites which are closer to bigger loops or branches are less effective for RNAi (Yiu et al., 2005). The large number of unpaired nucleotides on target mRNA sites are more available for siRNA binding. A value of delta G (dG) has been used to describe how the severity of a secondary formation. This value is calculated by the summation of free energy values from individual loops, bulges, and stacks (Shao et al., 2007; Sun et al., 2013). The  $\Delta G$  of the secondary structure of mRNA target is -1539.20 kcal/mol. The calculated  $\Delta G$  results were correlated to the PvGW182 knockdown efficiency of two dsRNA-GW182 constructs.

Another reason for the low knockdown efficiency is probably due to the half-life of both dsRNA-GW182s and PvGW182. Normally, the half-life of long dsRNA in shrimp is about 5 days (Ongvarrasopone et al., 2008; Yodmuang et al., 2006). However, according to Figure 0.1b, the suppression of dsRNA-GW182#1 recovered on day 3 indicating that the dsRNA-GW182 half-life seems to be 3 days or less. Moreover, the mRNA half-life examination in *Drosophila* revealed that the GW182 mRNA had a short half-life (Behm-Ansmant et al., 2006). The short half-life of GW182 mRNA might accelerate the rate of GW182 mRNA recovery and reduce the knockdown efficiency of dsRNA-GW182s.

Overall, the low knockdown efficiency of dsRNA-GW182s which all target to middle regions of the PvGW182 mRNA is probably due to the upregulation of PvGW182 mRNA level upon the administration of dsRNA, the target regions on the PvGW182 mRNA and the short half-life of both dsRNA-GW182 and GW182 mRNA.



dG = -1539.20 kcal/mole PmGW182

Figure 0.2 A schematic shows a secondary structure of the PvGW182 mRNA. The light blue color represents the dsRNA-GW182 target regions.

#### 4 CONCLUSIONS

- **1.** The level of *P. vannamei* GW182 mRNA in the WSSV-infected shrimp was not significantly different when compared with either before injection (0 hpi) or the NaCl-injected group.
- 2. The level of PvGW182 mRNA in the YHV-infected shrimp was up-regulated at 24 after YHV challenge compared with NaCl-injected shrimp.
- **3.** The recombinant plasmids for dsRNA-GW182 production were amplified by the primers designed from PmGW182. The partial coding regions of PvGW182 that were used as dsRNA-GW182 constructions were aligned nucleotide sequences with ORF of PmGW182. The dsRNA-GW182#1 and dsRNA-GW182#2 region similar to the nucleotide sequences of *P.monodon* GW182 at 98.46 and 98.41% identity.
- **4.** The dsRNA-GW182#1 and dsRNA-GW182#2 were produced by *in vivo* HT115 *E. coli* strain expression and extracted by an ethanol extraction method. The expected size of dsRNA-GW182#1 and #2 are 454 bp and 502 bp, respectively. The concentration of dsRNA-GW182#1 and #2 are 2 and 2.5 mg/ml, respectively.
- **5.** PvGW182 was specifically suppressed by dsRNA-GW182#1 or dsRNA-GW182#2 injection not by any dsRNA such as dsRNA-GFP.
- **6.** All dsRNA-GW182 injection conditions including the 2.5  $\mu$ g/g shrimp of dsRNA-GW182#1, #2 and the combination of 1.25  $\mu$ g/g shrimp per each of dsRNA-GW182#1 and #2 could be suppressed PvGW182 mRNA level about 40-60% compared to the NaCl-injected group.
- **7.** The combination of dsRNA-GW182#1 and #2 and the double injection of dsRNA-GW182#2 could not improve the knockdown GW182 mRNA efficiency.
- **8.** The 2.5  $\mu$ g/g shrimp of dsRNA-GW182#1 was further used for suppression PvGW182 mRNA level.
- **9.** The PvGW182 mRNA level was up-regulated in an administration of 2.5  $\mu$ g/g shrimp of dsRNA-GFP.
- 10. The GW182 mRNA expression upon 2.5  $\mu$ g/g shrimp of dsRNA-GW182#1 injection was partially knockdown at 63% after 2 days post-injection compared with shrimp before injection (0 hpi).

# 5 Future direction: studying the knockdown effect of PvGW182 in YHVinfected shrimp

The preliminary result showed that suppression PvGW182 suppression reduced YHV infection at day 2 post YHV injection because there was a delay in YHV infection in shrimp injected with dsRNA-GW182#1 compared to the NaCl-injected and the dsRNA-GFP-injected groups. This is probably due to the induction of an antiviral immunity by non-specific dsRNA injection (Labreuche et al., 2010) as well as the depletion of GW182. This experiment is still on-going since the preliminary result lacks the appropriate controls including the dsRNA-GW182#1 and the dsRNA-GFP negative YHV.

Together, the GW182 expression was up-regulated during YHV post-injection, while the WSSV-injected shrimp did not show any significant change in the PvGW182 mRNA expression. The PvGW182 mRNA level was suppressed by the single of 2.5  $\mu$ g/ g shrimp dsRNA-GW182#1 injection. In the further study, the PvGW182 function will be investigated in the virus-infected shrimp. The shrimp will be injected with 2.5  $\mu$ g/ g shrimp dsRNA-GW182#1 followed by virus challenge. The number of virus-infected shrimp after PvGW182 knockdown and also shrimp mortality assay need to be carried out to characterize the function of this gene (Figure 5.1).

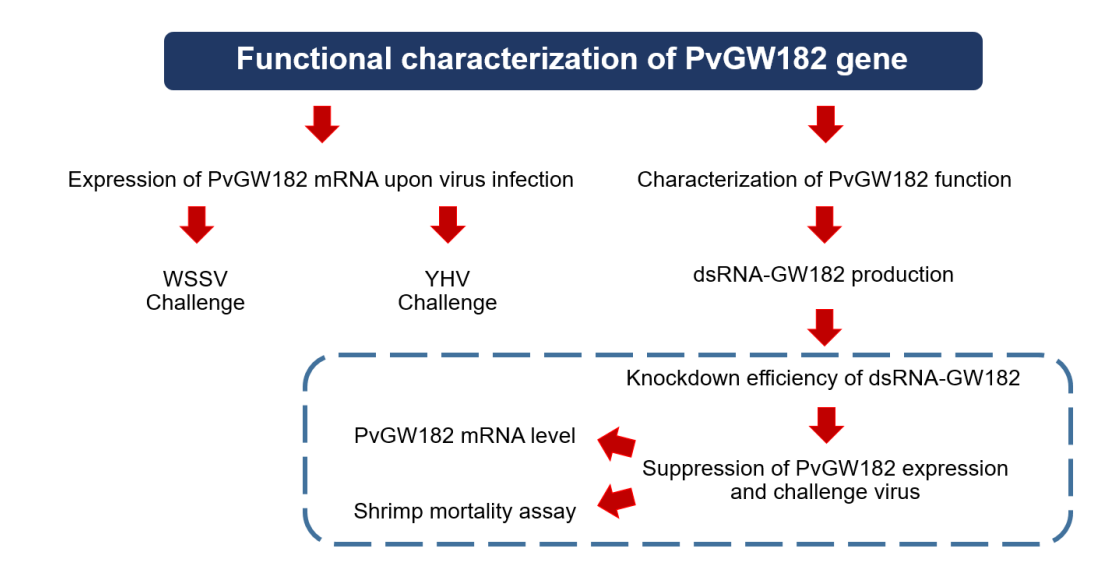


Figure 5.1 A schematic diagram represents the functional characterization of PvGW182 gene that will be performed in the future.

#### 6 References

- Attasart, P., Kaewkhaw, R., Chimwai, C., Kongphom, U., Namramoon, O., Panyim, S., 2009. Inhibition of white spot syndrome virus replication in *Penaeus monodon* by combined silencing of viral rr2 and shrimp PmRab7.

  Virus Res. 145, 127–133. doi:10.1016/j.virusres.2009.06.018
- Attasart, P., Namramoon, O., Kongphom, U., Chimwai, C., Panyim, S., 2013. Ingestion of bacteria expressing dsRNA triggers specific RNA silencing in shrimp. Virus Res. 171, 252–256. doi:10.1016/j.virusres.2012.11.012
- Behm-Ansmant, I., Rehwinkel, J., Doerks, T., Stark, A., Bork, P., Izaurralde, E., 2006. mRNA degradation by miRNAs and GW182 requires both CCR4:NOT deadenylase and DCP1:DCP2 decapping complexes. Genes Dev. 20, 1885–1898. doi:10.1101/gad.1424106
- Bohnsack, M.T., Czaplinski, K., GÖRLICH, D., 2004. Exportin 5 is a RanGTP-dependent dsRNA-binding protein that mediates nuclear export of pre-miRNAs. Rna 10, 185–191.
- Bukong, T.N., Hou, W., Kodys, K., Szabo, G., 2013. Ethanol facilitates hepatitis C virus replication via up-regulation of GW182 and heat shock protein 90 in human hepatoma cells. Hepatology 57, 70–80. doi:10.1002/hep.26010
- Chable-Bessia, C., Meziane, O., Latreille, D., Triboulet, R., Zamborlini, A., Wagschal, A., Jacquet, J.-M., Reynes, J., Levy, Y., Saib, A., Bennasser, Y., Benkirane, M., 2009. Suppression of HIV-1 replication by microRNA effectors. Retrovirology 6, 26. doi:10.1186/1742-4690-6-26
- Chahar, H.S., Chen, S., Manjunath, N., 2013. P-body components LSM1, GW182, DDX3, DDX6 and XRN1 are recruited to WNV replication sites and positively regulate viral replication. Virology 436, 1–7. doi:10.1016/j.virol.2012.09.041
- Chang, P., Lo, C., Wang, Y., Kou, G., 1996. Identification of white spot syndrome associated baculovirus (WSBV) target organs in the shrimp *Penaeus monodon* by in situ hybridization. Dis. Aquat. Organ. 27, 131–139.
- Chen, Y.H., Jia, X.T., Zhao, L., Li, C.Z., Zhang, S., Chen, Y.G., Weng, S.P., He, J.G., 2011. Identification and functional characterization of Dicer2 and five single VWC domain proteins of *Litopenaeus vannamei*. Dev. Comp. Immunol. 35, 661–671. doi:10.1016/j.dci.2011.01.010
- Chen, Y.H., Zhao, L., Jia, X.T., Li, X.Y., Li, C.Z., Yan, H., Weng, S.P., He, J.G., 2012. Isolation and characterization of cDNAs encoding Ars2 and Pasha homologues, two components of the RNA interference pathway in *Litopenaeus vannamei*. Fish Shellfish Immunol. 32, 373–380. doi:10.1016/j.fsi.2011.11.032
- Chou, H.Y., Huang, C.Y., Wang, C.H., Chiang, H.C., Lo, C.F., 1995. Pathogenicity of a baculovirus infection causing

  White Spot Syndrome in cultured Penaeid shrimp in Taiwan. Dis. Aquat. Org. Dis. AQUAT ORG 23,

  165–173.
- Dechklar, M., Udomkit, A., Panyim, S., 2008. Characterization of Argonaute cDNA from Penaeus monodon and

- implication of its role in RNA interference. Biochem. Biophys. Res. Commun. 367, 768–774. doi:10.1016/j.bbrc.2008.01.031
- Ding, S.-W., 2010. RNA-based antiviral immunity. Nat. Rev. Immunol. 10, 632-44. doi:10.1038/nri2824
- Eulalio, A., Helms, S., Fritzsch, C., Fauser, M., Izaurralde, E., 2009. A C-terminal silencing domain in GW182 is essential for miRNA function. RNA 15, 1067–77. doi:10.1261/rna.1605509
- Fauquet CM, Mayo MA, Maniloff J, Desselberger U, B. LA, 2005. VIIIth Report of the International Committee on Taxonomy of Viruses.
- Fire, A., Xu, S., Montgomery, M.K., Kostas, S.A., Driver, S.E., Mello, C.C., 1998. Potent and specific genetic interference by double-stranded RNA in *Caenorhabditis elegans*. Nature 391, 806–811. doi:10.1038/35888
- Flegel, T.W., 2012. Historic emergence, impact and current status of shrimp pathogens in Asia. J. Invertebr. Pathol. 110, 166–173. doi:10.1016/j.jip.2012.03.004
- Flegel, T.W., 2006. Detection of major penaeid shrimp viruses in Asia, a historical perspective with emphasis on Thailand. Aquaculture. doi:10.1016/j.aquaculture.2006.05.013
- Flegel, T.W., Lightner, D. V, Lo, C.H.U.F., Owens, L., 2008. Shrimp Disease Control: Past, Present and Future. Dis.

  Asian Aquac. VI 355–378.
- Ganjoor, M., 2015. A Short Review on Infectious Viruses in Cultural Shrimps ( Penaeidae Family ). Fish. Aquac. J. 6. doi:10.4172/2150-3508.1000136
- Holen, T., Amarzguioui, M., Wiiger, M.T., Babaie, E., Prydz, H., 2002. Positional effects of short interfering RNAs targeting the human coagulation trigger Tissue Factor. Nucleic Acids Res. 30, 1757–1766.
- Huang, T., Zhang, X., 2012. Contribution of the Argonaute-1 Isoforms to Invertebrate Antiviral Defense. PLoS One 7. doi:10.1371/journal.pone.0050581
- Kohlway, A., Pirakitikulr, N., Ding, S.C., Yang, F., Luo, D., Lindenbach, B.D., Pyle, A.M., 2014. The Linker Region of NS3 Plays a Critical Role in the Replication and Infectivity of Hepatitis C Virus. J. Virol. 88, 10970–10974. doi:10.1128/JVI.00745-14
- Labreuche, Y., Veloso, A., de la Vega, E., Gross, P.S., Chapman, R.W., Browdy, C.L., Warr, G.W., 2010. Non-specific activation of antiviral immunity and induction of RNA interference may engage the same pathway in the Pacific white leg shrimp *Litopenaeus vannamei*. Dev. Comp. Immunol. 34, 1209–1218. doi:10.1016/j.dci.2010.06.017
- Labreuche, Y., Warr, G.W., 2013. Insights into the antiviral functions of the RNAi machinery in penaeid shrimp. Fish Shellfish Immunol. 34, 1002–1010. doi:10.1016/j.fsi.2012.06.008
- Lee, R.C., Feinbaum, R.L., Ambros, V., 1993. The *C. elegans* heterochronic gene lin-4 encodes small RNAs with antisense complementarity to lin-14. Cell 75, 843–854. doi:10.1016/0092-8674(93)90529-Y
- Lee, Y., Ahn, C., Han, J., Choi, H., Kim, J., Yim, J., Lee, J., Provost, P., Radmark, O., Kim, S., 2003. The nuclear RNase

- III Drosha initiates microRNA processing. Nature 425, 415-419.
- Lee, Y.S., Nakahara, K., Pham, J.W., Kim, K., He, Z., Sontheimer, E.J., Carthew, R.W., 2004. Distinct roles for *Drosophila* Dicer-1 and Dicer-2 in the siRNA/miRNA silencing pathways. Cell 117, 69–81.
- Leebonoi, W., Sukthaworn, S., Panyim, S., Udomkit, A., 2015. A novel gonad-specific Argonaute 4 serves as a defense against transposons in the black tiger shrimp *Penaeus monodon*. Fish Shellfish Immunol. 42, 280–288. doi:10.1016/j.fsi.2014.11.014
- Li, X., Yang, L., Jiang, S., Fu, M., Huang, J., Jiang, S., 2013. Identification and expression analysis of Dicer2 in black tiger shrimp (*Penaeus monodon*) responses to immune challenges. Fish Shellfish Immunol. 35, 1–8. doi:10.1016/j.fsi.2013.03.370
- Lo, C.-F., Ho, C.-H., Chen, C.-H., Liu, K.F., Chiu, Y.L., Yeh, P.Y., Peng, S.E., Hsu, H.C., Liu, H.C., Chang, C.F., 1997.

  Detection and tissue tropism of white spot syndrome baculovirus (WSBV) in captured brooders of 

  Penaeus monodon with a special emphasis on reproductive organs. Dis. Aquat. Organ. 30, 53–72.
- Luo, K.Q., Chang, D.C., 2004. The gene-silencing efficiency of siRNA is strongly dependent on the local structure of mRNA at the targeted region. Biochem. Biophys. Res. Commun. 318, 303–310.
- Majzoub, K., Imler, J.-L., Majzoub, K., Imler, J., 2015. RNA Interference to Treat Virus Infections. Rev. Cell Biol. Mol. Med. 1, 192–228. doi:10.1002/3527600906.mcb.201500003
- Mayo, Ma., 2002. A summary of taxonomic changes recently approved by ICTV. Arch. Virol. 147, 1655-1656.
- Moerman, D.G., Baillie, D.L., 1979. Genetic Organization in CAENORHABDITIS ELEGANS: Fine-Structure Analysis of the unc-22 Gene. Genetics 91, 95–103. doi:10.2307/2177236
- Mohammed, A.M.A., Dlab, M.R., Abdelsattar, M., Khalil, S.M.S., 2017. Characterization and RNAi-mediated knockdown of Chitin Synthase A in the potato tuber moth, Phthorimaea operculella. Sci. Rep. 7, 1–12. doi:10.1038/s41598-017-09858-y
- Mueller, S., Gausson, V., Vodovar, N., Deddouche, S., Troxler, L., Perot, J., Pfeffer, S., Hoffmann, J.A., Saleh, M.-C., Imler, J.-L., 2010. RNAi-mediated immunity provides strong protection against the negative-strand RNA vesicular stomatitis virus in *Drosophila*. Proc. Natl. Acad. Sci. U. S. A. 107, 19390–5. doi:10.1073/pnas.1014378107
- Myles, K.M., Wiley, M.R., Morazzani, E.M., Adelman, Z.N., 2008. Alphavirus-derived small RNAs modulate pathogenesis in disease vector mosquitoes. Proc. Natl. Acad. Sci. U. S. A. 105, 19938–19943. doi:10.1073/pnas.0803408105
- Napoli, C., Lemieux, C., Jorgensen, R., 1990. Introduction of a Chimeric Chalcone Synthase Gene into Petunia Results in Reversible Co-Suppression of Homologous Genes in trans. Plant Cell 2, 279–289. doi:10.1105/tpc.2.4.279
- Nilsen, P., Karlsen, M., Sritunyalucksana, K., Thitamadee, S., 2017. White spot syndrome virus VP28 specific double-

- stranded RNA provides protection through a highly focused siRNA population. Sci. Rep. doi:10.1038/s41598-017-01181-w
- Ongvarrasopone, C., Chanasakulniyom, M., Sritunyalucksana, K., Panyim, S., 2008. Suppression of PmRab7 by dsRNA inhibits WSSV or YHV infection in shrimp. Mar Biotechnol 10, 374–381. doi:10.1007/s10126-007-9073-6
- Ongvarrasopone, C., Roshorm, Y., Panyim, S., 2007. A simple and cost effective method to generate dsRNA for RNAi studies in invertebrates. ScienceAsia 33, 35–39.
- Pang, P.S., Jankowsky, E., Planet, P.J., Pyle, A.M., 2002. The hepatitis C viral NS3 protein is a processive DNA helicase with cofactor enhanced RNA unwinding. EMBO J. 21, 1168–1176. doi:10.1093/emboj/21.5.1168
- Pascut, D., Bedogni, G., Tiribelli, C., 2015. Silencing efficacy prediction: a retrospective study on target mRNA features.

  Biosci. Rep. 35, e00185.
- Pause, A., Kukolj, G., Bailey, M., Brault, M., Dô, F., Halmos, T., Lagacé, L., Maurice, R., Marquis, M., McKercher, G.,

  Pellerin, C., Pilote, L., Thibeault, D., Lamarrell, D., 2003. An NS3 serine protease inhibitor abrogates

  replication of subgenomic hepatitis C virus RNA. J. Biol. Chem. 278, 20374–20380.

  doi:10.1074/jbc.M210785200
- Perkin, L.C., Elpidina, E.N., Oppert, B., 2017. RNA interference and dietary inhibitors induce a similar compensation response in Tribolium castaneum larvae. Insect Mol. Biol. 26, 35–45. doi:10.1111/imb.12269
- Phetrungnapha, A., Ho, T., Udomkit, A., Panyim, S., Ongvarrasopone, C., 2013. Molecular cloning and functional characterization of Argonaute-3 gene from *Penaeus monodon*. Fish Shellfish Immunol. 35, 874–882. doi:10.1016/j.fsi.2013.06.025
- Phetrungnapha, A., Kondo, H., Hirono, I., Panyim, S., Ongvarrasopone, C., 2015. Molecular cloning and characterization of Mj-mov-10, a putative RNA helicase involved in RNAi of kuruma shrimp. Fish Shellfish Immunol. 44, 241–247. doi:10.1016/j.fsi.2015.02.028
- Posiri, P., Ongvarrasopone, C., Panyim, S., 2013. A simple one-step method for producing dsRNA from E. coli to inhibit shrimp virus replication. J Virol Methods 188, 64–69. doi:10.1016/j.jviromet.2012.11.033
- Posiri, P., Panyim, S., Ongvarrasopone, C., 2016. Rab5, an early endosomal protein required for yellow head virus infection of *Penaeus monodon*. Aquaculture 459, 43–53. doi:10.1016/j.aquaculture.2016.03.026
- Raney, K.D., Sharma, S.D., Moustafa, I.M., Cameron, C.E., 2010. Hepatitis C virus non-structural protein 3 (HCV NS3):

  A multifunctional antiviral target. J. Biol. Chem. 285, 22725–22731. doi:10.1074/jbc.R110.125294
- Reinhart, B.J., Slack, F.J., Basson, M., Pasquinelli, a E., Bettinger, J.C., Rougvie, a E., Horvitz, H.R., Ruvkun, G., 2000. The 21-nucleotide let-7 RNA regulates developmental timing in *Caenorhabditis elegans*. Nature 403, 901–906. doi:10.1038/35002607
- Roniviridae, 2012. . Virus Taxon. 829-834. doi:10.1016/B978-0-12-384684-6.00069-0

- Sanitt, P., Attasart, P., Panyim, S., 2014. Protection of yellow head virus infection in shrimp by feeding of bacteria expressing dsRNAs. J. Biotechnol. 179, 26–31. doi:10.1016/j.jbiotec.2014.03.016
- Sarathi, M., Simon, M.C., Venkatesan, C., Hameed, A.S.S., 2008. Oral administration of bacterially expressed VP28dsRNA to protect *Penaeus monodon* from white spot syndrome virus. Mar. Biotechnol. 10, 242–249. doi:10.1007/s10126-007-9057-6
- Schubert, S., Grünweller, A., Erdmann, V.A., Kurreck, J., 2005. Local RNA target structure influences siRNA efficacy: systematic analysis of intentionally designed binding regions. J. Mol. Biol. 348, 883–893.
- Shao, Y., Chan, C.Y., Maliyekkel, A., Lawrence, C.E., Roninson, I.B., Ding, Y., 2007. Effect of target secondary structure on RNAi efficiency. RNA 13, 1631–1640. doi:10.1261/rna.546207
- Slack, F.J., Basson, M., Liu, Z., Ambros, V., Horvitz, H.R., Ruvkun, G., 2000. The lin-41 RBCC Gene Acts in the *C. elegans* Heterochronic Pathway between the let-7 Regulatory RNA and the LIN-29 Transcription Factor.

  Mol. Cell 5, 659–669. doi:10.1016/S1097-2765(00)80245-2
- Sritunyalucksana, K., Wannapapho, W., Lo, C.F., Flegel, T.W., 2006. PmRab7 Is a VP28-Binding Protein Involved in White Spot Syndrome Virus Infection in Shrimp. J. Virol. 80, 10734–10742. doi:10.1128/JVI.00349-06
- Su, J., Oanh, D.T.H., Lyons, R.E., Leeton, L., van Hulten, M.C.W., Tan, S.H., Song, L., Rajendran, K. V., Walker, P.J., 2008. A key gene of the RNA interference pathway in the black tiger shrimp, *Penaeus monodon*: Identification and functional characterisation of Dicer-1. Fish Shellfish Immunol. 24, 223–233. doi:10.1016/j.fsi.2007.11.006
- Sun, Y., Gui, J., Chen, Z., 2013. The influence of RNA secondary structure on efficiency of siRNA silencing. IFMBE Proc. 39 IFMBE, 398–401. doi:10.1007/978-3-642-29305-4 106
- Taengchaiyaphum, S., Nakayama, H., Srisala, J., Khiev, R., January Aldama-Cano, D., Thitamadee, S., Sritunyalucksana, K., 2017. Vaccination with multimeric recombinant VP28 induces high protection against white spot syndrome virus in shrimp. Dev. Comp. Immunol. 76.
- Takahashi, Y., Itami, T., Kondo, M., Maeda, M., Fujii, R., Tomonaga, S., Supamattaya, K., Boonyaratpalin, S., 1994.

  Electron microscopic evidence of bacilliform virus infection in kuruma shrimp (*Penaeus japonicus*). Fish

  Pathol. 29, 121–125.
- Tang, X., Hew, C.L., 2007. Expression, purification and crystallization of two major envelope proteins from white spot syndrome virus. Acta Crystallogr. Sect. F Struct. Biol. Cryst. Commun. 63, 624–626.
- Thammasorn, T., Sangsuriya, P., Meemetta, W., Senapin, S., Jitrakorn, S., Rattanarojpong, T., Saksmerprome, V., 2015.

  Large-scale production and antiviral efficacy of multi-target double-stranded RNA for the prevention of white spot syndrome virus (WSSV) in shrimp. BMC Biotechnol. 15, 110. doi:10.1186/s12896-015-0226-9
- Thitamadee, S., Prachumwat, A., Srisala, J., Jaroenlak, P., Salachan, P.V., Sritunyalucksana, K., Flegel, T.W.,

- Itsathitphaisarn, O., 2016. Review of current disease threats for cultivated penaeid shrimp in Asia. Aquaculture 452, 69–87. doi:10.1016/j.aquaculture.2015.10.028
- Timmons, L., Court, D.L., Fire, A., 2001. Ingestion of bacterially expressed dsRNAs can produce speci ® c and potent genetic interference in *Caenorhabditis elegans* 263, 103–112.
- Tritschler, F., Huntzinger, E., Izaurralde, E., 2010. Role of GW182 proteins and PABPC1 in the miRNA pathway: a sense of déjà vu. Nat. Rev. Mol. Cell Biol. 11, 379–384. doi:10.1038/nrm2885
- Unajak, S., Boonsaeng, V., Jitrapakdee, S., 2006. Isolation and characterization of cDNA encoding Argonaute, a component of RNA silencing in shrimp (*Penaeus monodon*). Comp. Biochem. Physiol. B. Biochem. Mol. Biol. 145, 179–187. doi:10.1016/j.cbpb.2006.07.002
- van der Krol, A.R., Mur, L.A., Beld, M., Mol, J.N., Stuitje, A.R., 1990. Flavonoid genes in petunia: addition of a limited number of gene copies may lead to a suppression of gene expression. Plant Cell 2, 291–299. doi:10.1105/tpc.2.4.291
- van Hulten, M.C.W., Witteveldt, J., Peters, S., Kloosterboer, N., Tarchini, R., Fiers, M., Sandbrink, H., Lankhorst, R.K., Vlak, J.M., 2001. The white spot syndrome virus DNA genome sequence. Virology 286, 7–22.
- Verbruggen, B., Bickley, L.K., Aerle, R. Van, Bateman, K.S., Stentiford, G.D., Santos, E.M., Tyler, C.R., 2016. Molecular Mechanisms of White Spot Syndrome Virus Infection and Perspectives on Treatments 1–29. doi:10.3390/v8010023
- Wang, S., Chen, A.J., Shi, L.J., Zhao, X.F., Wang, J.X., 2012. TRBP and elF6 homologue in *Marsupenaeus japonicus* play crucial roles in antiviral response. PLoS One 7, 1–10. doi:10.1371/journal.pone.0030057
- Wongteerasupaya, C., Vickers, J.E., Sriurairatana, S., Nash, G.L., Akarajamorn, A., Boonsaeng, V., Panyim, S., Tassanakajon, A., Withyachumnarnkul, B., Flegel, T.W., 1995. A non-occluded, systemic baculovirus that occurs in cells of ectodermal and mesodermal origin and causes high mortality in the black tiger prawn *Penaeus monodon*. Dis. Aquat. Organ. 21, 69–77.
- Wongteerasupaya, C., Wongwisansri, S., Boonsaeng, V., Panyim, S., Pratanpipat, P., Nash, G.L., Withyachumnarnkul, B., Flegel, T.W., 1996. DNA fragment of *Penaeus monodon* baculovirus PmNOBII gives positive in situ hybridization with white-spot viral infections in six penaeid shrimp species. Aquaculture 143, 23–32.
- Xu, D., Liu, W., Alvarez, A., Huang, T., 2014. Cellular immune responses against viral pathogens in shrimp. Dev. Comp. Immunol. 47, 287–297. doi:10.1016/j.dci.2014.08.004
- Yang, L., Li, X., Huang, J., Zhou, F., Su, T., Jiang, S., 2013. Isolation and characterization of homologous TRBP cDNA for RNA interference in *Penaeus monodon*. Fish Shellfish Immunol. 34, 704–711. doi:10.1016/j.fsi.2012.11.022
- Yang, L., Li, X., Jiang, S., Qiu, L., Zhou, F., Liu, W., Jiang, S., 2014. Characterization of Argonaute2 gene from black tiger shrimp (*Penaeus monodon*) and its responses to immune challenges. Fish Shellfish Immunol. 36,

#### 261-269. doi:10.1016/j.fsi.2013.11.010

- Yang, Z.-K., Niu, Y.-F., Ma, Y.-H., Xue, J., Zhang, M.-H., Yang, W.-D., Liu, J.-S., Lu, S.-H., Guan, Y., Li, H.-Y., 2013.

  Molecular and cellular mechanisms of neutral lipid accumulation in diatom following nitrogen deprivation.

  Biotechnol. Biofuels 6, 67. doi:10.1186/1754-6834-6-67
- Yao, X., Wang, L., Song, L., Zhang, H., Dong, C., Zhang, Y., Qiu, L., Shi, Y., Zhao, J., Bi, Y., 2010. A Dicer-1 gene from white shrimp *Litopenaeus vannamei*: Expression pattern in the processes of immune response and larval development. Fish Shellfish Immunol. 29, 565–570. doi:10.1016/j.fsi.2010.05.016
- Yi, R., Qin, Y., Macara, I.G., Cullen, B.R., 2003. Exportin-5 mediates the nuclear export of pre-microRNAs and short hairpin RNAs. Genes Dev. 17, 3011–3016.
- Yiu, S.M., Wong, P.W.H., Lam, T.W., Mui, Y.C., Kung, H.F., Lin, M., Cheung, Y.T., 2005. Filtering of ineffective siRNAs and improved siRNA design tool. Bioinformatics 21, 144–151. doi:10.1093/bioinformatics/bth498
- Yodmuang, S., Tirasophon, W., Roshorm, Y., Chinnirunvong, W., Panyim, S., 2006. YHV-protease dsRNA inhibits YHV replication in *Penaeus monodon* and prevents mortality. Biochem. Biophys. Res. Commun. 341, 351–356. doi:10.1016/j.bbrc.2005.12.186
- Zhou, Q., Xu, L., Li, H., Qi, Y.-P., Yang, F., 2009. Four major envelope proteins of white spot syndrome virus bind to form a complex. J. Virol. 83, 4709–4712.

# 7 Output จากโครงการวิจัยที่ได้รับทุนจาก สกว.

- 1. ผลงานตีพิมพ์ในวารสารวิชาการนานาชาติ (ระบุชื่อผู้แต่ง ชื่อเรื่อง ชื่อวารสาร ปี เล่ม ที่ เลขที่ และหน้า) หรือผลงานตามที่คาดไว้ในสัญญาโครงการ
  - เนื่องจากโครงการที่ดำเนินการอยู่ยังไม่ประสบผลสำเร็จ จึงขอใช้งานวิจัยเรื่อง "Identification, characterization and heparin binding capacity of a sporewall, virulence protein from the shrimp microsporidian, Enterocytozoon hepatopenaei (EHP)" เพื่อปิดโครงการวิจัยนี้ ผลงานวิจัยนี้มี ดร. อรชุมา อิฐ สถิตไพศาล เป็น corresponding author และได้รับการตอบรับการตีพิมพ์แล้ว จากวราสาร Parasite & Vector (Quartile 1)
- 2. การนำผลงานวิจัยไปใช้ประโยชน์
  - เชิงวิชาการ (มีการพัฒนาการเรียนการสอน/สร้างนักวิจัยใหม่)
    - ผลิตนักศึกษาระดับปริญญาโท สาขาชีวเคมี (หลักสูตรนานาชาติ) คณะ วิทยาศาสตร์ มหาวิทยาลัยมหิดล 1 คน
    - ผลิตนักศึกษาระดับปริญญาดุษฎีบัณฑิต สาขาชีวเคมี (หลักสูตรนานาชาติ) คณะวิทยาศาสตร์ มหาวิทยาลัยมหิดล 1 คน
- 3. อื่นๆ (เช่น ผลงานตีพิมพ์ในวารสารวิชาการในประเทศ การเสนอผลงานในที่ประชุม วิชาการ หนังสือ การจดสิทธิบัตร)
  - นำเสนอผลงานแบบโปสเตอร์ โดย นางสาว พชา สุดสัตย์ (นักศึกษาระดับปริญญาโท) Sudsat P, Ananphongmanee V, Jitrakorn S, Prachumwat A, Ongvarrasopone C, Panyim S, and <u>Itsathitphaisarn O</u>. An investigation into the effect of GW182 knockdown in WSSV-infected Penaeus vannamei. The 5th International Biochemistry and Molecular Biology conference (BMB), Songkhla, Thailand, 23-25 May 2016
  - ผลงานดีพิมพ์แบบ Proceedings ของนางสาวพชา สุดสัยต์ Sudsat P, Posiri P, Ongvarrasopone C, Panyim S, and <u>Itsathitphaisarn O</u>. 'Comparison of Knockdown Efficiency of GW182 by dsRNAs Specific to GW182. The 5<sup>th</sup> International Conference on Agriculture, Ecology and Biological Engineering (AEBE), Chonburi, Thailand, 2-4 May 2017

From: Parasite & Vectors em@editorialmanager.com

Subject: Decision has been reached on your submission to Parasites & Vectors - PARV-D-17-01200R3

Date: 27 กุมภาพันธ์ 2561 21:32

To: Ornchuma Itsathitphaisarn ornchuma.its@mahidol.ac.th

#### PARV-D-17-01200R3

Identification, characterization and heparin binding capacity of a spore-wall, virulence protein from the shrimp microsporidian, Enterocytozoon hepatopenaei (EHP)

Pattana Jaroenlak; Dominic Wiredu Boakye; Rapeepun Vanichviriyakit; Bryony A. P. Williams; Kallaya Sritunyalucksana; Ornchuma Itsathitphaisarn

Parasites & Vectors

Dear Dr. Itsathitphaisarn,

I am pleased to inform you that your manuscript "Identification, characterization and heparin binding capacity of a spore-wall, virulence protein from the shrimp microsporidian, Enterocytozoon hepatopenaei (EHP)" (PARV-D-17-01200R3) has been accepted for publication in Parasites & Vectors.

Before publication, our production team will check the format of your manuscript to ensure that it conforms to the standards of the journal. They will be in touch shortly to request any necessary changes, or to confirm that none are needed.

Any final comments from our reviewers or editors can be found, below. Please quote your manuscript number, PARV-D-17-01200R3, when inquiring about this submission.

We look forward to publishing your manuscript and I do hope you will consider Parasites & Vectors again in the future.

Best wishes,

Frank Katzer, D.Phil Parasites & Vectors https://parasitesandvectors.biomedcentral.com/

Comments:



# **Parasites & Vectors**

Identification, characterization and heparin binding capacity of a spore-wall, virulence protein from the shrimp microsporidian, Enterocytozoon hepatopenaei (EHP)

--Manuscript Draft--

Manuscript Number:	PARV-D-17-01200R3		
Full Title:		zation and heparin binding capacity of a spore-wall, virulence microsporidian, Enterocytozoon hepatopenaei (EHP)	
Article Type:	Research		
Section/Category:	Protozoan Biology and Disease		
Funding Information:	Agricultural Research Development Agency (CRP5905020530)	Ornchuma Itsathitphaisarn	
	Thailand Research Fund (IRG5980008)	Ornchuma Itsathitphaisarn	
	Thailand Research Fund (TRG5780032)	Ornchuma Itsathitphaisarn	
	Newton Institutional Links (IL) program to BIOTEC, Thailand and Cefas, UK	Kallaya Sritunyalucksana	
	Science Achievement Scholarship of Thailand (SAST)	Mr. Pattana Jaroenlak	
Abstract:	Background: The microsporidian Enterocytozoon hepatopenaei (EHP) is a spore-forming, intracellular parasite that causes an economically debilitating disease (hepatopancreatic microsporidiosis or HPM) in cultured shrimp. HPM is characterized by growth retardation and wide size variation that can result in economic loss for shrimp farmers. Currently, the infection mechanism of EHP in shrimp is poorly understood, especially at the level of host-parasite interaction. In other microsporidia, spore wall proteins have been reported to be involved in host cell recognition. For the host, heparin, a glycosaminoglycan (GAG) molecule found on cell surfaces, has been shown to be recognized by many parasites such as Plasmodium spp. and Leishmania spp.  Results: We identified and characterized the first spore wall protein of EHP (EhSWP1). EhSWP1 contains three heparin binding motifs (HBMs) at its N-terminus and a Binamphiphysin-Rvs-2 (BAR2) domain at its C-terminus. A phylogenetic analysis revealed that EhSWP1 is similar to an uncharacterized spore wall protein from Enterospora canceri. In a cohabitation bioassay using EHP-infected shrimp with naïve shrimp, the expression of EhSWP1 was detected by RT-PCR in the naïve test shrimp at 20 days after the start of cohabitation. Immunofluorescence analysis confirmed that EhSWP1 was localized in the walls of purified, mature spores. Subcellular localization by an immunoelectron assay revealed that EhSWP1 was distributed in both the endospore and exospore layers. An in vitro binding assay, a competition assay and mutagenesis studies revealed that EhSWP1 is a bona fide heparin binding protein. Conclusions: Based on our results, we hypothesize that EhSWP1 is an important host-parasite interaction protein involved in tethering spores to host-cell-surface heparin during the process of infection.		
Corresponding Author:	Ornchuma Itsathitphaisarn Department of Biochemistry and Center of Excellence for Shrimp Molecular Biology and Biotechnology (Centex Shrimp), Faculty of Science, Mahidol University, Bangkok THAILAND		
Corresponding Author Secondary Information:			
Corresponding Author's Institution:	Department of Biochemistry and Center of Excellence for Shrimp Molecular Biology and Biotechnology (Centex Shrimp), Faculty of Science, Mahidol University, Bangkok		
Corresponding Author's Secondary Institution:			
First Author:	Pattana Jaroenlak		

First Author Secondary Information:	
Order of Authors:	Pattana Jaroenlak
	Dominic Wiredu Boakye
	Rapeepun Vanichviriyakit
	Bryony A. P. Williams
	Kallaya Sritunyalucksana
	Ornchuma Itsathitphaisarn
Order of Authors Secondary Information:	
Response to Reviewers:	Dear Editor,
	We write to resubmit the final revised version of our manuscript entitled "Identification, characterization and heparin binding activity of a spore-wall, virulence protein from the shrimp microsporidian, Enterocytozoon hepatopenaei"
	Changes in the manuscript were revised and accepted. They did not affect the scientific meaning of the manuscript. I, however, prefer the unitalicized version of via.
	Additional information and requested clarifications were provided. The final revised file is PARV-D-17-01200_R2 EDIT SC_PJ_OI.docx
	Thank you very much for considering our work for publication at Parasites and Vectors.
	Sincerely,
	Ornchuma Itsathitphaisarn
	Ornchuma Itsathitphaisarn Lecturer of Biochemistry
Additional Information:	
Question	Response
Are you submitting to an Article Collection?	No

Please, use this copy edited file for revision, there are many formatting changes. Do not change the file name, just add your initials.

Identification, characterization and heparin binding capacity of a spore-wall, virulence protein from the shrimp microsporidian, *Enterocytozoon hepatopenaei* (EHP)

Pattana Jaroenlak<sup>1,2</sup>, Dominic Wiredu Boakye<sup>3</sup>, Rapeepun Vanichviriyakit<sup>2,4</sup>, Bryony A. P. Williams<sup>3</sup>, Kallaya Sritunyalucksana<sup>5,6</sup> and Ornchuma Itsathitphaisarn<sup>1,2\*</sup>

<sup>1</sup>Department of Biochemistry, Faculty of Science, Mahidol University, Bangkok, Thailand.

<sup>2</sup>Center of Excellence for Shrimp Molecular Biology and Biotechnology (Centex Shrimp), Faculty of Science, Mahidol University, Bangkok, Thailand.

<sup>3</sup>Biosciences, College of Life and Environmental Sciences, University of Exeter, Devon, United Kingdom.

<sup>4</sup>Department of Anatomy, Faculty of Science, Mahidol University, Bangkok, Thailand.

<sup>5</sup>National Center for Genetic Engineering and Biotechnology (BIOTEC), National Science and Technology Development Agency (NSTDA), Pathumthani, Thailand.

<sup>6</sup>Shrimp Pathogen Interaction Laboratory (SPI), National Center for Genetic Engineering and Biotechnology (BIOTEC), Bangkok, Thailand.

\*Correspondence: ornchuma.its@mahidol.ac.th

E-mails

Pattana Jaroenlak: p.jaroenlak@gmail.com

Dominic Wiredu Boakye: d.wiredu-boakye@exeter.ac.uk

Rapeepun Vanichviriyakit: vrapeepun@gmail.com

Bryony A. P. Williams: b.a.p.williams@exeter.ac.uk

Kallaya Sritunyalucksana: kallaya@biotec.or.th

Ornchuma Itsathitphaisarn: ornchuma.its@mahidol.ac.th

### **Abstract**

intracellular parasite that causes an economically debilitating disease (hepatopancreatic microsporidiosis or HPM) in cultured shrimp. HPM is characterized by growth retardation and wide size variation that can result in economic loss for shrimp farmers. Currently, the infection mechanism of EHP in shrimp is poorly understood, especially at the level of host-parasite interaction. In other microsporidia, spore wall proteins have been reported to be involved in host cell recognition. For the host, heparin, a glycosaminoglycan (GAG) molecule found on cell surfaces, has been shown to be recognized by many parasites such as *Plasmodium* spp. and *Leishmania* spp. **Results:** We identified and characterized the first spore wall protein of EHP (EhSWP1). EhSWP1 contains three heparin binding motifs (HBMs) at its N-terminus and a Bin-amphiphysin-Rvs-2 (BAR2) domain at its C-terminus. A phylogenetic analysis revealed that EhSWP1 is similar to an uncharacterized spore wall protein from Enterospora canceri. In a cohabitation bioassay using EHPinfected shrimp with naïve shrimp, the expression of *EhSWP1* was detected by RT-PCR in the naïve test shrimp at 20 days after the start of cohabitation. Immunofluorescence analysis confirmed that EhSWP1 was localized in the walls of purified, mature spores. Subcellular localization by an immunoelectron assay revealed that EhSWP1 was distributed in both the endospore and exospore layers. An *in vitro* binding assay, a competition assay and mutagenesis studies revealed that

**Background:** The microsporidian *Enterocytozoon hepatopenaei* (EHP) is a spore-forming,

**Conclusions:** Based on our results, we hypothesize that EhSWP1 is an important host-parasite interaction protein involved in tethering spores to host-cell-surface heparin during the process of infection.

**Keywords:** EHP, *Enterocytozoon hepatopenaei*, Spore wall protein, SWP, Heparin, Heparin binding protein

# Background

EhSWP1 is a *bona fide* heparin binding protein.

Microsporidia are obligate, intracellular, spore-forming parasites and currently considered as a sister group to fungi [1]. Microsporidia are important pathogens that infect a wide range of animal hosts from beneficial invertebrate to vertebrate species [2, 3]. Since the discovery of the first microsporidian *Nosema bombycis* in silkworms in the nineteenth century [4], it remains the cause of a fatal disease referred to as Pébrine that causes economic losses in the sericulture industry [5, 6].

Enterocytozoon hepatopenaei (EHP) is a close evolutionarily relative of Enterocytozoon bieneusi and other human-infecting microsporidia in the genus Encephalitozoon that cause life-threatening diarrhea in immunocompromized humans [7]. In aquatic animals, infection of microsporidia in fish leads to reduction in growth rate and productivity [8], and this is true also for EHP in shrimp [9].

Microsporidia display many unique cellular and genetic characteristics. At the cellular level, microsporidia lack peroxisomes and a typical Golgi structure [10, 11]. Their mitochondria are structurally and functionally reduced into organelles called mitosomes [12, 13]. Their genomes are remarkably compact due to the loss of genes in metabolic pathways and reduction in intergenic spaces [14]. The 2.3 Mbp genome of *E. intestinalis* is the smallest eukaryotic genome known to date [15]. In addition, microsporidia have developed a characteristic invasion mechanism that involves the polar tube and the spore wall [16]. At the first step of infection, the spore wall proteins are capable of interacting with host cell glycosaminoglycans (GAGs) [17, 18]. Under suitable conditions, the polar tube is extruded to pierce the host cell membrane. This process rapidly occurs in less than 2 milliseconds [11, 19]. The polar tube then serves as a conduit to transfer an infectious sporoplasm into the host cell to begin the parasitic, intracellular phase of the life cycle [11].

The spore walls of microsporidia consist of two layers, a proteinaceous electron dense exospore layer and a chitinous electron lucent endospore layer [20]. Many spore wall proteins (SWPs) are found in these layers [21]. They participate in the host cell recognition process and provide structural support for the spore wall [17, 21, 22]. SWPs have been extensively characterized for the genera *Nosema* and *Encephalitozoon*. These include NbSWP5, NbSWP11, NbSWP12, NbSWP16, NbSWP25 and NbSWP26 from *N. bombycis* [22–27], EcEnP1, EcEnP2 and chitin deacetylase (EcCDA) from *E. cuniculi* [28, 29], and EiEnP1 from *E. intestinalis* [18]. Recently, *Antonospora locustae* SWP2 (AlocSWP2) has been shown to be involved in sporulation [30].

Hepatopancreatic microsporidiosis (HPM) in cultivated shrimp is characterized by slow growth and wide size variation, making the causative agent *E. hepatopenaei* (EHP) an economically important pathogen for shrimp farmers [31, 32]. EHP was initially reported as a new, undescribed microsporidian in hepatopancreatic tissue of the black tiger shrimp *Penaeus monodon* in Thailand in 2004 [33], but it was not characterized and named as a new species until 2009 [34]. Thus, it was an endemic pathogen that was also able to cause disease in the exotic Pacific-white shrimp *P. vannamei* [35] that replaced *P. monodon* as the dominant and most economically important shrimp species cultivated in Thailand. Currently, EHP is known to occur widely in Asia (e.g. Thailand, China, India, Vietnam, Indonesia and Malaysia) and it has been reported more recently from Venezuela

[34, 36–38]. In Thailand, EHP is now the third most serious problem for shrimp farmers after white spot disease (WSD) caused by white spot syndrome virus and acute hepatopancreatic necrosis disease (AHPND) caused by unique *Vibrio* isolates that produce Pir-like toxins [9].

Since EHP is a threat to the global shrimp industry, a better understanding of its infection mechanisms and virulence is urgently needed to facilitate the development of preventative and therapeutic strategies. Previously, a cohabitation assay revealed that EHP can be horizontally transmitted via water in shrimp cultivation ponds [39]. Thus, any treatment or management protocol that would stop or interfere with transmission would constitute an effective control measure. However, knowledge of how EHP interacts with the host is still poorly understood. This study therefore aimed at a better understanding of the process. From whole genome sequencing of EHP [40], the spore wall protein EhSWP1 was first identified and its gene sequence was used to develop a more specific PCR detection method called SWP-PCR [31]. Here, we functionally characterize EhSWP1, show that it contains three heparin binding motifs (HBMs) and one Bin-amphiphysin-Rvs-2 (BAR2) domain, that it is localized in the exospore and endospore layers, and that interacts with heparin via its HBMs. We hypothesize that EHP uses this recognition process to initiate host cell infection, and we hope that this understanding may lead to identification of vulnerable targets for development of preventative and therapeutic methods to control EHP in the shrimp aquaculture industry.

### **Methods**

#### **Shrimp and EHP specimens**

With permission from the farm owners to collect specimens for this study from their properties, EHP-infected *P. vannamei* (7–10 g) were collected from commercial shrimp farms in Thailand. Hepatopancreata of EHP-infected shrimp were dissected as previously described [31] to obtain spores for purification by discontinuous Percoll gradient centrifugation [40]. The purified spores were washed with sterile distilled water and stored at room temperature.

#### **Bioinformatics analysis**

In this study, we used predicted proteins encoded by the genomes of 23 microsporidian species (*Enterospora canceri*, *Enterocytozoon hepatopenaei*, *Hepatospora eriocheir*, *Hepatospora eriocheir* canceri, *Anncaliia algerae*, *Ordospora colligata*, *Trachipleistophora hominis*, *Spraguea lophii*,

Vittaforma corneae, Encephalitozoon romaleae, Vavraia culicis, Edhazardia aedis, Encephalitozoon hellem Swiss, Encephalitozoon hellem ATCC, Nematocida parisii ERTm1, Nematocida parisii ERTm3, Nematocida sp. ERTm2, Nematocida sp. ERTm6, Enterocytozoon bieneusi, Encephalitozoon intestinalis, Encephalitozoon cuniculi, Nosema bombycis and Nosema ceranae). These were downloaded from public databases NCBI and MicrosporidiaDB. Ortholog clusters in which these proteins belonged were identified by initially querying the proteins from all 23 microsporidian genomes against their own database by using BLASTP with an e-value cut-off of 1e-03 [41]. An ortholog prediction program, ORTHOMCL on its default settings, was then used to convert the BLASTP output into ortholog clusters [42]. Phylogenetic assessment of the ortholog groups in which EHP SWPs were grouped was performed as follows. The proteins in the two ortholog groups in which EHP SWPs were clustered were first aligned with the online MAFFT program using the L-INS-I iterative refinement setting and then trimmed with GBLOCKS with less stringent settings (allowing smaller final blocks, gap positions in the final blocks and less strict flanking positions). A Bayesian inference method was also used to infer the phylogenetic relationship between the proteins in the ortholog clusters. Here, the trimmed alignment was passed to the online MR BAYES tool on the CIPRES online portal. MR BAYES was run using an LG+GAMMA model and default settings [43]. Subsequent phylogenetic analyses performed on the SWP12 clade were performed following the same protocols as explained above. Although EHP00 1468 did not cluster with any microsporidian protein in our ORTHOMCL analyses, we included it in our phylogenetic analyses as it had 98% identity to EHP00\_350 in initial BLASTP analyses.

Conserved domains of proteins were predicted with MOTIF SCAN
(http://www.genome.jp/tools/motif/). MOTIF SCAN searches protein sequences against a PFAM library of Hidden Markov Models (HMMs). To further assess the conservation of BAR2 domains within proteins in the SWP ortholog clusters, a pairwise alignment with the EMBOSS STRETCHER tool (https://www.ebi.ac.uk/Tools/psa/emboss\_stretcher/) of each protein against the PFAM BAR2 consensus sequence was performed. This is the consensus alignment sequence of seed proteins used by PFAM for the construction of the BAR2 HMM. The complete PFAM seed library for various functional domains can be downloaded from ftp://ftp.ebi.ac.uk/pub/databases/Pfam/current\_release/Pfam-A.seed.gz. Phosphorylation site prediction was carried out by SCANPROSITE tool (http://prosite.expasy.org/prosite.html).

NETNGLYC (http://www.cbs.dtu.dk/services/NetNGlyc/) and NETOGLYC

(http://www.cbs.dtu.dk/services/NetOGlyc/) were used to predict N- and O-glycosylation sites, respectively.

#### Reverse transcription PCR (RT-PCR) analysis

To achieve EHP infections, naïve, uninfected, test P. vannamei were co-habitated with EHPinfected P. vannamei as previously described [39]. Briefly, naïve P. vannamei shrimp were kept in tanks containing 150 l artificial seawater (Mariscience Co. Ltd, Bangkok, Thailand) at 25 ppt and 28 °C with a basket cage containing EHP-infected P. vannamei in the center of the tank. At 0, 5, 7, 9, 11 and 20 days after cohabitation, shrimp were collected and their hepatopancreatic tissue was aseptically removed for RNA extraction. Total RNA was extracted using Ribozol RNA extraction reagent (Amresco, Philadelphia, USA) and used as template RNA in reverse transcription reactions employing ImPromp-II reverse transcriptase (Promega, Wisconsin, USA) to produce cDNA using an oligo-dT primer. cDNA was subsequently used as the template for standard PCR with Green PCR master mix containing Taq DNA polymerase (Biotechrabbit, Hennigsdorf, Germany). The fulllength EhSWP1 gene was amplified by specific primer pairs, EHP\_SWP01\_F; 5'--ATA TCC ATG GGC ATG TTA GAA GAT GCA AAG-3' and EHP SWP01 R; 5'-ATA TCT CGA GAG AAA ATT TTT CAA GGT G-3'. Specific primer pairs for the actin gene of *P. vannamei (PvActin)* were used as an internal control (Actin\_F; 5'-CCT CGC TGG AGA AGT CCT AC3' and Actin\_R; 5'-TGG TCC AGA CTC GTC GTA CTC-3') [31, 44]. The PCR protocol for both EhSWP1 and PvActin was as follows: denaturation at 95 °C for 5 min followed by 30 cycles of 30 s denaturation at 95 °C, 30 s annealing at 55 °C and 45 s extension at 68 °C, with a final extension for 5 min at 68 °C. The expected PCR amplicons were 687 bp and 401 bp for *EhSWP1* and *PvActin*, respectively. The amplicons were analyzed by 1.5% agarose gel electrophoresis with ethidium bromide staining.

#### Molecular cloning, expression, and purification of recombinant EhSWP1

The complete ORF of *EhSWP1* (687 bp) was amplified from cDNA obtained from the hepatopancreas of EHP-infected shrimp (GenBank accession no. MG015710). PCR conditions were the same as previously described in the RT-PCR analysis section. The gene was inserted between *NcoI* and *XhoI* restriction sites of the pET28 expression vector (Novagen, Queensland, Australia) to generate a pET28a\_SWP1 that was transformed into *Escherichia coli* BL21 Star (DE3). Positive clones were analyzed by restriction endonuclease analysis and confirmed by DNA sequencing (Macrogen, South Korea). A selected positive clone was grown in Luria-Bertani (LB) medium and

induced with 0.4 mM IPTG (isopropyl  $\beta$ -D-1-thiogalactopyranoside) at 37 °C for 4 h. Bacterial cells were harvested by centrifugation at 14,000 × g at 4 °C for 10 min.

To purify recombinant EhSWP1, a bacterial cell pellet was re-suspended with 1× PBS and broken by sonication. After that, the mixture was centrifuged at 14,000 × *g* at 4 °C for 15 min. The supernatant was collected and mixed with protein lysis buffer (50 mM NaH<sub>2</sub>PO<sub>4</sub>, 300 mM NaCl, 10 mM imidazole; pH 8) prior to loading onto a Ni<sup>2+</sup>-NTA affinity column (Qiagen, Hilden, Germany). Protein and Ni<sup>2+</sup>-beads were incubated for 1 h at 4 °C. Then, the column was washed with 10 column volumes of wash buffer (50 mM NaH<sub>2</sub>PO<sub>4</sub>, 300 mM NaCl, 20 mM imidazole; pH 8). The purified recombinant EhSWP1 was eluted with elution buffer (50 mM NaH<sub>2</sub>PO<sub>4</sub>, 300 mM NaCl, 250 mM imidazole; pH 8). All protein fractions were analyzed by 12.5% SDS-PAGE. Protein concentrations were measured using Bradford reagent (BioRad, California, USA). The purified recombinant EhSWP1 was dialyzed against 1× PBS at 4 °C overnight.

## Polyclonal antibody production and Western blot analysis

To produce a polyclonal antibody against EhSWP1, purified recombinant EhSWP1 was sent to a commercial antibody production facility (Singapore Advanced Biologics, Singapore) to immunize rabbits. After the third immunization, rabbit sera containing anti-EhSWP1 antibody were collected and specificity of anti-EhSWP1 antibody was tested by Western blot analysis.

For Western blot analysis, purified recombinant EhSWP1 was separated by 12.5% SDS-PAGE and transferred to a nitrocellulose membrane. The membrane was blocked with blocking solution (5% skim milk in 1× PBS) for 1 h at room temperature (RT) followed by incubation with 1:2,000 anti-EhSWP1 antibody or naïve rabbit serum as a negative control in blocking solution for 1 h at RT. After six washes with PBST buffer (1× PBS, 0.05% Tween 20), 1:3,000 goat anti-rabbit IgG conjugated with alkaline phosphatase enzyme (GAR-AP) was applied for 1 h at RT and later washed with PBST buffer three times. Finally, colorimetric signals were developed by BCIP/NBT phosphatase substrate (Millipore, Massachusetts, USA).

#### Immunofluorescence analysis (IFA)

Purified EHP spores were added onto poly-lysine coated slides and dried at RT overnight. The spores were fixed with 4% paraformaldehyde at RT for 15 min followed by washing with  $1 \times PBS$  three times and permeabilized with 1% Triton X-100 at RT for 30 min. Next, the spores were blocked with blocking reagent (10% normal goat serum, 5% bovine serum albumin in  $1 \times PBS$ ) at

RT for 90 min prior to incubation with 1:100 anti-EhSWP1 antibody in blocking reagent at RT for 3 h. The negative control group was incubated with naïve rabbit serum. After six washes, 1:200 goat anti-rabbit antibody conjugated with Alexa 488 (GAR-Alexa488) was added and incubated at RT for 1 h. 1:2,000 TO-PRO-3 dye was used to stain nuclei for 5 min at RT. Finally, slides were mounted with 50% glycerol. The fluorescence signals were examined using a confocal laser scanning microscope (Olympus FV10i-DOC).

#### Immunoelectron analysis (IEM)

Purified EHP spores and EHP-infected hepatopancreatic tissue were fixed with 4% paraformaldehyde and 0.5% glutaraldehyde in 0.1 M sodium cacodylate buffer pH 7.2 for 1 h at RT and then rinsed with 1× PBS four times. The samples were dehydrated with a graded ethanol series including 50%, 75% and 100% for 15 min each step followed by permeabilizing and embedding in LR-white (Electron Microscopy Sciences, Pennsylvania, USA). LR-white was polymerized at 65 °C overnight. Next, ultrathin sections were placed onto 300-mesh nickel grids. For immunostaining, the grids were blocked with blocking solution (1% bovine serum albumin, 0.02% NaN<sub>3</sub>, 5% normal goat serum in 1× PBS) for 2 h at RT and incubated with 1:10 anti-EhSWP1 antibody in blocking solution for 2 h at RT. For the negative control group, naïve rabbit serum was used instead of anti-EhSWP1 antibody. After six washes with 1× PBS, 1:100 anti-rabbit IgG conjugated with 10 nm gold particles (Sigma-Aldrich, Massachusetts, USA) in blocking solution was applied onto the grids for 1 h at RT and then washed with distilled water. Finally, the grids were counterstained using 4% uranyl acetate for 2 min and gold particles were examined under a Hitachi H7100 transmission electron microscope (TEM) at an accelerating voltage of 100 kV.

## Site-directed mutagenesis of *EhSWP1*

Basic amino acid residues of all three HBMs found in *EhSWP1* gene were mutated into glycine or serine using a gene synthesis facility (Synbio Technologies, USA). *EhSWP1*(B→G) contained the following mutations: R11G, K12G, K14G, K15G, R35G, K36G, R38G, K62G, H63G, H65G and H66G, while *EhSWP1*(B→S) contained mutations R11S, K12S, K14S, K15S, R35S, K36S, R38S, K62S, H63S, H65S and H66S. After that, mutated *EhSWP1* genes were subcloned into the pET28a expression vector (Novagen, Queensland, Australia). Protein expression and purification were followed as previously described for EhSWP1 WT.

#### Heparin bead binding and competition assays

Purified recombinant EhSWP1 (20  $\mu$ g) or 20  $\mu$ g of bovine serum albumin (Sigma-Aldrich, Massachusetts, USA) were mixed with 50  $\mu$ l of pre-equilibrated heparin-sepharose beads (50% slurry) with 1× PBS (GE Healthcare, Buckinghamshire, UK) at 4 °C for 1 h with radial rotation. For the heparin competition assay, various concentrations (0.1, 1, 10 and 100 mg/ml) of porcine heparin sodium salt (Sigma-Aldrich, Massachusetts, USA) were mixed with recombinant EhSWP1 prior to incubation with heparin-sepharose beads. The beads were then washed three times with 1× PBS (5 min incubation in each washing step). Proteins were eluted with elution buffer (2 M NaCl in 1× PBS). All protein fractions were visualized by 12.5% SDS-PAGE with Coomassie blue staining. To quantify the level of heparin binding, the intensity of the protein band was quantified using Scion Image software (Version 4.0). Level of heparin binding in the group without competitor (0 mg/ml heparin group) was used for normalization.

#### **Statistical analysis**

The percentages of heparin binding were expressed as means  $\pm$  standard error of the mean (SEM). The difference between each heparin concentration was tested using one-way ANOVA.

#### **Results**

#### **Identification and characterization of EhSWP1**

To better understand the pathogenesis of EHP, a search for its potential virulence factors was carried out by analyzing the EHP genome [40] and categorizing genes according to their functions (Table 1). Putative EHP virulence factors included genes involved in host cell invasion, spore attachment, energy parasitism and host cell manipulation. To infect their host cells, microsporidia have been reported to utilize SWPs as a recognition system [17, 45]. Herein, we describe identification of a spore wall protein, EhSWP1 (EHP00\_686). The full-length coding sequence of *EhSWP1* is 687 bp encoding a deduced protein of 228 amino acids (GenBank accession no. MG015710), with a molecular mass of 27 kDa and a theoretical isoelectric point of 8.45.

#### Phylogenetic analysis of EhSWP1

An initial NCBI word search for SWP in the genomic assembly of EHP identified proteins with the following accession numbers OQS53864.1 (EHP00\_686), OQS55031.1 (EHP00\_944), OQS55055.1

(EHP00\_1468) and OQS53422.1 (EHP00\_350). In this study, we focused on EHP00\_686, which we named EhSWP1. Our orthology analyses revealed that EhSWP1 (EHP00\_686) and EHP00\_350 were in a different ortholog cluster from EHP00\_944 (Fig. 1). Interestingly, EHP00\_1468 did not cluster with any other microsporidian protein used in this analysis despite having a 98% identity to EHP00\_350 in our BLASTP search results. Bayesian inference (BI) analyses resulted in a tree that had representative proteins from the two ortholog clusters in two distinct clades (Fig. 1). The clade in which EhSWP1, EHP00\_350 and EHP00\_1468 clustered contained other microsporidian proteins that were predominantly annotated as SWP12, whereas EHP00\_944 was grouped within a clade containing proteins that were predominantly annotated as SWP7. Both SWP12 and SWP7 were previously described in *Nosema bombycis* [24, 46] and they were used as the name of the clades in this study. The phylogenetic relationship between these clades was however poorly supported statistically in both Bayesian and maximum likelihood (ML) analyses (Fig. 1). Apart from *Nematocida* species, all other microsporidian species used in this analysis were represented by at least a single protein in both the SWP12 and SWP7 clades (Fig. 2).

An initial search for functional domains in proteins belonging to the SWP12 clade showed that some of them encoded a Bin-amphiphysin-Rvs-2 (BAR2) domain. Unlike proteins in the SWP12 clade, a scan for functional domains for proteins in the SWP7 clade showed that they did not share a common functional domain. When aligned against the consensus sequence of BAR2 HMM seed sequences, proteins in the SWP12 clade showed amino acid similarity ranging between 20–29 %. The BAR2 domain of *Saccharomyces cerevisiae* protein YP148 that was one of the seed sequences used in the construction of the BAR2 HMM was 29% similar to the consensus sequence (data not shown). Proteins belonging to *V. corneae* and members of the family Encephalitozoonidae displayed the highest amino acid similarity (Fig. 2). Contrary to MOTIF SCAN results that predicted the BAR2 domains of most SWP12 clade proteins to be located in their C-terminus, amino acid pair-wise alignment analyses showed that the BAR2 domain spanned the entire length of these proteins.

A regular expression search predicted all proteins in the SWP12 clade to encode, at least, a single heparin binding motif (HBM) whereas only M896\_121080 (*Ordospora colligata*), EDEG\_03348 (*Edhazardia aedis*), NBO\_63g0026 (*Nosema bombycis*) and ECANGB1\_2681 (*Enterospora canceri*) in the SWP7 clade encoded heparin binding motifs. In this study, three HBMs were identified at the N-terminus of EhSWP1 (EHP00\_686). The position of the first XBBXBBX HBM was conserved only in the family Enterocytozoonidae whereas that of the second

XBBXBX HBM was conserved among most but not all microsporidian species (Fig. 2). Interestingly, the position of the third XBBXBX HBM was conserved only in EhSWP1 and ECANGB1\_2216. EHP00\_350 and EHP00\_1468 were the only proteins in this analyses that contained the XBBBXXBX HBM signature sequence.

EhSWP1 was among the few proteins that were not predicted to possess any O-glycosylation sites (see yellow stars in Fig. 2). While all proteins in the SWP12 clade were predicted to contain phosphorylation sites, none of them were positive for signal peptide sequences, GPI anchoring and transmembrane domains.

#### Gene expression pattern of EhSWP1 during an infection

To investigate the expression pattern of the *EhSWP1* gene, single step RT-PCR analysis was performed using cDNA generated from hepatopancreatic tissue of naïve shrimp collected on days 0, 5, 7, 9, 11 and 20 after cohabitation with EHP-infected shrimp. Positive RT-PCR amplicons for the *EhSWP1* gene were detected in the naïve shrimp at 20 days after the start of cohabitation (Fig. 3). However, subsequent testing using a more sensitive nested RT-PCR method revealed a low level of *EhSWP1* at 11 days after cohabitation (Additional file 1: Figure S1). This indicated that a measurable level of infection was evident much earlier than 20 days and that progression of the infection was not very rapid.

#### **Immunolocalization of EhSWP1**

Purified EhSWP1-His<sub>6</sub> was expressed in *E. coli*. After induction with IPTG, a 27 kDa overexpressed band of recombinant EhSWP1 was observed (Fig. 4a). Purification with Ni<sup>2+</sup>-NTA affinity chromatography showed that purified protein was found in fractions 2 to 5 (Fig. 4a: lanes E2–E5) after elution with 300 mM imidazole (Fig. 4b). Later, purified protein was pooled prior to immunization of rabbits to generate polyclonal antibody against EhSWP1. Specificity of the antibody was tested by western blot analysis (Fig. 4c). The result revealed a strong positive band at 27 kDa that was consistent with the size of recombinant EhSWP1 (Fig. 4c). Thus, anti-EhSWP1 antibody specifically bound to recombinant EhSWP1 and was suitable for localization studies.

When rabbit anti-EhSWP1 was used to perform immunofluorescence analysis (IFA) with purified spores of EHP, green fluorescence from Alexa-488 dye revealed that EhSWP1 was localized on their periphery (Fig. 5a). TO-PRO-3 dye (blue fluorescence) revealed the nucleus

within EHP spores (Fig. 5). For the negative control group, no green fluorescence was detected (Fig. 5b). Therefore, these data confirmed that EhSWP1 was an EHP spore-wall protein.

Further immunoelectron analysis (IEM) to determine the subcellular localization of EhSWP1 revealed immunogold particles in both the exospore (Ex) and endospore layers (En), but not in the plasmalemma (Fig. 6a, b) or in the spore cytoplasm. No immunogold particles were found in the negative control group (Fig. 6c).

#### Interaction of EhSWP1 with heparin and a competition assay

Since sequence analysis revealed that EhSWP1 had three heparin binding motifs at its N-terminus, preliminary assays were carried out to test its ability to bind with heparin *in vitro*. When recombinant EhSWP1 and BSA (Fig. 7a) were incubated with heparin beads, only recombinant EhSWP1 (but not BSA) was bound and subsequently eluted (Fig. 7b). It was possible but unlikely that the band in Fig. 7b arose from a contaminant *E. coli* protein of the same electrophoretic mobility as recombinant EhSWP1, but this possibility was eliminated in the following experiment below.

In addition, since previous studies [47, 48] showed that basic residues in HBM are important for its binding activity to negatively-charged heparin, we used in vitro mutation to determine whether the function of HBM in EhSWP1 was related to heparin binding. Positively charged amino acids arginine, lysine and histidine in the three HBMs were mutated to uncharged glycine [EhSWP1(B $\rightarrow$ G)], or to partially negative serine [EhSWP1(B $\rightarrow$ S)]. Due to the substitution of larger side chains with smaller side chains, EhSWP1(B→G) and EhSWP1(B→S) were1-kDa lower in molecular weight than EhSWP1 wild type (EhSWP1 WT). Mutation to alanine was also carried out. However, almost all of the overexpressed alanine mutant proteins were insoluble (data not shown). Input proteins for the binding experiment are shown in Fig. 8a. After incubation of EhSWP1 WT, EhSWP1( $B \rightarrow G$ ) and EhSWP1( $B \rightarrow S$ ) with heparin beads followed by elution with 2 M NaCl, only EhSWP1 WT was found in the elution fraction, not EhSWP1( $B \rightarrow G$ ) or EhSWP1( $B \rightarrow S$ ) (Fig. 8b). Western blot results using the anti-EhSWP1 antibody confirmed that only EhSWP1 WT did bind to heparin, while EhSWP1(B $\rightarrow$ G) and EhSWP1(B $\rightarrow$ S) did not (Fig. 8). This result confirmed that EhSWP1-HBMs are important for heparin binding. Since all three recombinant proteins were produced using the same E. coli expression system, the negative western blot results for EhSWP1( $B \rightarrow G$ ) or EhSWP1( $B \rightarrow S$ ) (Fig. 8b) also eliminated the unlikely possibility that the band

in Fig. 7b and the immunopositive band in Fig. 8b arose from a contaminant *E. coli* protein of the same electrophoretic mobility as recombinant EhSWP1.

To confirm specificity of the binding, competition assays using soluble heparin were carried out. By pre-incubating four different concentrations of soluble heparin with recombinant EhSWP1 prior to mixing with heparin-sepharose beads, it was shown that 10 mg/ml of soluble heparin could reduce the binding by more than 40% (Fig. 9, Additional file 2: Figure S2). Increasing the soluble heparin to 100 mg/ml reduced the binding by 84% (Fig. 9c). However, there was no reduction in binding when there was no exogenous heparin or heparin at 0.1 mg/ml (Fig. 9c). This result suggests that exogenous heparin can inhibit the interaction of EhSWP1 with heparin in a dose dependent manner and that heparin is indeed an EhSWP1 binding partner.

## **Discussion**

## Diversity and phylogeny of spore wall proteins

The microsporidian infection process is unique compared to that of other intracellular parasites [49, 50]. Their spores possess a special organelle called a polar tube that is extruded to pierce host cell membranes and serve as a conduit to transfer the infectious spore contents (sporoplasm) into the host cell cytoplasm [16]. However, microsporidia require relatively close proximity to host cells for the first step of infection [17, 45]. Previous studies have revealed that SWPs are important in the attachment of microsporidian spores to their hosts [17, 18].

Orthology clustering and phylogenetic analyses performed in this study identified the four proteins annotated as SWPs in EHPs genomic assembly [40] to fall under two distinct clades of microsporidian SWPs, SWP12 and SWP7. Signature sequences of HBMs are well characterized, namely XBBXBX, XBBXBBX, XBBBXXBX and XBBBXXBBBXXBBX, where X represents a hydrophobic amino acid and B represents a positively charged amino acid [48, 51, 52]. Although XBBXBX and XBBXBBX HBMs appeared to be highly conserved across the SWP12 clade in our analysis, their exact positioning and enrichment was specific to microsporidian families and sometimes, species (Fig. 2). In light of the importance of SWP HBMs in parasite-host tethering [18, 24], this family/species-specific HBM positioning and enrichment perhaps reflect the different host environs and cell types with which these proteins have evolved to interact. Our phylogenetic analysis suggests there was a duplication of the *SWP12* gene in the common ancestor of species belonging to the family Enterocytozoonidae, with positional conservation of HBMs only being

maintained in subclade 1 (Fig. 2). This duplication event, unique to the Enterocytozoonidae, hints at the importance of this particular protein in the life cycle of species within this family. Gene duplication is known to facilitate innovation in genomes by allowing the duplicate gene to develop new functional properties via the accruement of non-deleterious mutations, a process referred to as neofunctionalization. Finally, our analyses corroborated previous research that predicted NbSWP12 (NBO\_28g0066) and *E. intestinalis* EnP1 to contain 1 and 2 HBMs, respectively [18, 24].

Our alignment results suggest that the BAR2 domain is conserved across all proteins that clustered within the SWP12 clade. Known functions of this domain include membrane shaping and signalling control processes, but its role in microsporidian proteins is yet to be elucidated [53]. The conservation of this domain in the SWP12 clade, however, alludes to its importance in the function of SWP12 proteins [24].

### **Expression profiles of spore wall proteins**

Expression profiles of SWPs vary in different microsporidian species. Feeding of fourth instar silkworm larvae with mulberry leaves contaminated with *N. bombycis* spores showed that NbSWP5, NbSWP12 and NbSWP15 were expressed on day 3 post-infection [22, 24, 25]. In contrast, transcripts of NbSWP11 appeared at a low level on day 1 post-infection and gradually rose until day 7 [23]. Moreover, starvation treatment of third instar nymph locusts followed by feeding with *A. locustae* spores revealed that *Aloc*SWP2 expression was detected on day 9 after spore inoculation [30]. Our cohabitation study between naïve shrimp and EHP-infected shrimp showed that EhSWP1 transcripts were observed only at 20 days after the start of cohabitation. However, by using RT-PCR followed by nested-PCR analysis specific to the *EhSWP1* gene, a low level of expression was found at 11 days after cohabitation. The result may suggest that EHP requires at least 11 days to develop into mature spores. However, this needs to be confirmed by other analyses.

## **EhSWP1:** its role in host-cell tethering

Heparin is a member of the GAG family and has been extensively studied in vertebrate species. A major function of heparin is to serve as a blood anticoagulant [54]. It is also used as an antithrombotic agent against heart and vascular thrombosis [55]. In mammals, heparin is mainly distributed in the lungs, intestine and liver [56]. Heparin is not only found in vertebrates, but also in invertebrates including crustaceans, molluscs, annelids, echinoderms and chidarians [57]. However, there are very few studies on localization of heparin in organs and cell types. In the northern quahog

clam, heparin was found at the proximal to epithelial surfaces of cells in the intestine, palp and siphon [58]. For shrimp, there has been no study on heparin distribution. However, heparin has been successfully extracted from the cephalothorax (where the gills, heart, intestine and hepatopancreas are located [59]) in the red-spotted shrimp *P. brasilliensis* and the Pacific white shrimp *P. vannamei* [60, 61]. Transcriptomic analysis of the hepatopancreas of *P. vannamei* showed that genes involved in the GAG biosynthesis pathway were active [62] and suggested that heparin might be present in the hepatopancreas. In this study, we showed that EhSWP1 could bind to heparin using the *in vitro* heparin binding assay. From immunofluorescence and immunoelectron analyses of EHP spores, we also showed that EhSWP1 is localized in both the exospore and endospore layers, similar to what has been previously described for SWPs from other microsporidians including EiEnP1, NbSWP9 and NbSWP26 [18, 27, 63]. The results support our hypothesis that EHP uses EhSWP1 to bind to heparin of target cells in shrimp hepatopancreatic tissue (Fig. 10) [33, 34].

It is not only EHP that utilizes heparin for attachment to host cells. Other intracellular parasites such as *Trypanosoma cruzi* also use heparin-binding proteins for host cell recognition. Incubation of its epimastigote stage with heparin and heparin sulfate can inhibit parasite binding to immobilized heparin and also inhibit parasite binding to midgut epithelial cells of their insect vectors [64]. In the malarial parasite *Plasmodium falciparum*, BAEBL protein binding to erythrocytes was disrupted by addition of soluble heparin [65]. The competition assay presented here showed that soluble heparin inhibited interaction between EhSWP1 and immobilized heparin beads in a dose dependent manner and suggests that heparin would inhibit EhSWP1 binding to shrimp host cells via their surface heparin.

Since there is no EHP infection model in hepatopancreatic cell cultures or any immortal shrimp cell line, *in vivo* tests of spore adherence could not be carried out but should constitute a future goal to confirm whether exogenous soluble heparin could reduce or inhibit EHP spore attachment to host cells. Similar tests would also show whether or not the antibody against EhSWP1 could reduce spore adherence. From previous studies, anti-EcEnP1 antibody inhibited spore adherence by 56% [18], while anti-NbSWP16 antibody reduced adherence by 20% [25]. Such *in vivo* assays with host cells are required to fully understand the function of EhSWP1.

# **Conclusions**

In summary, this is the first report on characterization of a spore wall protein from the microsporidian *E. hepatopenaei* (EhSWP1). It is present in both the exospore and endospore layers of mature spore walls and it has been shown to bind with heparin, indicating a possible role in attachment to host cells via surface heparin as an early step in the host cell infection process and constituting an important role in virulence (Fig. 10). This knowledge may lead to the development of novel therapeutics to combat to EHP infection.

# **Additional files**

**Additional file 1: Figure S1.** Transcriptional pattern of EhSWP1 using one-step RT-PCR and nested RT-PCR analysis of RNA template from naïve shrimp cohabitated with EHP-infected shrimp.

**Additional file 2: Figure S2.** Experimental replicates of the heparin competition assay. (a) replicate II and (b) replicate III.

### **Abbreviations**

**EHP:** *Enterocytozoon hepatopenaei*, **EhSWP1:** Spore wall protein 1 of EHP, **HBM:** Heparin binding motif, **ORF:** Open reading frame, **ppt:** parts per trillion.

### Acknowledgements

The authors would like to thank Professor T. W. Flegel for assistance in designing the study, supervising the project and editing the manuscript, and Asst. Professor Danaya Pakotiprapha for providing heparin sepharose beads and giving very useful comments.

### **Declarations**

### Ethics approval and consent to participate

At the time this work was carried out, there was no official standard of the Ethical Principles and Guidelines for the Use of Animals of the National Research Council of Thailand (1999) for invertebrates. However, its principles for vertebrates were adapted for shrimp. The guidelines of the New South Wales State Government (Australia) for the humane harvesting of fish and crustaceans were also followed (http://www.dpi.nsw.gov.au/agriculture/livestock/animal-welfare/general/fish/shellfish) with respect to details regarding the transport of the shrimp and their

laboratory maintenance. With respect to processing of the shrimp for histological analysis or for killing at the end of an experiment, the saltwater/ice slurry method was used as recommended in the Australian guidelines.

# **Consent for publication**

Not applicable.

# Availability of data and materials

All data generated or analysed during this study are included in this published article and its supplementary information files.

# **Competing interests**

The authors declare that they have no competing interests.

# **Funding**

This project was supported by the Agricultural Research Development Agency (ARDA) of Thailand under project CRP5905020530, by the Thailand Research Fund (TRF) under project IRG5980008 and TRG5780032, by the Newton Institutional Links (IL) program to BIOTEC, Thailand and Cefas, UK, and by Mahidol University. PJ would like to thank the Science Achievement Scholarship of Thailand (SAST) for a PhD scholarship.

### **Author contributions**

PJ, OI and KS designed the study. OI and KS obtained the funding. PJ and RV performed experiments. DWB and BAPW performed bioinformatics analyses. OI, KS and RV supervised the project. PJ, DWB and OI wrote and edited the manuscript. All authors read and approved the final manuscript.

### **Author details**

<sup>1</sup>Department of Biochemistry, Faculty of Science, Mahidol University, Bangkok, Thailand.

<sup>2</sup>Center of Excellence for Shrimp Molecular Biology and Biotechnology (Centex Shrimp), Faculty of Science, Mahidol University, Bangkok, Thailand.

<sup>3</sup>Biosciences, College of Life and Environmental Sciences, University of Exeter, Devon, United Kingdom.

<sup>4</sup>Department of Anatomy,

Faculty of Science, Mahidol University, Bangkok, Thailand. <sup>5</sup>National Center for Genetic Engineering and Biotechnology (BIOTEC), National Science and Technology Development Agency (NSTDA), Pathumthani, Thailand. <sup>6</sup>Shrimp Pathogen Interaction Laboratory (SPI), National Center for Genetic Engineering and Biotechnology (BIOTEC), Bangkok, Thailand.

### References

- 1. Choi J, Kim SH. A genome tree of life for the Fungi kingdom. Proc Natl Acad Sci USA. 2017;114:9391–6.
- 2. Keeling PJ, Fast NM. Microsporidia: biology and evolution of highly reduced intracellular parasites. Annu Rev Microbiol. 2002;56:93–116.
- 3. Stentiford GD, Feist SW, Stone DM, Bateman KS, Dunn AM. Microsporidia: diverse, dynamic, and emergent pathogens in aquatic systems. Trends Parasitol; 2013;29:567–78.
- 4. Nägeli KW. Über die neue krankheit der seidenraupe und verwandte organismen. Bot Z. 1857;15:760–1.
- 5. Bhat SA, Bashir I, Kamili AS. Microsporidiosis of silkworm, *Bombyx mori* L. (Lepidopterabombycidae): a review. African J Agric Res. 2009;4:1519–23.
- 6. Becnel JJ, Andreadis TG. Microsporidia in insects. In: Weiss LM, Becnel JL, editors. Microsporidia: Pathogens of Opportunity. First Ed. West Sussex, UK: Wiley Blackwell; 2014. p. 521–70.
- 7. Kotler DP, Orenstein JM. Clinical syndromes associated with microsporidiosis. Adv Parasitol. 1998;40:321–49.
- 8. Rodriguez-Tovar LE, Speare DJ, Markham RJF. Fish microsporidia: immune response, immunomodulation and vaccination. Fish Shellfish Immunol. 2011;30:999–1006.
- 9. Thitamadee S, Prachumwat A, Srisala J, Jaroenlak P, Salachan PV, Sritunyalucksana K, et al. Review of current disease threats for cultivated penaeid shrimp in Asia. Aquaculture. 2016;452:69–87.
- 10. Takvorian PM, Cali A. Enzyme histochemical identification of the Golgi apparatus in the microsporidian, *Glugea stephani*. J Eukaryot Microbiol. 1993;41:63–64.
- 11. Franzen C. Microsporidia: how can they invade other cells? Trends Parasitol. 2004;20:275–9.
- 12. Williams BAP, Hirt RP, Lucocq JM, Embley TM. A mitochondrial remnant in the microsporidian *Trachipleistophora hominis*. Nature. 2002;418:865–9.

- 13. Burri L, Williams BAP, Bursac D, Lithgow T, Keeling PJ. Microsporidian mitosomes retain elements of the general mitochondrial targeting system. Proc Natl Acad Sci USA. 2006;103:15916–20.
- 14. Peyretaillade E, El Alaoui H, Diogon M, Polonais V, Parisot N, Biron DG, et al. Extreme reduction and compaction of microsporidian genomes. Res Microbiol. 2011;162:598–606.
- 15. Corradi N, Pombert J-F, Farinelli L, Didier ES, Keeling PJ. The complete sequence of the smallest known nuclear genome from the microsporidian *Encephalitozoon intestinalis*. Nat Commun. 2010;1:77–84.
- 16. Weidner E. The microsporidian spore invasion tube. the ultrastructure, isolation, and characterization of the protein comprising the tube. J Cell Biol. 1976;71:23–34.
- 17. Hayman JR, Southern TR, Nash TE. Role of sulfated glycans in adherence of the microsporidian *Encephalitozoon intestinalis* to host cells *in vitro*. Infect Immun. 2005;73:841–8.
- 18. Southern TR, Jolly CE, Lester ME, Hayman JR. EnP1, a microsporidian spore wall protein that enables spores to adhere to and infect host cells *in vitro*. Eukaryot Cell. 2007;6:1354–62.
- 19. Frixione E, Ruiz L, Cerbón J, Undeen AH. Germination of *Nosema algerae* (Microspora) spores: conditional inhibition by D2O, ethanol and Hg2+ suggests dependence of water influxupon membrane hydration and specific transmembrane pathways. J Eukaryot Microbiol. 1997;44:109–16.
- 20. Vávra J, Lukeš J. Microsporidia and "the art of living together". Adv Parasitol. 2013;82:253–319
- 21. Weiss LM, Delbac F, Hayman JR, Pan G, Dang X, Zhou Z. The microsporidian polar tube and spore wall. In: Weiss LM, Becnel JL, editors. Microsporidia: Pathogens of Opportunity. First Ed. West Sussex, UK: Wiley Blackwell; 2014. p. 261–306.
- 22. Li Z, Pan G, Li T, Huang W, Chen J, Geng L, et al. SWP5, a spore wall protein, interacts with polar tube proteins in the parasitic microsporidian *Nosema bombycis*. Eukaryot Cell. 2012;11:229–37.
- 23. Yang D, Dang X, Peng P, Long M, Ma C, Qin JJG, et al. NbHSWP11, a microsporidia *Nosema bombycis* protein, localizing in the spore wall and membranes, reduces spore adherence to host cell BME. J Parasitol. 2014;100:623–32.
- 24. Chen J, Geng L, Long M, Li T, Li Z, Yang D, et al. Identification of a novel chitin-binding spore wall protein (NbSWP12) with a BAR-2 domain from *Nosema bombycis* (microsporidia). Parasitology. 2013;140:1394–402.
- 25. Wang Y, Dang X, Ma Q, Liu F, Pan G, Li T, et al. Characterization of a novel spore wall protein

NbSWP16 with proline-rich tandem repeats from *Nosema bombycis* (microsporidia). Parasitology. 2014;142:534–42.

- 26. Wu Z, Li Y, Pan G, Zhou Z, Xiang Z. SWP25, a novel protein associated with the *Nosema bombycis* endospore. J Eukaryot Microbiol. 2009;56:113–8.
- 27. Li Y, Wu Z, Pan G, He W, Zhang R, Hu J, et al. Identification of a novel spore wall protein (SWP26) from microsporidia *Nosema bombycis*. Int J Parasitol. 2009;39:391–8.
- 28. Peuvel-Fanget I, Polonais V, Brosson D, Texier C, Kuhn L, Peyret P, et al. EnP1 and EnP2, two proteins associated with the *Encephalitozoon cuniculi* endospore, the chitin-rich inner layer of the microsporidian spore wall. Int J Parasitol. 2006;36:309–18.
- 29. Brosson D, Kuhn L, Prensier G, Vivarès CP, Texier C. The putative chitin deacetylase of *Encephalitozoon cuniculi*: a surface protein implicated in microsporidian spore-wall formation. FEMS Microbiol Lett. 2005;247:81–90.
- 30. Chen L, Li R, You Y, Zhang K, Zhang L. A novel spore wall protein from *Antonospora locustae* (Microsporidia: Nosematidae) contributes to sporulation. J Eukaryot Microbiol. 2017;64:779–791.
- 31. Jaroenlak P, Sanguanrut P, Williams BAP, Stentiford GD, Flegel TW, Sritunyalucksana K, et al. A nested PCR assay to avoid false positive detection of the microsporidian *Enterocytozoon hepatopenaei* (EHP) in environmental samples in shrimp farms. PLoS One. 2016;11:e0166320.
- 32. Sritunyalucksana K, Sanguanrut P, Salachan PV, Thitamadee S, Flegel TW. Urgent appeal to control spread of the shrimp microsporidian parasite *Enterocytozoon hepatopenaei* (EHP). Network of Aquaculture Centres in Asia-Pacific (NACA). 13 Dec 2014;4–6.
- enaca.org/publications/health/disease-cards/urgent-appeal-to-control-ehp-3.pdf
- 33. Chayaburakul K, Nash G, Pratanpipat P, Sriurairatana S, Withyachumnarnkul B. Multiple pathogens found in growth-retarded black tiger shrimp *Penaeus monodon* cultivated in Thailand. Dis Aquat Org. 2004;60:89–96.
- 34. Tourtip S, Wongtripop S, Stentiford GD, Bateman KS, Sriurairatana S, Chavadej J, et al. *Enterocytozoon hepatopenaei* sp. nov. (Microsporida: Enterocytozoonidae), a parasite of the black tiger shrimp *Penaeus monodon* (Decapoda: Penaeidae): fine structure and phylogenetic relationships. J Invertebr Pathol. 2009;102:21–9.
- 35. Tangprasittipap A, Srisala J, Chouwdee S, Somboon M, Chuchird N, Limsuwan C, et al. The microsporidian *Enterocytozoon hepatopenaei* is not the cause of white feces syndrome in whiteleg shrimp *Penaeus* (*Litopenaeus*) *vannamei*. BMC Vet Res. 2013;9:139.
- 36. Tang KFJ, Pantoja CR, Redman RM, Han JE, Tran LH, Lightner DV. Development of in situ

hybridization and PCR assays for the detection of *Enterocytozoon hepatopenaei* (EHP), a microsporidian parasite infecting penaeid shrimp. J Invertebr Pathol. 2015;130:37–41.

- 37. Rajendran KV, Shivam S, Ezhil PP, Joseph SRJ, Sathish KT, Avunje S, et al. Emergence of *Enterocytozoon hepatopenaei* (EHP) in farmed *Penaeus* (*Litopenaeus*) vannamei in India. Aquaculture. 2016;454:272–80.
- 38. Tang KFJ, Aranguren LF, Piamsomboon P, Han JE, Maskaykina IY, Schmidt MM. Detection of the microsporidian *Enterocytozoon hepatopenaei* (EHP) and Taura syndrome virus in *Penaeus vannamei* cultured in Venezuela. Aquaculture. 2017;480:17–21.
- 39. Salachan PV, Jaroenlak P, Thitamadee S, Itsathitphaisarn O, Sritunyalucksana K. Laboratory cohabitation challenge model for shrimp hepatopancreatic microsporidiosis (HPM) caused by *Enterocytozoon hepatopenaei* (EHP). BMC Vet Res. 2016;13:9.
- 40. Wiredu Boakye D, Jaroenlak P, Prachumwat A, Williams TA, Bateman KS, Itsathitphaisarn O, et al. Decay of the glycolytic pathway and adaptation to intranuclear parasitism within Enterocytozoonidae microsporidia. Environ Microbiol. 2017;19:2077–89.
- 41. Camacho C, Coulouris G, Avagyan V, Ma N, Papadopoulos J, Bealer K, et al. BLAST+: architecture and applications. BMC Bioinformatics. 2009;10:421.
- 42. Li L, Stoeckert CJJ, Roos DS. OrthoMCL: Identification of ortholog groups for eukaryotic genomes. Genome Res. 2003;13:2178–89.
- 43. Ronquist F, Teslenko M, Van Der Mark P, Ayres DL, Darling A, Höhna S, et al. MrBayes 3.2: Efficient bayesian phylogenetic inference and model choice across a large model space. Syst Biol. 2012;61:539–42.
- 44. Somchai P, Jitrakorn S, Thitamadee S, Meetam M, Saksmerprome V. Use of microalgae *Chlamydomonas reinhardtii* for production of double-stranded RNA against shrimp virus. Aquac Reports. 2016;3:178–83.
- 45. Southern TR, Jolly CE, Hayman JR. Augmentation of microsporidia adherence and host cell infection by divalent cations. FEMS Microbiol Lett. 2006;260:143–9.
- 46. Yang D, Pan L, Peng P, Dang X, Li C, Li T, et al. Interaction between SWP9 and PTPs of the microsporidian *Nosema bombycis* and SWP9 as a scaffolding protein contributes to the polar tube tethering to spore wall. Infect Immun. 2016;85:00872-16.
- 47. Proudfoot AEI, Fritchley S, Borlat F, Shaw JP, Vilbois F, Zwahlen C, et al. The BBXB motif of RANTES is the principal site for heparin binding and controls receptor selectivity. J Biol Chem. 2001;276:10620–6.

- 48. Marinò M, Friedlander JA, McCluskey RT, Andrews D. Identification of a heparin-binding region of rat thyroglobulin involved in megalin binding. J Biol Chem. 1999;274:30377–86.
- 49. Bigliardi E, Sacchi L. Cell biology and invasion of the microsporidia. Microbes Infect. 2001;3:373–9.
- 50. Weiss LM, Becnel JJ. Pathogens of Opportunity. First Ed. West Sussex, UK: Wiley Blackwell; 2014.
- 51. Cardin AD, Weintraub HJ. Molecular modeling of protein-glycosaminoglycan interactions. Arteriosclerosis. 1989;9:21–32.
- 52. Capila I, Linhardt RJ. Heparin-protein interactions. Angew Chemie. 2002;41:390–412.
- 53. Kessels MM, Qualmann B. Different functional modes of BAR domain proteins in formation and plasticity of mammalian postsynapses. J Cell Sci. 2015;128:3177–85.
- 54. Linhardt RJ. Heparin: structure and activity. J Med Chem. 2003;46:2551–64.
- 55. Arias E, Smith BL. Deaths: preliminary data for 2001. Natl Vital Stat Rep. 2003;51:1–44.
- 56. Nader HB, Lopes CC, Rocha HAO, Santos EA, Dietrich CP. Heparins and heparinoids: occurrence, structure and mechanism of antithrombotic and hemorrhagic activities. Curr Pharm Des. 2004;10:951–66.
- 57. Volpi N. Occurrence and structural characterization of heparin from molluscs. ISJ. 2005;2:6–16.
- 58. Ulrich PN, Boon JK. The histological localization of heparin in the northern quahog clam, *Mercenaria mercenaria*. J Invertebr Pathol. 2001;78:155–9.
- 59. Bell TA, Lightner DV. A handbook of normal penaeid shrimp histology. Baton Rouge: World Aquaculture Society; 1988.
- 60. Brito AS, Cavalcante RS, Palhares LC, Hughes AJ, Andrade GP, Yates EA, et al. A non-hemorrhagic hybrid heparin/heparan sulfate with anticoagulant potential. Carbohydr Polym. 2014;99:372–8.
- 61. Dietrich CP, Paiva JF, Castro RAB, Chavante SF, Jeske W, Fareed J, et al. Structural features and anticoagulant activities of a novel natural low molecular weight heparin from the shrimp *Penaeus brasiliensis*. Biochim Biophys Acta-Gen Subj. 1999;1428:273–83.
- 62. Chen K, Li E, Li T, Xu C, Wang X, Lin H, et al. Transcriptome and molecular pathway analysis of the hepatopancreas in the Pacific white shrimp *Litopenaeus vannamei* under chronic low-salinity stress. PLoS One. 2015;10:1–22.
- 63. Yang D, Pan G, Dang X, Shi Y, Li C, Peng P, et al. Interaction and assembly of two novel proteins in the spore wall of the microsporidian species *Nosema bombycis* and their roles in

adherence to and infection of host cells. Infect Immun. 2015;83:1715–31.

64. Oliveira FOR, Alves CR, Souza-Silva F, Calvet CM, Côrtes LMC, Gonzalez MS, et al. *Trypanosoma cruzi* heparin-binding proteins mediate the adherence of epimastigotes to the midgut epithelial cells of *Rhodnius prolixus*. Parasitology. 2012;139:735–43.

65. Kobayashi K, Kato K, Sugi T, Takemae H, Pandey K, Gong H, et al. *Plasmodium falciparum* BAEBL binds to heparan sulfate proteoglycans on the human erythrocyte surface. J Biol Chem. 2010;285:1716–25.

# Legends to figures

**Fig. 1** Sequence analysis of EHP SWPs. Bayesian Inference phylogenetic analyses of proteins that were grouped in the same ORTHOMCL ortholog clusters with *Enterocytozoon hepatopenaei* proteins annotated as SWP in its genomic assembly. The dotted line arcs delineate the two distinct clades made up of SWP12 and SWP7 proteins. *E. hepatopenaei* proteins are indicated with asterisk (\*). Red arrowhead represents EhSWP1 (EHP00\_686). Numbers on nodes are Bayesian posterior probability values

**Fig. 2** Domain organization of EHP SWPs. Bayesian inference analyses of proteins in the SWP12 clade. Blue rounded rectangles represent conservation of the BAR2 domain across this clade with their hues reflecting their level of similarity to the BAR2 HMM seed consensus sequence. Hues assigned with the heat map module in R STUDIO. Conservation of Heparin Binding Motifs (HBMs) is represented with small grey curved rectangles. Subclades have been delimitated with different background colors. Numbers on nodes are Bayesian posterior probability values. EHP SWPs are indicated with asterisk (\*) and red arrowhead represents EhSWP1 (EHP00\_686)

**Fig. 3** EhSWP1 transcripts can be detected 20 days after cohabitation. The mRNA expression of EhSWP1 was analyzed by RT-PCR using RNA template extracted from hepatopancreatic tissue of naïve shrimp cohabitated with EHP-infected shrimp. Shrimp samples were collected at 0, 5, 7, 9, 11 and 20 days after the start of cohabitation between naïve shrimp and EHP-infected shrimp. The actin gene of *P. vannamei* (PvActin) was used as an internal control

**Fig. 4** Expression, purification and Western blot analysis of recombinant EhSWP1. **a** SDS-PAGE gel compared between uninduced *E. coli* BL21 star(DE3) cells and induced *E. coli* cells with 0.4

mM IPTG. **b** SDS-PAGE gel showing purified recombinant EhSWP1 obtained using Ni<sup>2+</sup>-NTA affinity chromatography. Lane FT shows the flow-through fraction; W1 and W5 are wash fractions 1 and 5, respectively; E1–E5 are elution fractions 1–5. **c** Immunoblot of recombinant EhSWP1 probed with rabbit anti-SWP1 antibody and naïve rabbit serum as a negative control. The recombinant EhSWP1 band is indicated by a black arrow. Lane M:protein molecular weight marker

**Fig. 5** Immunofluorescence analysis (IFA) reveals the localization of EhSWP1 in the spore wall. Green fluorescence (Alexa-488) indicates the localization of EhSWP1 in mature spores. Phase shows the phase contrast micrographs. TO-PRO-3 was used to stain the nuclei of EHP spores (blue fluorescence). **a** Anti-SWP1 antibody was used as a primary antibody. A higher magnification is shown in the inset. **b** Naïve rabbit serum was used a negative control

**Fig. 6** Subcellular localization of EhSWP1 using Immunoelectron analysis (IEM). **a, b** Electron micrographs reveal the localization of EhSWP1. Exposure to anti-SWP1 antibody followed by GAR-IgG conjugated with 10 nm gold particles revealed immunogold particles (indicated with white arrows) indicating the presence of EhSWP1 in the exospore and endospore of EHP. **c** Negative control probed with naïve rabbit serum shows no immunogold signals. *Abbreviations*: Ex, exospore layer; En, endospore layer

**Fig. 7** Recombinant EhSWP1 binds to heparin *in vitro*. **a** SDS-PAGE gel showing input recombinant EhSWP1 (black arrow) and bovine serum albumin (BSA, white arrow) prior to mixing with heparin sepharose beads. **b** SDS-PAGE gel showing fractions eluted with 2 M NaCl and indicating that only EhSWP1 (black arrow) was captured and eluted from the heparin beads

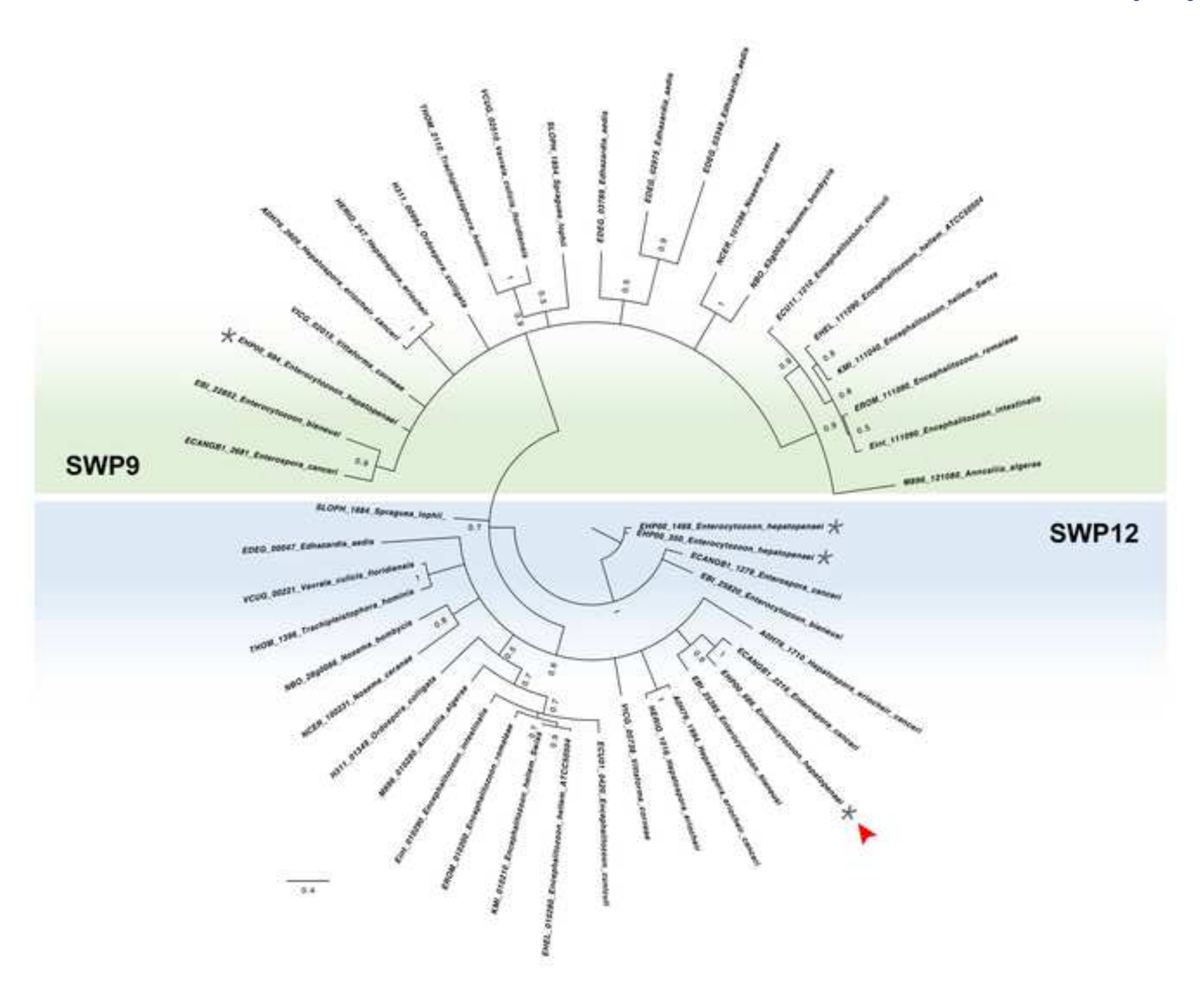
**Fig. 8** EhSWP1-HBM mutants fail to bind to heparin beads. **a** SDS-PAGE gel showing input proteins EhSWP1 WT, EhSWP1(B→G) and EhSWP1(B→S) (black arrow) with molecular weights of 27 kDa, 26 kDa and 26 kDa, respectively. **b** SDS-PAGE gel showing elution fractions after incubation with heparin sepharose beads and revealing that only EhSWP1 WT (black arrow) was captured and eluted from the beads. Lower panels (indicated as WB) are western blots probed with anti-EhSWP1 antibody to confirm protein identity as EhSWP1 (black arrows)

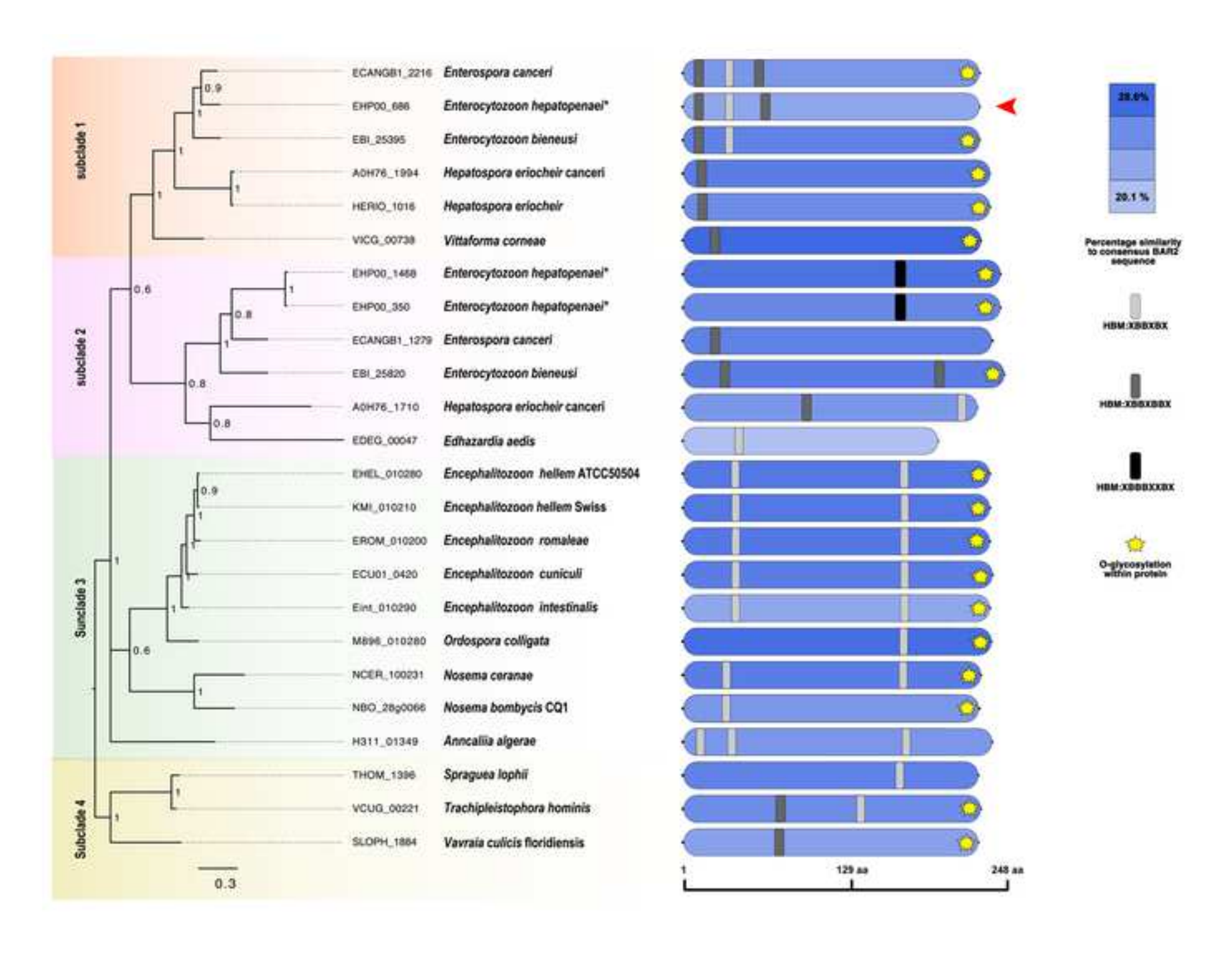
**Fig. 9** Heparin competition assay. **a** SDS-PAGE gel showing input recombinant EhSWP1 (black arrow) with different concentrations of soluble porcine heparin. **b** SDS-PAGE gel shows elution fractions after 1 h competition and revealing that binding of EhSWP1 (black arrow) to heparin beads was blocked at 100 mg/ml. **c** Bar graph showing percentage of heparin binding quantified from the protein bands from 3 with replicates gels (Additional file 2: Figure S2). Error bars indicate the mean  $\pm$  SEM. Level of heparin binding at 0 mg/ml was used for normalization. \* $P \le 0.01$ ; \*\*\* $P \le 0.0001$ 

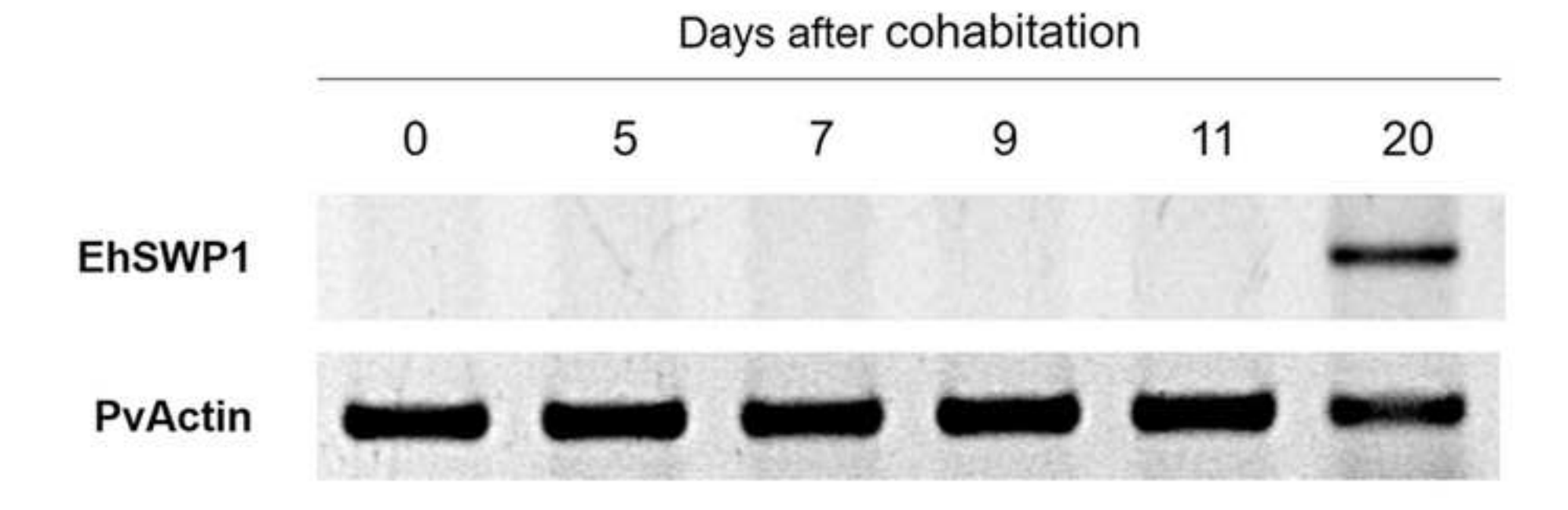
**Fig. 10** A schematic model of how EhSWP1 functions in host cell attachment. In order to invade shrimp cells, EHP must be in close proximity to tubule epithelial cells of shrimp hepatopancreas. From our results, we hypothesize that spores of EHP are attracted to the epithelial cells through the electrostatic interactions between positively charged residues (Arg, Lys and His) in the three HBMs of EhSWP1 and negatively charged heparin on cell surface. Once anchored, the EHP spores extrude their polar tube to pierce the host cell membrane and release sporoplasm into host cytoplasm where the next developmental stages occur

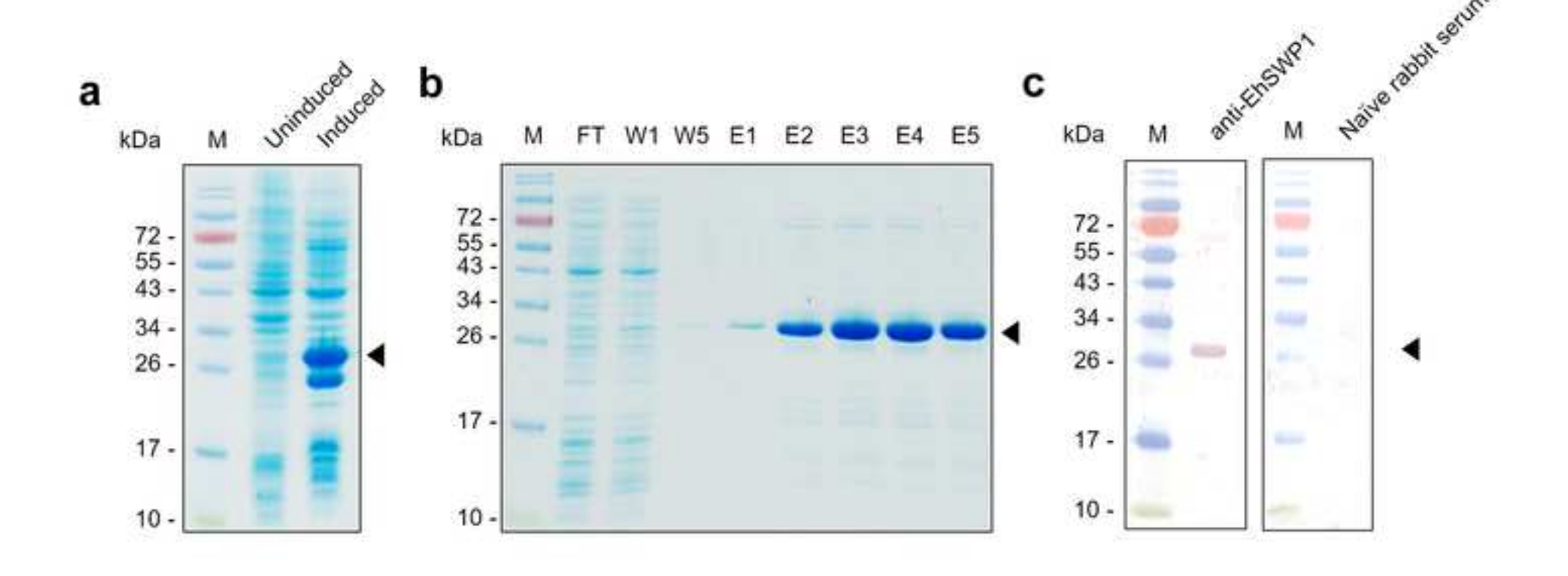
**Table 1** Putative virulence factors of EHP

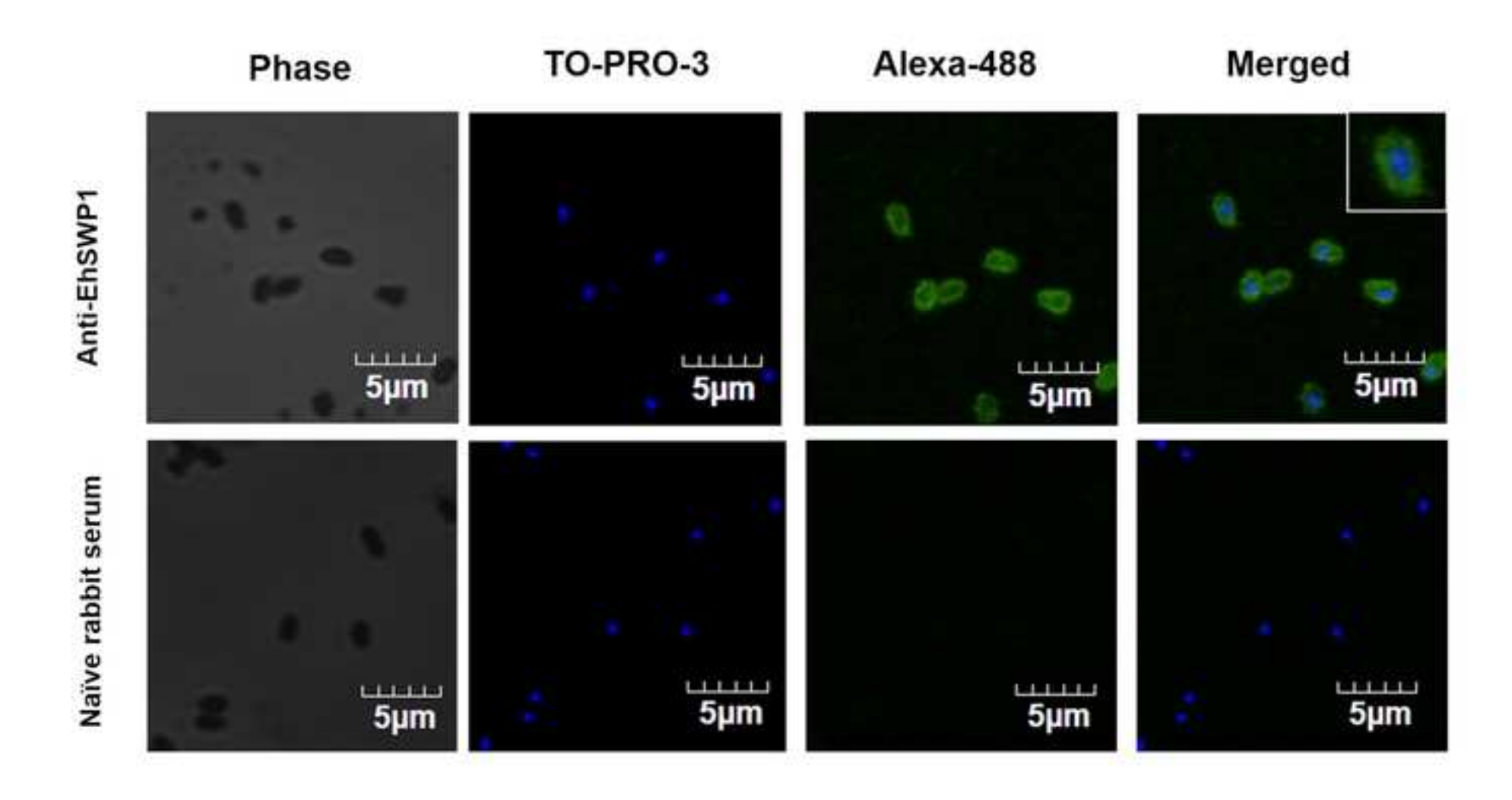
Function	Gene
Host cell invasion and spore attachment	Polar tube proteins (PTPs)
	Spore wall proteins (SWPs)
	Endochitinases
	Chitin synthases
Energy parasitism	ADP/ATP transporters
Host cell manipulation	Mitogen-activated protein kinases
	Transferases
	Splicing machineries

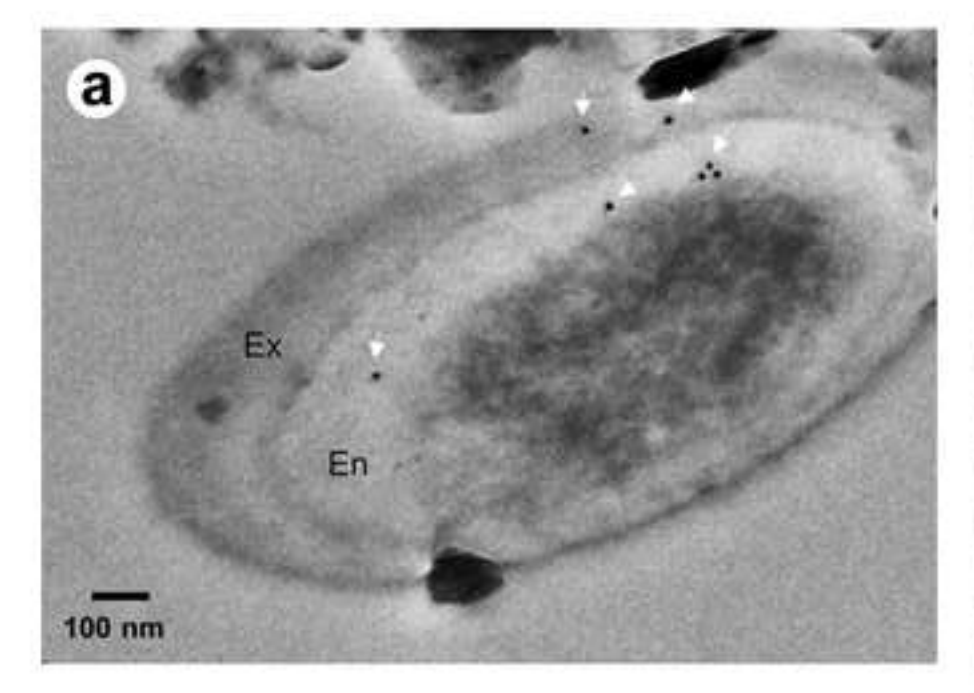


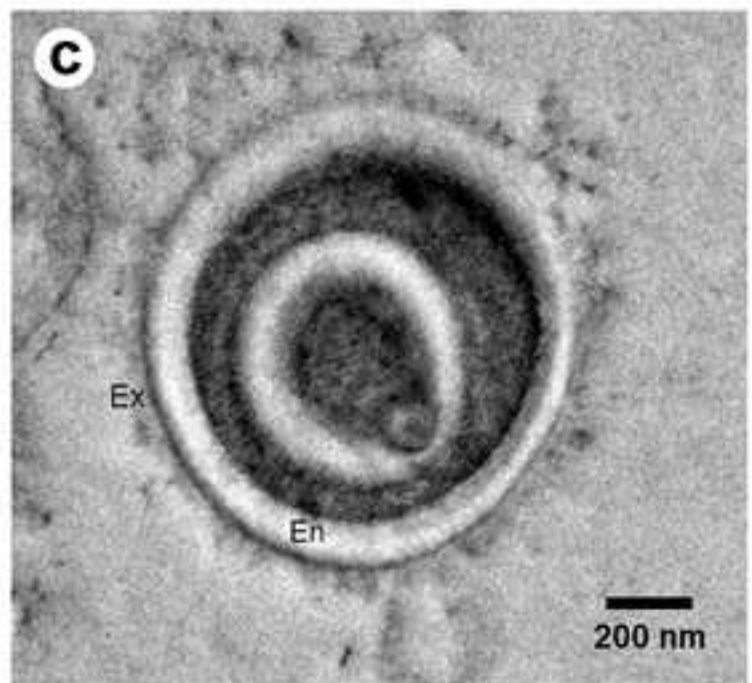


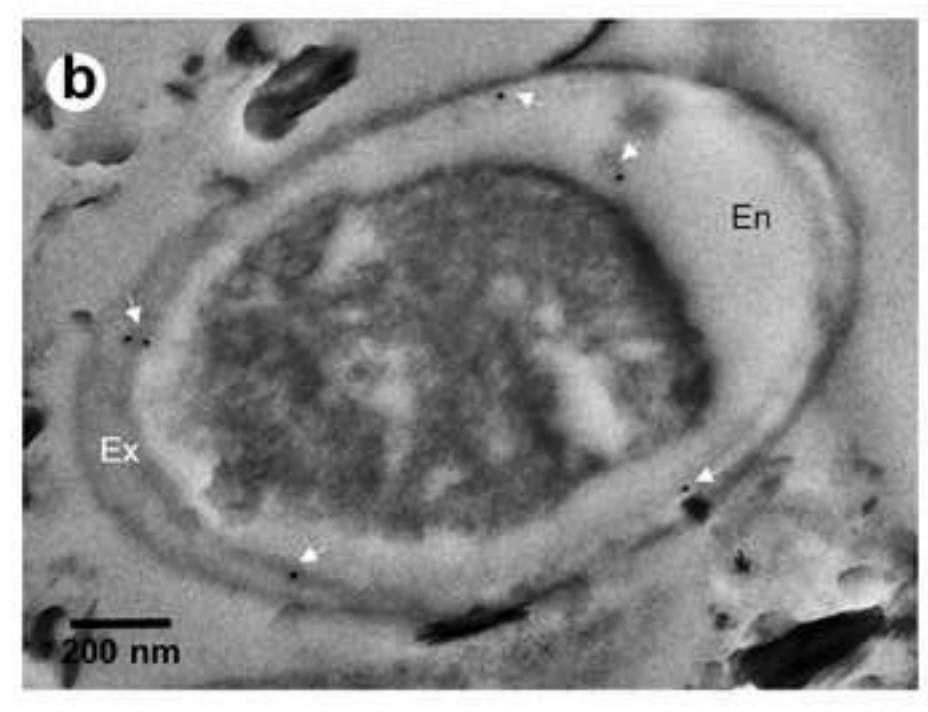


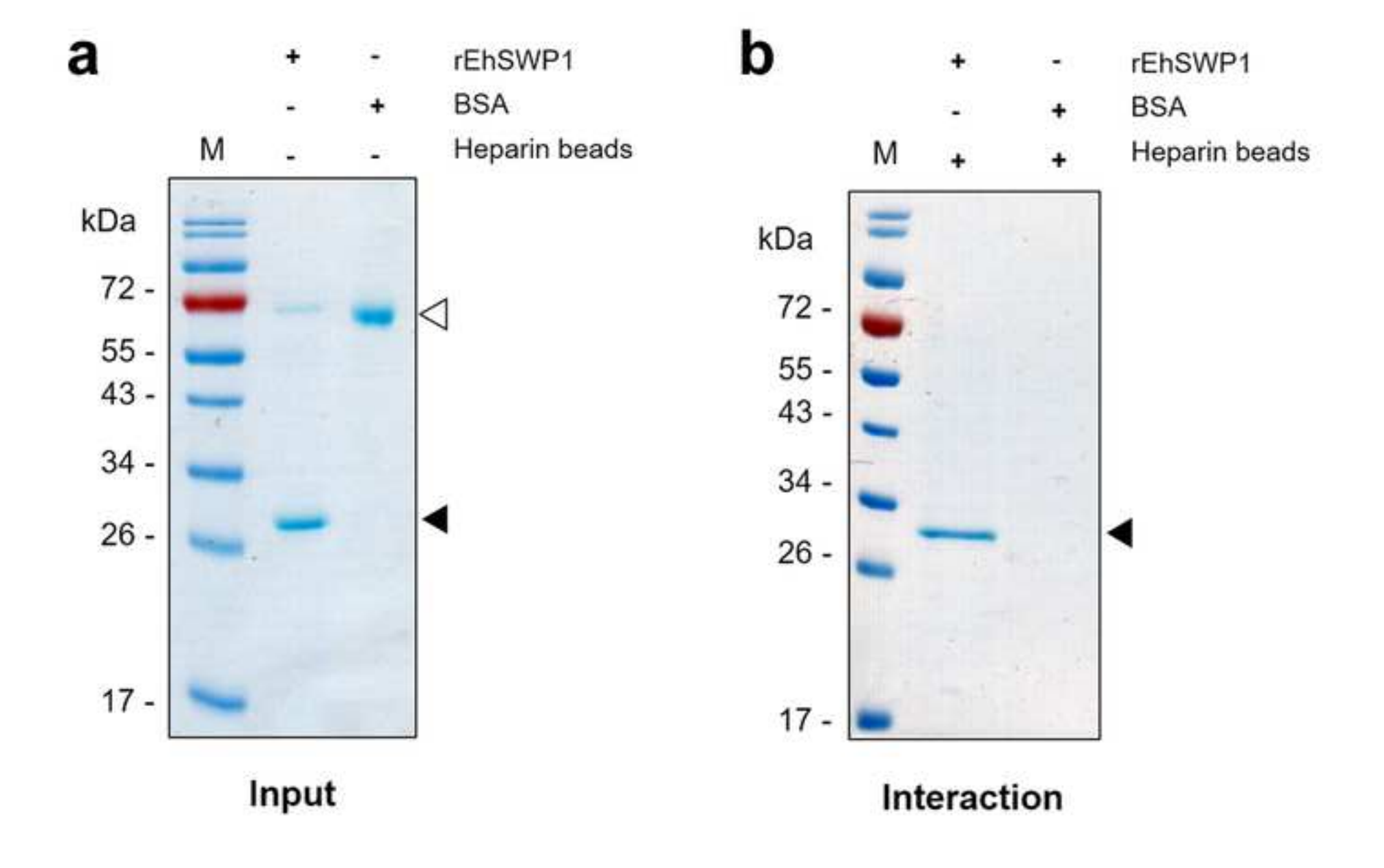


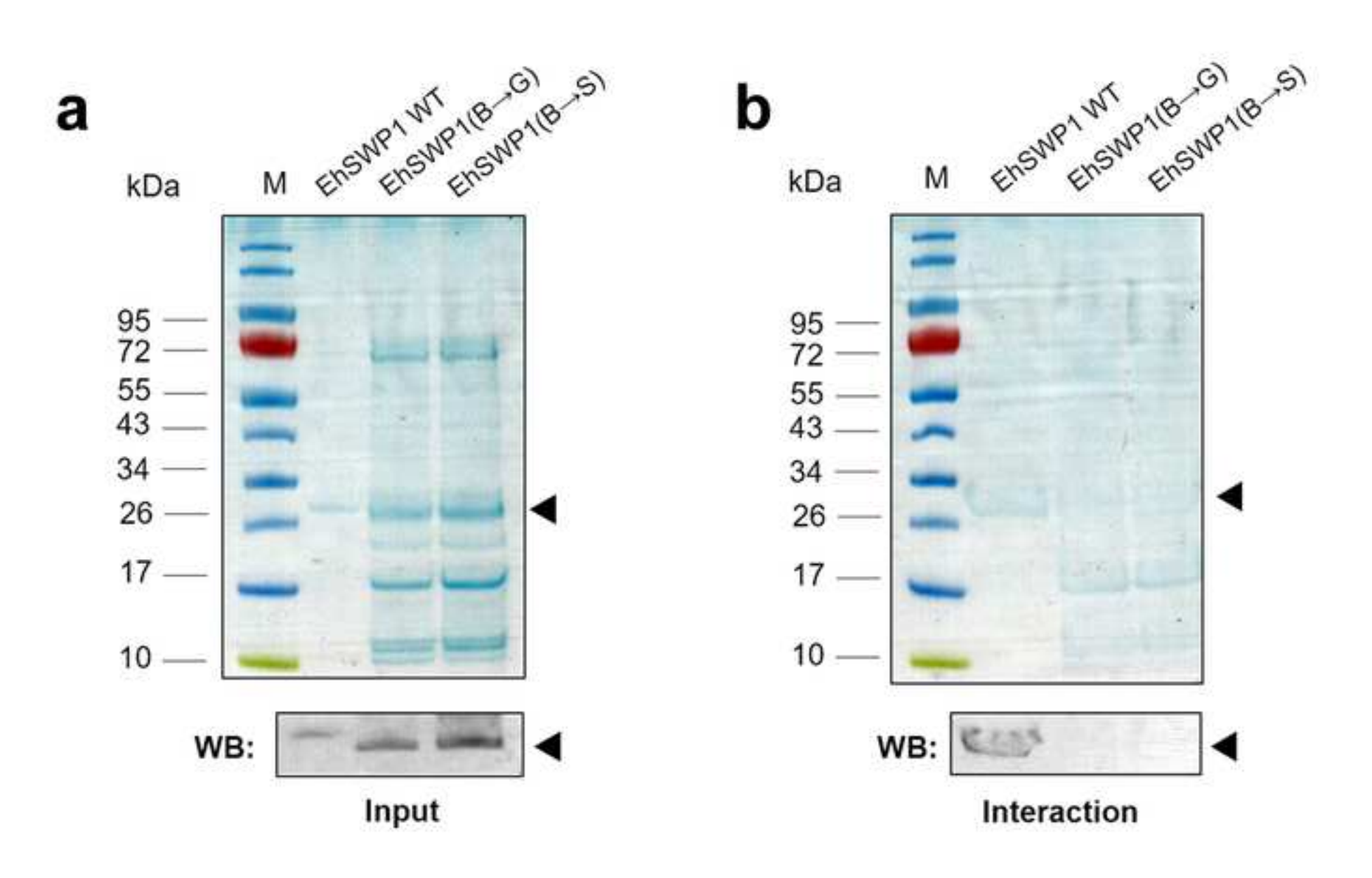


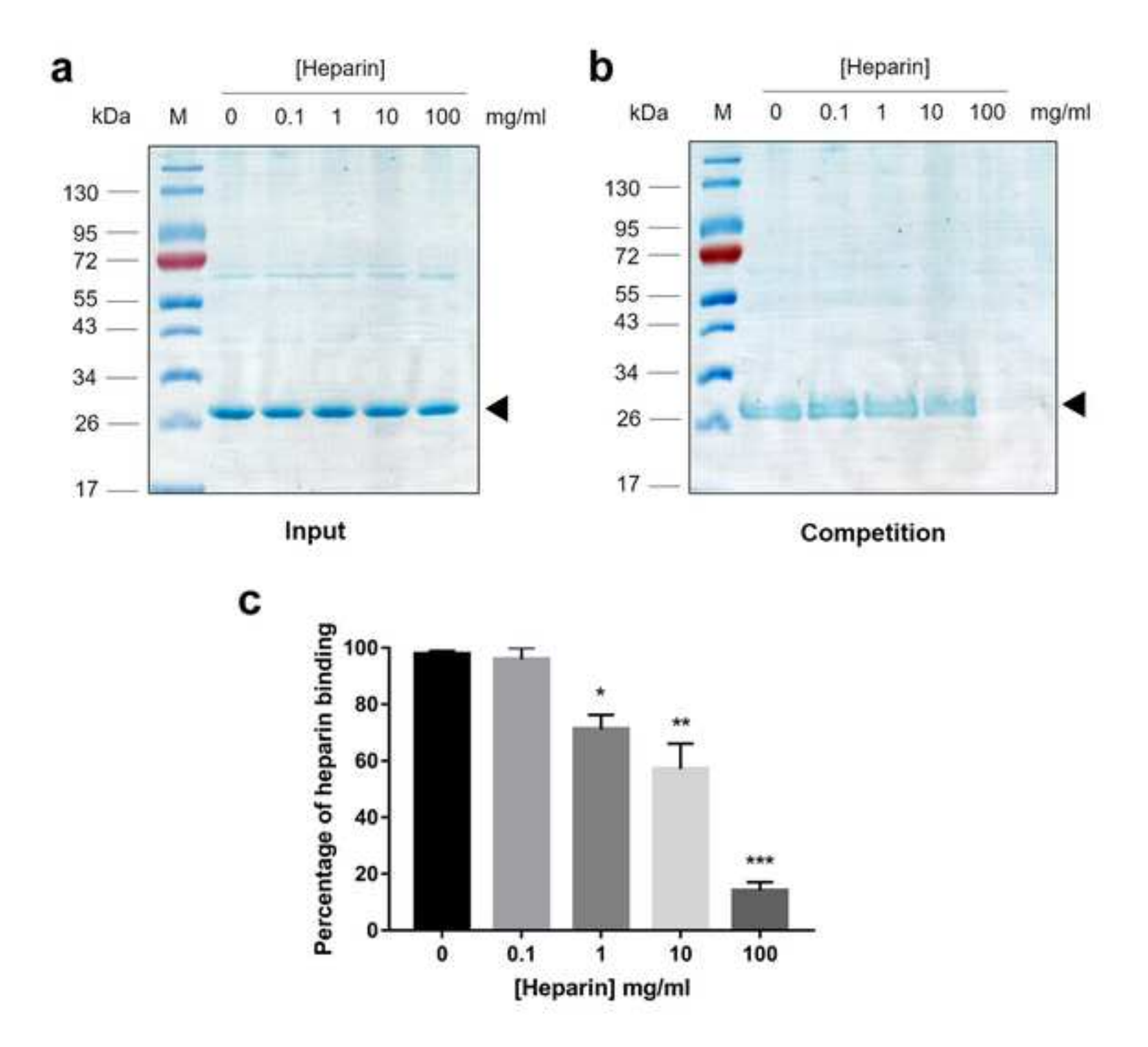












# EhSWP1 Heparin-binding protein Heparin Binding Motifs (HBMs) B\* is a positively charged amino acid EHP spore EhSWP1 Heparin Binding Motifs (HBMs) Heparin Heparin Heparin Heparin

Tubule epithelial cells of shrimp hepatopancreas

Additional file 1

Click here to access/download **Supplementary Material**Additional file 1.tif

Additional file 2

Click here to access/download **Supplementary Material**Additional file 2.tif



Department of Biochemistry Center of Excellence for Shrimp Molecular Biology and Biochemistry (Centex Shrimp) Faculty of Science, Mahidol University 272 Rama VI Road, Ratchathewi, Bangkok, Thailand 10400

> Ornchuma Itsathitphaisarn, PhD Lecturer of Biochemistry

Telephone: +6602 201 5873 *Fax:* +6602 354 7344

Email: ornchuma.its@mahidol.ac.th

October 10, 2017

Dear Editor,

We write to resubmit the final revised version of our manuscript entitled "Identification, characterization and heparin binding activity of a spore-wall, virulence protein from the shrimp microsporidian, Enterocytozoon hepatopenaei"

Changes in the manuscript were revised and accepted. They did not affect the scientific meaning of the manuscript. I, however, prefer the unitalicized version of via.

Additional information and requested clarifications were provided. The final revised file is PARV-D-17-01200\_R2 EDIT SC\_PJ\_OI.docx

Thank you very much for considering our work for publication at Parasites and Vectors.

Sincerely,

Ornchuma Itsathitphaisarn

Ornchuma Itsathitphaisarn Lecturer of Biochemistry